uOttawa

L'Université canadienne
Canada's university

FACULTÉ DES ÉTUDES SUPÉRIEURES ET POSTOCTORALES

u Ottawa

L'Université canadienne
Canada's university

FACULTY OF GRADUATE AND POSDOCTORAL STUDIES

Kathleen Hurst

AUTEUR DE LA THÈSE / AUTHOR OF THESIS

M.Sc. (Cellular and Molecular Medicine)

GRADE / DEGREE

Department of Cellular and Molecular Medicine

FACULTÉ, ÉCOLE, DÉPARTEMENT / FACULTY, SCHOOL, DEPARTMENT

NF-kB Function and Activation in Mouse Mammary Stem Cells and it's Interplay with the Downstream Target, Ciap2 IN mmtv-eRBb2 Induced Tumourigenesis

TITRE DE LA THÈSE / TITLE OF THESIS

Dr. Pratt

DIRECTEUR (DIRECTRICE) DE LA THÈSE / THESIS SUPERVISOR

CO-DIRECTEUR (CO-DIRECTRICE) DE LA THÈSE / THESIS CO-SUPERVISOR

Michael McBurney

Rob Surgaton

Gary W. Slater

Le Doyen de la Faculté des études supérieures et postdoctorales / Dean of the Faculty of Graduate and Postdoctoral Studies

NF-κB function and activation in mouse mammary stem cells and its interplay with the downstream target, cIAP2 in MMTV-ErbB2 induced tumourigenesis

Kathleen M. Hurst

This thesis is submitted as a partial fulfillment of the M.Sc. program in Cellular Molecular Medicine

University of Ottawa

Ottawa, Ontario, Canada

February 24, 2010

Your file Votre référence
ISBN: 978-0-494-65529-0
Our file Notre référence
ISBN: 978-0-494-65529-0

ABSTRACT

The process of tumourigenesis in breast cancer involves a number of cellular proteins that work in concert to allow for cellular survival, proliferation, angiogenesis and continued tumour growth. The transcription factor NF-κB, which is often constitutively expressed in mammary carcinoma, signals through a number of downstream targets, one of which is cIAP2, to promote cellular growth and evasion of apoptosis. It is unclear if the NF-κB in cancer is needed for mammary stem cell or tumour-initiating cell survival. In the first part of this two-part study, it was shown that MMTV-ErbB2 mice lacking cIAP2 expression developed tumours with increased latency compared to MMTV-ErbB2 mice with cIAP2 expression. These tumours exhibited no change in cellular mitotic index or levels of tumour-associated macrophage infiltration, but did exhibit an increase in the number of apoptotic cells and an increase in angiogenesis. Preliminary data also suggests that tumours in knockout mice also exhibit a decrease in ErbB2 transgene expression levels, and an associated decrease in the expression of phospho-Akt, which may be associated with an increase in transgene silencing with age. It is proposed that cIAP2 knockout tumours have circumvented the absence of this survival gene in part by signaling angiogenesis, but the exact mechanism driving tumour formation remains unclear.

In the second part of this study, mouse mammary epithelial stem and progenitor cells from dissociated mammary glands of NF-κB EGFP reporter mice were analyzed for NF-κB expression by flow cytometry and by fluorescent staining for nuclear p65 (NF-κB). Mouse mammary repopulating units (MRUs) and mammary colony forming cells (Ma-CFCs) were analyzed; these cell types have been previously described. MRUs have

been characterized as basal-like mammary cells, and Ma-CFCs express markers characteristic of luminal mammary cells. It was found that only 6% of MRUs exhibited NF-κB expression, whereas 100% of the Ma-CFCs contained NF-κB expression. Analysis of tumours from MMTV-ErbB2 mice expressing the NF-κB EGFP reporter transgene was also completed. Sorting MMTV-ErbB2 induced mammary tumour cells based on CD44 surface staining (a previously reported tumour initiating cell marker) was unsuccessful, suggesting that CD44 may not be a putative marker for the cancer stem cell. These data suggest that NF-κB is activated during differentiation in the luminal Ma-CFC progenitor population, but not in the stem cell enriched populations.

ACKNOWLEDGEMENTS

I would like to thank Dr. Robert Haché for taking me into his lab, providing me with a positive working environment and giving me the confidence to continue my degree. I would also like to thank Dr. Sebastien Soubeyrand and Louise Pope for their guidance and assistance in the lab. I am also very grateful for the support and advice provided to me by committee, Dr. David Lohnes and Dr. Stephen Lee.

My sincere gratitude towards my family for their continued encouragement and love – Thank you Mom, Dad, Holly and Matt. You kept me smiling and wanting to strive for more. A huge thank you also to my future mother and father-in-law, Linda and Fred Bone. I have more support with you in my life than I could ever hope for.

Thank you also to my good friend Stephanie Grainger for laughter and awesomeness.

Finally, I would like to thank my fiancé and best friend, Jamie Bone, who I respect and love endlessly and overwhelmingly for his ability to keep me grounded, and calm me down.

"Misfortune shows those who are not really friends". – Aristotle

STATEMENT

Please note that the data presented herein was completed in Dr. Christine Pratt's lab at the University of Ottawa in the Department of Cellular and Molecular Medicine, Faculty of Medicine until August 2008 (from May 2007). This work was supported by Grant # FRN 79304 from the Canadian Institutes of Health Research/Canadian Breast Cancer Research Alliance and the Cancer Research Society Incorporated to Dr. Pratt. I would like to thank her for her help in writing my thesis. The data outlined in Appendix 3 was completed in Dr. Robert Haché's lab (my current supervisor) at the University of Ottawa in the Department of Biochemistry, Faculty of Medicine and covers work completed between September 2008 and April 2009. The work was supported by a grant to Robert Haché from the Canadian Institute of Health Research.

Graduate Studentships from both the Ontario Graduate Scholarship Program and the Canadian Institute of Health Research to Kathleen Hurst also supported this research.

TABLE OF CONTENTS

LIST OF ABBREVIATIONS

Abbreviation	Full Name
Akt	V-akt murine thymoma viral oncogene homolog
AML	Acute myelogenous leukemia
APAF-1	Apoptotic peptidase activating factor 1
ARD	Ankryin repeat domain
ATP	Adenosine triphosphate
β-TrCP-SCF	Beta transducin repeat containing protein-Skp1 cullin F box protein
BAFF	B-cell activating factor
Bcl-2, Bcl-3	B cell CLL/lymphoma 2, 3
Bcr-Abl	Breakpoint cluster region-v-ABL Abelson murine leukemia viral oncogene homolog 1
BIRC2, 3	Baculoviral inhibitor of apoptosis repeat-containing 2, 3
BMS	4(2'-aminoethyl)amino-1,8-dimethylimidazo(1,2-a)quinoxaline
BRCA1	Breast cancer 1, early onset
BSA	Bovine serum albumin
CAST	CAZ-associated structural protein
CAZ	Cytomatrix at the active zone
CO_2	Carbon dioxide
COX-2	Cyclooxygenase-2
CD	Cell differentiation marker
CDK	Cyclin dependent kinase
cIAP1, 2	Cellular inhibitor of apoptosis 1, 2
CK2	Casein kinase 2
CSC	Cancer stem cell
CYLD	Cylindromatosis
DAPI	4'-6-diamidino-2-phenylindole
DIABLO	Direct IAP binding factor with low pI
DMBA	7,12-dimethyl benz(*a*)anthracene
DNase	Deoxyribonuclease
E	Embryonic day
ECM	Extracellular matrix
EDTA	Ethylenediaminetetraacetic acid
EGFP	Enhanced green fluorescent protein
EGF	Epidermal growth factor
EGFR	Epidermal growth factor receptor
EMSA	Electrophoretic mobility shift assay
ER	Estrogen receptor
ErbB2	v-erb-b2 erythroblastic leukemia viral oncogene homolog 2
ERC1	ELKS/RAB-6-interacting/CAST family member 1
Erk	Extracellular signal related kinase
ESA	Epithelial specific antigen

FBS	Fetal bovine serum
FACS	Fluorescence activated cell sorting
FSC	Forward scatter
FVB/NJ	Female friend virus B NIH Jackson
GFP	Green fluorescent protein
Grb2	Growth factor receptor bound protein 2
Ha-Ras	Harvey retrovirus-associated DNA sequences
HBSS	Hank's balanced salt solution
HER2	Human epidermal growth factor receptor 2
HF	Hank's balanced salt solution with 2% FBS
HFE	Hank's balanced salt solution with 2% FBS and 2 mmol/L EDTA
HGF	Hepatocyte growth factor
HRG	Heregulin
HSA	Heat stable antigen
IAP	Inhibitor of apoptosis
IBC	Inflammatory breast cancer
ICAD	Inhibitor of caspase activated deoxyribonuclease
IHC	Immunohistochemistry
IκB	Inhibitor of NF-κB
$I\kappa B^{SR}$	Inhibitor of NF-κB super repressor
IKK	Inhibitor of NF-κB (IκB) kinase
IKKAP1	IKK associated protein 1
JNK	c-Jun NH2-terminal kinase
Kip	Kinase inhibitor protein
Lin-	Lineage negative
LTβR	Lymphotoxin beta receptor
LZ	Leucine zipper
Ma-CFC	Mammary colony forming cell
MAPK	Mitogen activated protein kinase
MaSC	Mammary stem cell
MEK	MAP-Erk kinase
MMTV	Mouse mammary tumour virus
MPA	Medroxyprogesterone acetate
MRU	Mammary repopulating units
Myc	v-myc myelocytomatosis viral oncogene homolog
NEMO	NF-κB essential modulator
NF-κB	Nuclear factor kappa-light chain enhancer of activated B cells
NIK	NF-κB inducing kinase
OCT	Optimal cutting temperature
OHRI	Ottawa Hospital Research Institute
PBS	Phosphate buffered saline
PE	Phycoerythrin

PECAM-1	Platelet endothelial cell adhesion molecule 1
PEST	Proline (P), glutamic acid (E), serine (S), threonine (T)
PFA	Paraformaldehyde
pI	Isoelectric point
PI3K	Phosphatidylinositol 3-kinase
PR	Progesterone receptor
RAB	Ras-related in the brain
RING	Really interesting new gene
Rip1	Receptor interacting protein 1
rh bFGF	Recombinant human basic fibroblast growth factor
RHD	Rel-homology domain
RNS	Reactive nitrogen species
ROS	Reactive oxygen species
RTK	Receptor tyrosine kinase
SAPK	Stress activated protein kinase
Sca-1	Stem cell antigen 1
SH2	Sarcoma-homology domain 2
Skp1	S-phase kinase associated protein 1
SMAC	Second mitochondrial derived activator of caspases
Sos	Son of Sevenless
Src	Sarcoma
SSC	Side scatter
Tac-1	Tachykinin precursor 1
Tak-1	Transforming growth factor beta-activated kinase 1
TAM	Tumour-associated macrophage
TAD	Transactivation domain
TEB	Terminal end bud
TGF-β	Transforming growth factor beta
TIC	Tumour initiating cell
TNFα	Tumour necrosis factor alpha
TNFR	Tumour necrosis factor receptor
TRADD	TNFR-associated death domain
TRAF	Tumour necrosis factor receptor associated factor
TUNEL	Terminal deoxynucleotidyl transferase dUTP nick end labeling
TWEAK	TNF-like wear inducer of apoptosis
XIAP	X-linked inhibitor of apoptosis

LIST OF FIGURES

CHAPTER ONE

INTRODUCTION

1.1 Mouse mammary gland development

The mammary glands are the organs that, in mammals, are responsible for producing nutrients in the form of milk in order to sustain offspring after birth (McClellan *et al.*, 2008). Mammary gland development is a strictly controlled process that relies heavily on hormonal cues from the surrounding cellular environment. Most of the development occurs postnatally, when the gland undergoes a complex cascade of invasive growth, branching, differentiation, secretion, apoptosis and remodeling during each pregnancy, or to a lesser extent estrous cycle (Richert *et al.*, 2000). Irregularities occurring during these events may result in tumourigenesis. Worldwide, breast cancer is the second most common type of cancer, and the fifth most common cause of cancer-related death (World Health Organization, 2009). In order to circumvent the ethical and economic issues involved with using humans in cancer studies, the mouse mammary gland is often used to study developmental events and the defects that could potentially lead to mammary tumour development.

1.1.1 The mouse mammary gland

The mouse mammary gland develops via a small number of ectodermally derived cells that generate a series of ducts terminating in lobules embedded in stromal tissue (Molyneux *et al*, 2007; Shackleton *et al.*, 2006; Stingl *et al.*, 2006). It is a continually changing, complex tissue consisting of parenchymal structures that invade the mammary fat pad. The mammary fat pad is located under the exterior nipples, which connect to the primary epithelial duct (Silberstein and Daniel, 1987). The fully developed mammary gland is made up of an inner layer of luminal cells that form the epithelial duct, and an

outer layer of contractile myoepithelial/basal cells (see below). The epithelial ductal structures allow for milk release during lactation. In the mouse, there are five pairs of fat pads which begin at the thoracic region of the underside of the mouse where there are three pairs, and extend to the inguinal region, where the remaining fat pads are located (Ward and Parsoneault, 2006). This area is known as the milk or mammary line (Bolander, 1990; Richert *et al.*, 2000).

Before birth, the mammary fat pad is invaded by rudimentary ductal structures; all development essentially halts until puberty at 3 weeks of age (Richert *et al.*, 2000). At puberty, terminal end buds (TEBs) first appear and begin ductal elongation up until 10-12 weeks, when they reach the end of the fat pad and regress (Richert *et al.*, 2000). Hormones produced during the estrous cycle cause gland branching to form alveolar buds (Richert *et al.*, 2000). Full differentiation of the alveolar buds occurs during pregnancy, when they are capable of milk secretion (Richert *et al.*, 2000). Following weaning, the mammary gland remodels through apoptosis, and regresses during a process called involution (Richert *et al.*, 2000). The mammary gland undergoes the process of lactation and involution during each pregnancy. For a more complete description of development, see below.

1.1.2 Embryonic development

The mouse mammary gland begins embryonic development as an epithelial bud, which penetrates the underlying mesenchyme at embryonic day (E) 10-11. By E14, the epithelial bud becomes bulb-shaped and elongates to form an embryonic sprout by E16, which invades the precursor mammary fat pad tissue (Sakakura *et al.*, 1987). In the male

mouse, development is identical to the female up until E13, when the testes begin androgen production; androgens decrease the volume of the primitive mammary gland and halt its development. At birth (E19.5), the mammary gland parenchyma has formed into a rudimentary mammary tree consisting of several branching ducts (Topper and Freeman, 1980). Each branch is composed of a single layer of epithelial cells that surround a lumen; these cells are referred to as luminal cells. Mammary luminal epithelial cells are identified by the presence of keratins 8, 11, 14, 20 and 22 (Asch and Asch, 1985). A myoepithelial cell layer is located beneath the epithelial cells, forming a basal cell layer resting on the basement membrane, separating the parenchyma from the stroma (Richert *et al.*, 2000). Myoepithelial cells at this stage stain positively for smooth muscle actin (Radice *et al.*, 1997). These cells are the contractile cell layer responsible for moving milk down the ductal structures during lactation; they are also responsible for the secretion of basement membrane components during all developmental stages (Richardson, 1949; Richert *et al.*, 2000).

1.1.3 Pubertal development

A period of rapid growth occurs at 3-6 weeks, the time period known as the pubertal development stage (Richert *et al.*, 2000). During this time, the mammary ducts lengthen and branch out, forming secondary and tertiary mammary structures that fully occupy the mammary fat pad by 3 months of age (Silberstein and Daniel, 1987). During the beginning of the ductal mammary growth period, the primary mammary epithelial structure is known as the TEB (Silberstein and Daniel, 1987). TEB structures are located at the ends of growing mammary ducts and are made up of multiple layers of epithelial

cells, with a layer of undifferentiated stem cells called cap cells on the outside (Richert *et al.*, 2000; Williams and Daniel, 1983). The ductal myoepithelial cells are eventually derived from the highly proliferative cap cells; cap cells also migrate into the epithelial cell layer to become luminal epithelial cells (Russo and Russo, 1996; Silberstein and Daniel, 1987). Proliferation and migration of the TEB cells results in an invasion of the mammary fat pad, and elongation of the duct. TEBs regress to form terminal ducts that become encased in basement membrane and stroma as they reach the edge of the fat pad (Richert *et al.*, 2000). At 10-12 weeks of age, most of the TEBs have regressed (Humphreys *et al.*, 1996).

Mammary lateral and alveolar bud development is initiated in response to the cycling ovarian hormones in a post-pubertal mouse (Andres and Strange, 1999). Lateral buds either form branches, or cleave to form alveolar buds (Richert *et al.*, 2000). Those that form branches have a layer of cap cells, and as branching occurs, connective tissue is degraded to allow for epithelial structure growth (Silberstein and Daniel, 1987). Alveolar buds form rudimentary alveolar structures composed of a single layer of epithelial cells with a hollow center. These alveolar buds progress into fully functional milk-secreting units during the highly proliferative stage associated with pregnancy (Robinson *et al.*, 1995). Once female mice have ceased lactation, the majority of the mammary epithelium undergoes apoptosis in a process called involution, after which the epithelium remains quiescent until the next pregnancy (Furth, 1999). The process of rapid proliferation, milk secretion and involution occurs with each pregnancy; proliferation and involution also occurs to a lesser extent with each estrous cycle (Brantley *et al.*, 2001).

1.2 Mouse mammary cell populations

1.2.1 The mouse mammary stem cell

It has been long established that the mammary gland consists of two lineages of epithelial cells, the inner luminal cell layer and the outer layer of myoepithelial cells. It has been recently postulated, however, that the mammary epithelium is arranged in a cellular hierarchy ranging from mammary stem cells to terminally differentiated cells (Stingl, 2009). Mammary stem cells (MaSCs) have been defined by their ability to generate both ductal and lobular mammary gland components, and to self-renew. MaSCs give rise to progenitor or transit amplifying cells, cells in the mammary gland that have proliferative potential (Shackleton *et al.*, 2006). Mammary stem and progenitor cells are of interest in the cancer field as it is thought that these cells may become the target for transformation into cells with malignant properties and tumourigenic potential.

1.2.2 Identification of mouse mammary stem cells

Many unique properties of mouse mammary gland development can be exploited in ways to increase understanding of mammary gland development in humans (Stingl, 2009). The ability to uniquely identify mammary stem cells is made easier in the mouse because the mouse mammary gland develops primarily postnatally (Richert *et al.*, 2000). This phenomenon has allowed for the study of mammary stem cells; early mammary structures can be efficiently removed in young mice, resulting in a mammary fat pad cleared of epithelial cells (Deome *et al.*, 1959). The cleared fat pad can then be used to transplant donor-derived mouse mammary tissue. Transplantation studies have shown that small mammary gland fragments transplanted into cleared fat pads can develop into

fully functional mammary glands, support for the presence of a stem cell-like population in the mammary gland (Daniel *et al.*, 1968). Transplant experiments have also demonstrated the existence of ductal and alveolar-restricted progenitor cells that are not necessarily primitive stem cells (Smith, 1996).

1.2.3 Experimental techniques to identify mammary stem cells

Many experimental techniques have been established to detect mouse MaSCs. The technique that has proven to be the most successful involves the removal of mammary glands from donor mice, their subsequent enzymatic and mechanical dissociation into a single-cell suspension, followed by transplantation into recipient weanling mice with cleared mammary fat pads (Stingl, 2009). These transplant experiments have demonstrated the existence of subset of mammary cells that are capable of regenerating new mammary tissue; these cells are known as mammary repopulating units (MRUs) (Stingl *et al.*, 2006). Interestingly, it has been shown using mammary glands from Rosa-26-mice that a single MRU has the multi-lineage differentiation and proliferative capacity to reconstitute a completely functional mammary gland (Shackleton *et al.*, 2006). In this study, single MRUs from Rosa-26 that carry a ubiquitously expressed *LacZ* transgene were transplanted into wild-type mice, and *LacZ* positive outgrowths were detected by staining for *LacZ* (β-galactosidase) activity by X-gal, or by PCR for *LacZ.* Rosa-26 mice were developed with random insertion of the retroviral gene-trap vector ROSA, or Reverse Orientation with Splice Acceptor, which contains the β-galactosidase gene; these mice ubiquitously express β-galactosidase in all tissues in the developing embryo and most tissues in the adult. *LacZ* positive outgrowths were

comprised of normal ductal structures with both luminal and myoepithelial cells; in pregnant recipients, outgrowths were capable of milk production and complete functional differentiation following birth. MRUs give rise to another progenitor-like cell, a mammary colony-forming cell (Ma-CFC) (Shackleton *et al.*, 2006; Stingl *et al.*, 2006). Ma-CFCs can be detected by an *in vitro* Ma-CFC assay, which involves dissociating mammary cells, and seeding them at low density onto a layer of irradiated fibroblasts (Shackleton *et al.*, 2006; Smalley, Titley and O'Hare, 1998; Stingl *et al.*, 1998). Alternatively, mammary epithelial cells can be grown in conditions that are similar to those encountered physiologically (Stingl, 2009); dissociated mammary cells can be plated onto a semi-solid matrix of Matrigel or on collagen-coated culture dishes. Using either method, the cells that are capable of growth and small colony formation after 1-2 weeks are the Ma-CFCs (Stingl *et al.*, 2006).

1.2.4 Analysis of stem cell populations

Mouse MRUs are found throughout the mouse mammary gland, with the highest frequency occurring at the TEB of the developing gland, and the lowest frequency in the alveoli of lactating mice (Stingl, 2009). Dissociation of a single mammary gland from a young virgin female mouse generates approximately 1400 MRUs and 30,000 Ma-CFCs (Stingl *et al.*, 2006; Figure 1). MRUs and Ma-CFCs can be distinguished from each other using a number of cellular markers, including cell differentiation marker (CD) 24, CD29, CD49f, CD14, CD61 and stem cell antigen 1 (Sca-1) (Shackleton *et al.*, 2006; Stingl *et al.*, 2006). Fluorescent activated cell sorting (FACS) analysis by flow cytometry (Appendix) sorting of lineage negative cells (hematopoietic (CD45+Ter119+) negative,

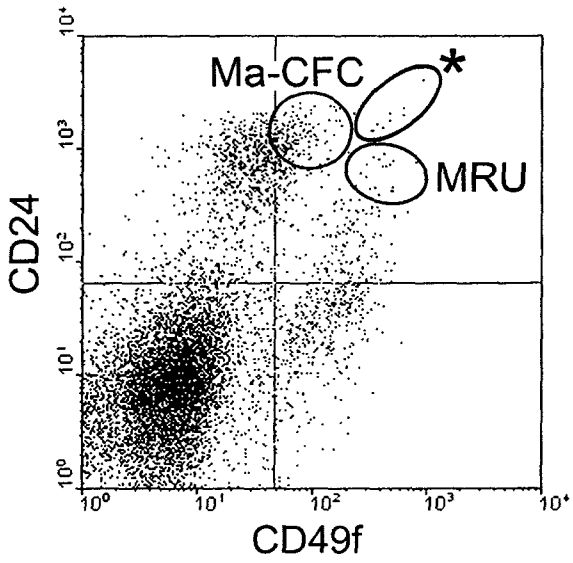
Ma-CFC
*
MRU
CD24
CD49f
10⁰
10¹
10²
10³
10⁴

Figure 1. Flow cytometric analysis of mouse mammary stem cells. Distribution of lineage negative stem cell according to the expression status of CD24 and CD49f. Mammary repopulating units (MRUs) are $CD24^{med}CD49f^{high}$ and have basal stem cell properties, whereas mammary colony forming cells (Ma-CFCs) are $CD24^{high}CD49f^{low}$ and exhibit luminal stem cell properties. Some mice exhibit small numbers of $CD24^{high}CD49f^{high}$ cells (indicated * in the dot plot), which may contain some stem cells. Used by permission from Macmillan Publishers Ltd: Nature, Stingl *et al.*, copyright 2009 (License Number 2284881111969, Appendix A.7).

endothelial (CD31+) negative) and subsequent transplantation into cleared fat pads has shown that these cell types differentially express CD49f and CD24: MRUs are characterized by $CD24^{med}CD49f^{high}$ expression, and Ma-CFCs by $CD24^{high}CD49f^{low}$ expression (Stingl *et al.*, 2006) (Figure 1). CD24 (also known as heat stable antigen, HSA) is an early cell adhesion protein that has been shown to modulate B cell receptor responses and is typically absent when cells reach differentiation (Kay *et al.*, 1991). CD49f is a cell surface antigen known to associate with either integrin β_1 (CD29) or integrin β_4 (CD104) to form receptors for laminin and kalinin, and is expressed on platelets, monocytes, T cells, placental trophoblasts, epithelial and endothelial cells. It is also involved in adhesion and can act as a co-stimulatory molecule for T cell activation and proliferation (Sonnenberg *et al.*, 1990).

Analysis of mammary stem cell populations by flow cytometry using the cell surface markers CD49f and CD24 has lead to a method whereby the MRU and Ma-CFC populations can be separated from the mammary gland for further analysis. A more differentiated myoepithelial cell population can also be sorted using this technique; these cells are present in the $CD24^{low}CD49f^{low}$ cellular fraction (Stingl *et al.*, 2006). The MRU fraction highly expresses the basal/myoepithelial markers keratin 5 and 14, smooth muscle myosin, vimentin and laminin, whereas the Ma-CFC fraction contains high expression levels for keratin 8, 18 and 19, and a variety of casein transcripts typical of luminal cells (Shackleton *et al.*, 2006; Sleeman *et al.*, 2006; Stingl *et al.*, 2006). These two cell types are most likely the progenitors for the differentiated basal and luminal cell layers present in a fully developed mammary gland (Stingl, 2009).

1.3 Models of cancer progression

1.3.1 The classical cancer model

The study of stem and progenitor cells within a given tissue is of great interest from a cancer research perspective as it has been recently suggested that these cells are initial targets for oncogenic transformation. The classical cancer model postulates a multi-hit process whereby normal cells acquire tumourigenic potential via a series of successive genetic mutations that upregulate growth and inhibit cell death, termed multi-step tumourigenesis (Figure 2A) (Moulder, 1998; Weinberg, 2007). This model states that all tumour cells are capable of forming new tumours and have high proliferative potential, and that cancer is therefore a proliferative disease (Tan *et al.*, 2006). Tumour progression in this model is driven by a random sequence of mutations and genetic alterations that affect genes involved in cellular proliferation, and survival. This process has been documented in a variety of human tissues, including the intestinal epithelia (Weinberg, 2007). The intestine is an easy system to use to study tumour progression since it is the most rapidly renewing epithelial cell layer in the body and is fairly accessible. In the intestine, epithelial cell populations are in a constant state of proliferation and renewal, and are the site of the pathological changes associated with colon carcinoma development (Grady and Markowitz, 2002; Weinberg, 2007). The multi-step progression towards the tumourigenic state in the colon has been documented histologically and genetically. This model, however, is over simplistic, as many genetic and environmental factors complicate the tumourigenic evolution (Weinberg, 2007).

A

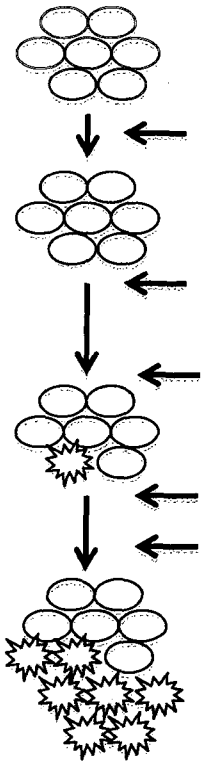

Normal cell population

Genotoxic injury from exposure to genotoxic agents or from random errors in DNA replication

Some normal cells are converted to pre-cancerous cells

Genotoxic injury (or injuries) from exposure to genotoxic agents or from random errors in DNA replication

Exposure to epigenetic influences

A pre-cancerous cell is converted to a cancer cell

Time

Exposure to epigenetic influences

A cancer develops from the cancer cell

B

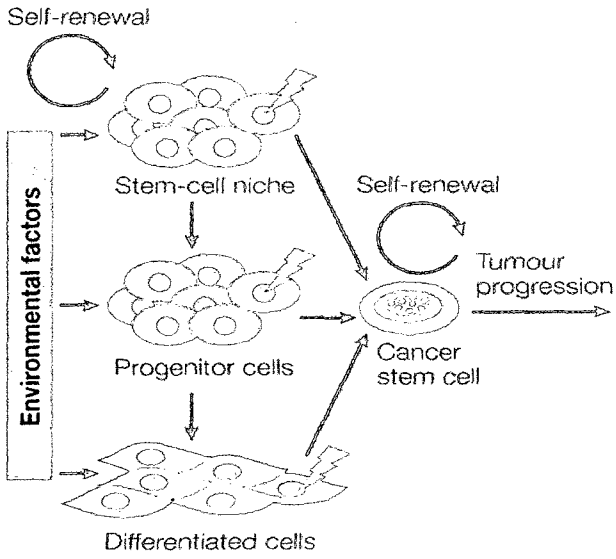

Figure 2. Proposed models of tumourigenesis. **A**, Classical multi-step tumourigenic model. Adapted from Moulder, 1998. **B**, Cancer stem cell hypothesis. Mutations in stem cells and or progenitor cells might give rise to cancer stem cells. Reprinted by permission from Macmillan Publishers Ltd: Nature Reviews Cancer, Bjerkvig *et al.*, copyright 2005 (License Number 2284911341687, Appendix A.7).

1.3.2 Downfalls to multi-step tumourigenesis

In experimental studies, tumours have only been able to form after a large number of tumour cells have been injected into nude (immunocompromised) mice, suggesting that only a small number of cells within the tumour cell population are capable of initiating new tumour growth (Dick, 2003). If every cell in the tumour were capable of initiating growth, injection of only a small number of cells would lead to tumour growth following injection into a nude mouse. There is growing evidence that tumours are initiated from a relatively small population of cells with properties similar to those of normal stem cell or progenitor cells (Liu *et al.*, 2007). FACS analysis of cancer cell populations by flow cytometry has shown the existence of a subset of tumourigenic stem cell-like cells in many cancer types. In acute myelogenous leukemia (AML), FACS analysis has identified a minority of cells with tumourigenic potential (Huntly and Gilliland, 2004). Similar results have been achieved using human breast cancer cells and brain tumour cells; FACS analysis has shown that approximately 2% of tumour cells have tumourigenic potential (Al-Hajj *et al.*, 2003). These experimental outcomes have caused many researchers to reconsider how multi-step tumour progression occurs; a linear path of tumourigenesis oversimplifies the reality of cancer progression (Weinberg, 2007).

1.3.3 The cancer stem cell hypothesis

The evidence suggesting that cancer progression is initiated by a subset of tumourigenic cells with stem cell like properties, or cancer stem cells (CSCs), has lead to the development of a new model of multi-step tumour progression. This new model, the

"cancer stem cell hypothesis" states that the upregulated cell growth needed to produce an evident tumour is due to a disruption in the mechanism of stem cell renewal (Figure 2B) (Bjerkvig *et al.*, 2005; Weinberg, 2007). Thus, CSCs/tumour-initiating cells (TICs) are defined by stem cell-like properties, including the ability to divide indefinitely, producing more TICs (self-renewal) and progeny that eventually make up the bulk of the tumour (Dick, 2003; Liu *et al.*, 2007). The term TIC is often preferred over CSC, as the as the cells that may lead to tumour development are not necessarily normal stem cells gone awry, but are transit amplifying cells or differentiated cells that have acquired stem-cell like properties (Weinberg, 2007). Stem and progenitor cells have the capacity to generate the large numbers of progeny needed to increase the probability that genetic mutations could lead to malignancy.

1.3.4 Cancer stem cells/tumour-initiating cells

TICs can differentiate into transit-amplifying cells, a subset of relatively undifferentiated cells that are generated by stem cell division, and are capable of exponential proliferation for a limited number of cell generations before leading to differentiated progeny (Pardal *et al.*, 2003; Weinberg, 2007). TICs represent only a small number of neoplastic cells in tumour masses, while transit-amplifying cells represent the majority of neoplastic tumour cells (Weinberg, 2007). Thus, mutations that strike the genomes of TICs can be transmitted to descendent tumour stem cells, and to transit-amplifying cells leading to an increase in genetic change. As tumour progression continues, tumour genomes often become increasingly unstable; mutation rates in stem

and progenitor cells may become elevated, increasing the number of distinct cell populations that arise from them within a tumour (Marx, 2003).

1.3.5 Identification of tumour-initiating cells

Identification of TICs in some tumour types has been successful based on expression of cell surface markers. In human breast cancer, TICs have been shown to express the early epithelial marker epithelial specific antigen (ESA) and the cell surface marker CD44, while non-tumourigenic cells express CD24 (Al-Hajj *et al.*, 2003). CD44 is a receptor for hyaluronic acid, a chief component of the extracellular matrix (ECM). It is involved in adhesion of leukocytes to endothelial cells, stromal cells, and the ECM, and has been implicated in tumour cell metastasis (Yasuda *et al.*, 2002). In other types of cancers, including small cell lung cancer and squamous cell carcinoma of the neck, CD24 is involved in cell adhesion, invasion, and metastasis tumourigenesis.

1.3.6 Tumour initiating cells and current cancer treatments

Breast cancers arise from the epithelial mammary cells and are highly heterogeneous. Classification of various breast cancer subtypes has been difficult due to this heterogeneity; however, our current understanding of mammary tumourigenesis has placed breast tumours in two general subgroups: luminal tumours and basal-like tumours based on estrogen receptor (ER) status; breast cancer can be further classified based on molecular data: luminal-like, which includes luminal A, B and C, basal-like, normal-like and ErbB2 positive (Kaklamani and Gradishar, 2006; Sotirou and Pusztai, 2009). Luminal A type breast cancers have high expression of the ER alpha (ERα) gene cluster,

and have low mutation levels of the tumour suppressor, p53. Luminal B type breast cancer have low to moderate expression of the ERα gene cluster, while luminal C breast cancer is similar to luminal B, but also expresses genes associated with basal and ErbB2 positive breast cancer (Sims *et al.*, 2007, Kaklamani and Gradishar, 2006; Sotirou and Pusztai, 2009). Basal-like tumours express cytokeratins 5, 14 and 17, but do not express ER, PR, and elevated HER2/ErbB2, and are thus referred to as triple negative. These tumours also have elevated p53 mutation levels (Korsching *et al.*, 2008; Kaklamani and Gradishar, 2006; Sotirou and Pusztai, 2009). Normal-like breast cancers express many genes known to be expressed by adipose tissue and other non-epithelial cells, and also have high basal gene expression and low luminal gene expression. Finally, ErbB2 positive breast cancer exhibits elevated levels of ErbB2 expression and may also exhibit high levels of p53 mutation (Kaklamani and Gradishar, 2006; Sotirou and Pusztai, 2009). In humans, primitive stem cells are generally ER negative, and give rise to ER-positive progenitors, suggesting that basal-like tumours arise from a subset of ER negative, and luminal tumours arise from the transformation of ER positive cells (Clarke, *et al.*, 2005; Sims *et al.*, 2007). Both ER negative and ER positive stem cells are relatively quiescent, posing a problem for current cancer targeting treatments. Traditional cancer treatments target highly proliferating cells and mammary stem cells are not highly proliferative; if progenitors of mammary stem cells give rise to TICs, they could "escape" conventional treatment. Residual TICs that are not eradicated following treatment could re-initiate tumour growth after cancer regression, and could be the cause relapse seen in a subset of breast and other cancer cases following apparently successful treatment (Behbod and Rosen, 2005).

1.3.7 CD44 and cancer

Recently, using double-staining immunohistochemistry to quantify CD44 and CD24 expression in characterized human breast tumours, a research group has found that the CD44+/CD24- phenotype was most often seen in a basal-like subgroup of breast tumours (Honeth *et al.*, 2008). This subgroup was characterized as being human epidermal growth factor receptor 2 (HER2)/v-erb-b2 erythroblastic leukemia viral oncogene homolog 2 (ErbB2) negative, and positive for cytokeratin 5/14 (Honeth *et al.*, 2008). In this study, it was also reported that 95% of BRCA1 tumours (basal-like), a subset of familial breast cancers with a germline mutation in BRCA1, exhibited the CD44+/CD24- phenotype. BRCA1 has an essential role in a number of biological functions including DNA damage repair, cell cycle checkpoint regulation, transcriptional activation and repression, and mammary tumour formation (Liu and West, 2002). Human epidermal growth factor receptor (HER2)/ErbB2 positive tumours, however, were more often CD44-/CD24+ (Honeth *et al.*, 2008). Thus, tumourigenic potential may not be attributed only to the CD44+/CD24- cellular subtype, and that other breast cancer cell markers need to be identified. Nevertheless, these markers (CD44+/CD24-) are still being used to positively identify breast cancer tumour-initiating cells. The differential expression of surface markers in breast cancer, and other cancers, has allowed for purification of TICs from the bulk tumour via FACS analysis (Liu *et al.*, 2007; Tan *et al.*, 2006). Characterization of normal stem cell populations in the mammary gland, including an understanding of which signaling pathways are active in each cell type, may lead to the characterization of a definitive breast cancer stem cell.

1.4 Mouse models of mammary cancer

1.4.1 Early mouse models

The mouse has been used as a model to provide a general understanding the progression of human breast cancer progresses for the past 75 years. Studies using inbred mouse strains provided researchers with the knowledge that specific genetic, hormonal or environmental factors, like chemical carcinogens, or the mouse mammary tumour virus (MMTV) increase susceptibility to developing certain cancer, including breast cancers (Allred and Medina, 2008; Medina, 2000). It was noted that both chemical carcinogens and MMTV induce pre-malignant lesions that can progress to malignant cancers, and specific genes become active, or mutations occur after exposure to either of these factors ((Deome *et al.*, 1959; Medina, 2000). Nude mice in which human cancer cell lines have been transplanted were a favourite model used in past cancer research as well (Medina, 2000).

1.4.2 Transgenic mouse models

With the understanding that specific gene mutations, gene activations or overexpression can lead to breast cancer progression, transgenic mouse models were generated based on a specific overexpression of oncogenes targeted to the mammary gland, or germline deletion of tumour suppressor genes (Allred and Medina, 2008). Transgenic models allow for the evaluation of the signal transduction pathways often involved in human breast cancer, the pathobiology of many cancer types, and the evaluation of the efficacy chemotherapeutic drugs. However, transgenic mouse models do have some limitations. It is difficult to control the extent of gene expression in an

overexpression study as multiple gene copies may be inserted throughout the mouse genome. Also, non-targeted or unconditional deletion of tumour suppressor genes may prove to be embryonic lethal; this has lead to the development of conditional mouse models of cancer tumourigenesis, allowing for the targeted activation or deletion of specific genes during any stage of development (Allred and Medina, 2008). The information that has been gained using mouse models has lead to a better understanding of the multitude of pathways that can be disrupted during tumourigenic progression.

1.4.3 Common models of breast cancer

In a mouse, mammary tumourigenesis can be induced in many ways. Two common methods of cancer induction are the subcutaneous implantation of a slow release medroxyprogesterone acetate (MPA) pellet followed by gavage with a chemical carcinogen like 7,12-dimethyl benz(*a*)anthracene (DMBA) or by the mammary specific overexpression of the ErbB2 oncogene (driven by the MMTV promoter) (Thompson, 2000). MPA generates a proliferative response in the mammary gland compartment, increasing the number of target cells at risk for mutation by DMBA, thus accelerating development and increasing latency of mammary tumours. Using this protocol to induce mammary tumours, MPA acts as a tumour promoter, while DMBA acts as an initiator, with a mean tumour growth latency of 99 ± 51 days (Aldaz *et al.*, 1996).

1.4.4. Chemical carcinogenesis

The induction of mouse mammary tumourigenesis using a chemical carcinogen like DMBA is based on the knowledge that chemical exposure can induce cancer in

humans through a variety of mechanisms, the most prominent being inflammation (Ohshima *et al.*, 2003). The first documented cases of chemically induced tumourigenesis date back to the late 18th century where it was noted that young male chimney sweeps often succumbed to a painful and fatal disease originating in their reproductive organs at puberty (Miller, 1978). In the more recent years, it is estimated that approximately 20% of the total documented cancers arise from an inflammatory response to infectious agents, including chemicals (Ohshima *et al.*, 2003).

Chemical exposure can induce an inflammatory response, which can, upon prolonged activation, cause DNA and tissue damage through the production of reactive oxygen and nitrogen species (ROS and RNS) (Figure 3) (Ohshima *et al.*, 2003; Waris and Ahsan, 2006). The ROS and RNS produced during an inflammatory response are capable of causing cellular damage in a number of ways. These species are capable of inducing direct DNA base modifications through oxidative damage; inflammatory oxidants react with reduced transition medals that are either free or DNA bound to generate highly toxic radicals or metal complexes that result in more than 30 different DNA and RNA base modifications (Dizdaroglu, 1994). These modifications can lead to the formation of single or double-strand DNA breaks, point and frame shift mutations, and chromosomal abnormalities that can increase the risk of cellular transformation (Christen *et al.*, 1999). ROS and RNS are also capable of inducing alterations in protein structure and function that can also contribute to carcinogenesis. Studies have shown that elevated levels of modified proteins are present in inflamed tissues, such as in patients with gastritis or lung cancer (Pignatelli *et al.*, 2001a; Pignatelli *et al.*, 2001b). Mammalian cells incubated with excess ROS accumulate the tumour suppressor p53;

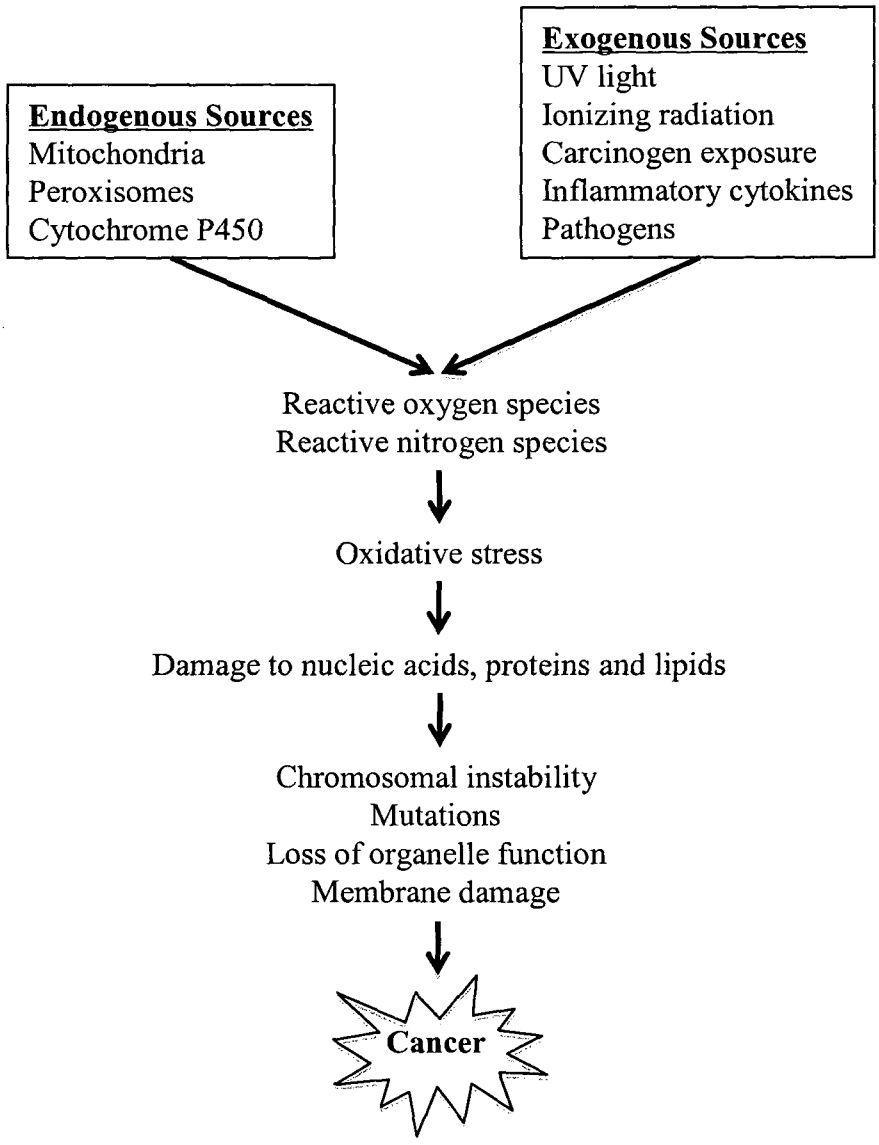
Endogenous Sources
Mitochondria
Peroxisomes
Cytochrome P450
Exogenous Sources
UV light
Ionizing radiation
Carcinogen exposure
Inflammatory cytokines
Pathogens
Reactive oxygen species
Reactive nitrogen species
Oxidative stress
Damage to nucleic acids, proteins and lipids
Chromosomal instability
Mutations
Loss of organelle function
Membrane damage
Cancer

Figure 3. Reactive oxygen species and cancer development. Pathways illustrating the sources of reactive oxygen species and its role in the development of cancer. In the mitochondria, ROS are produced as a normal byproduct of metabolism and the electron transport chain. Peroxisomes contribute to the production of ROS through their roe in the production and scavenging of hydrogen peroxide. Cytochrome P450 enzymes generate ROS through catalyzing the oxidation of a number of organic substances. Adapted from Waris and Ahsan, 2006.

however, in the presence of elevated ROS, p53 becomes modified by the ROS via inactivation leading to loss of p53 DNA binding capacity and its tumour suppressive ability (Calmels *et al.*, 1997; Cobbs *et al.*, 2001). Inactivation of p53 through mutations occurs in half of human cancers (Olivier *et al.*, 2002). Inflammation facilitates the malignant progression and transformation needed to induce tumour growth (Ohshima *et al.*, 2003). The various cytokines secreted by the immune system can trigger expression of various receptors on the tumour cells themselves, which can aid the growth of the tumour cells.

1.4.5 The ErbB2 transgenic model

Approximately 30% of human cancers originating in breast tissue involve an amplification or overexpression of the proto-oncogene ErbB2 (Her2/neu); its amplification and overexpression has also been detected in many other types of human cancer, including ovarian, lung, pancreactic, colonic, esophageal, prostate, endometrial and cervical cancers (Fajac *et al.*, 1995; Maurer *et al.*, 1998; Mosesson and Yarden, 2004; Osako *et al.*, 1998; Saffari *et al.*, 1995; Stephens *et al.*, 2004; Yu and Hung, 2000). Transgenic overexpression of wild-type ErbB2 in the mouse mammary epithelium under the control of MMTV induces focal mammary tumour formation in female mice at approximately 8 months of age (Muller *et al.*, 1996). The ErbB2 transgenic model allows researchers to study the effects of overexpression or knockout of other genes involved in mammary carcinoma on the ErbB2 background, since these mice will develop tumours without induction, and possess a phenotype similar to that seen in many human breast cancers.

The ErbB2 gene encodes a 185-kDa transmembrane glycoprotein that belongs to the subclass 1 of receptor tyrosine kinase (RTK) superfamily/epidermal growth factor receptor (EGFR) family, which includes three other ErbB receptors, ErbB1 (EGFR), ErbB3 and ErbB4 (Hynes and Lane, 2005). The EGFR family was the first growth factor receptor family identified in cancer cells (Carpenter *et al.*, 1975). In the mammary gland, ErbB2 expression and its subsequent overexpression in breast cancer has been localized to the luminal/Ma-CFC fraction of mammary cells. The ErbB receptors are implicated in the development of many cancer types, and may undergo various types of alterations, including gene amplification, and constitutive activation; many tumours are able to secrete factors that interact with the ErbB receptors (Salomon *et al.*, 1995). Overexpression of ErbB2 in cancer causes an activation of ErbB2 without the need for heterodimerization and ligand (see below). Patients with ErbB2 over-expressing tumours have a reduced overall survival rate, and also exhibit increased chance of relapse even if the primary tumour is initially successfully eradicated during treatment (Yu and Hung, 2000). The use of humanized monoclonal antibodies against the extracellular domain of ErbB2 in patients with metastatic breast cancer resistant to standard treatments has been shown to produce remission in 10-15% of cases (Eisenhauer, 2001).

1.4.6 ErbB2 signaling

EGFR family proteins are comprised of an (approximately) 1186 amino acid residue protein that is inserted into the cell membrane. The sequence identity of the EGFR family varies between the proteins and among domains, with the tyrosine kinase domains having the highest sequence identity, and the carboxy terminal domain the

lowest. It is important to note that ErbB3 is tyrosine kinase defective. The sequences of the EGFR family proteins can be characterized into a number of domains (Figure 4A and 4B) (Nair, 2005; Beselga and Swain, 2009). The extracellular portion is made up of four domains referred to as L1, CR1, L2 and CR2, with L referring to a "leucine rich" region and CR referring to a "cysteine rich" region (Burgess, 2008; Nair, 2005). ErbB2 functions in heterotrimeric complexes with other ErbB receptors, and is activated by ligands that include heregulins (HRGs), and those that bind the heterotrimeric complex, like growth factor. When the EGFR family proteins dimerize, the interaction exists between the CR1 regions of each receptor (Nair, 2005). None of the known EGFR ligands are capable of directly binding ErbB2 directly; in ErbB2, there exists a strong interaction between the L1 and L2 domains, rendering it incapable of ligand binding (Beselga and Swain, 2009). ErbB2 is characterized as an orphan receptor; however, ErbB2 is the preferred dimerization partner for all other ErbB receptors (Olayioye, 2001). The receptor is not capable of signaling until oligermization and ligation has occurred (Burgess, 2008). Heterodimerization following ligand binding leads to *trans* phosphorylation of carboxy-terminal tyrosine kinase residues in ErbB2 and its dimerization partner (Graus-Porta *et al.*, 1997).

EGFR tyrosine kinase activity plays an important role in many processes that affect tumour growth and progression, including proliferation, dedifferentiation, inhibition of apoptosis, cellular invasiveness and lack of adhesion dependence (Nair, 2005). The phosphorylated tyrosine kinases residues present in activated EGFR act as binding domains for proteins that activate many signaling pathways, including the mitogen-activated protein kinase (MAPK) pathway (the primary pathway), the nuclear

A

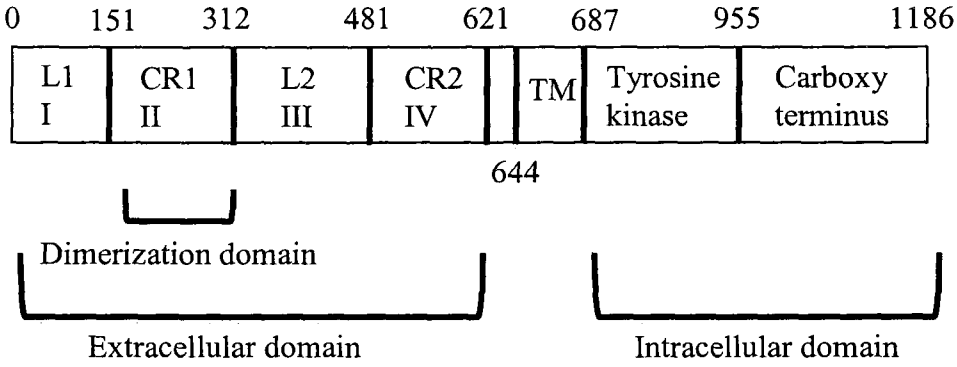
0
151
312
481
621
687
955
1186
L1
I
CR1
II
L2
III
CR2
IV
TM
Tyrosine kinase
Carboxy terminus
644
Dimerization domain
Extracellular domain
Intracellular domain

B

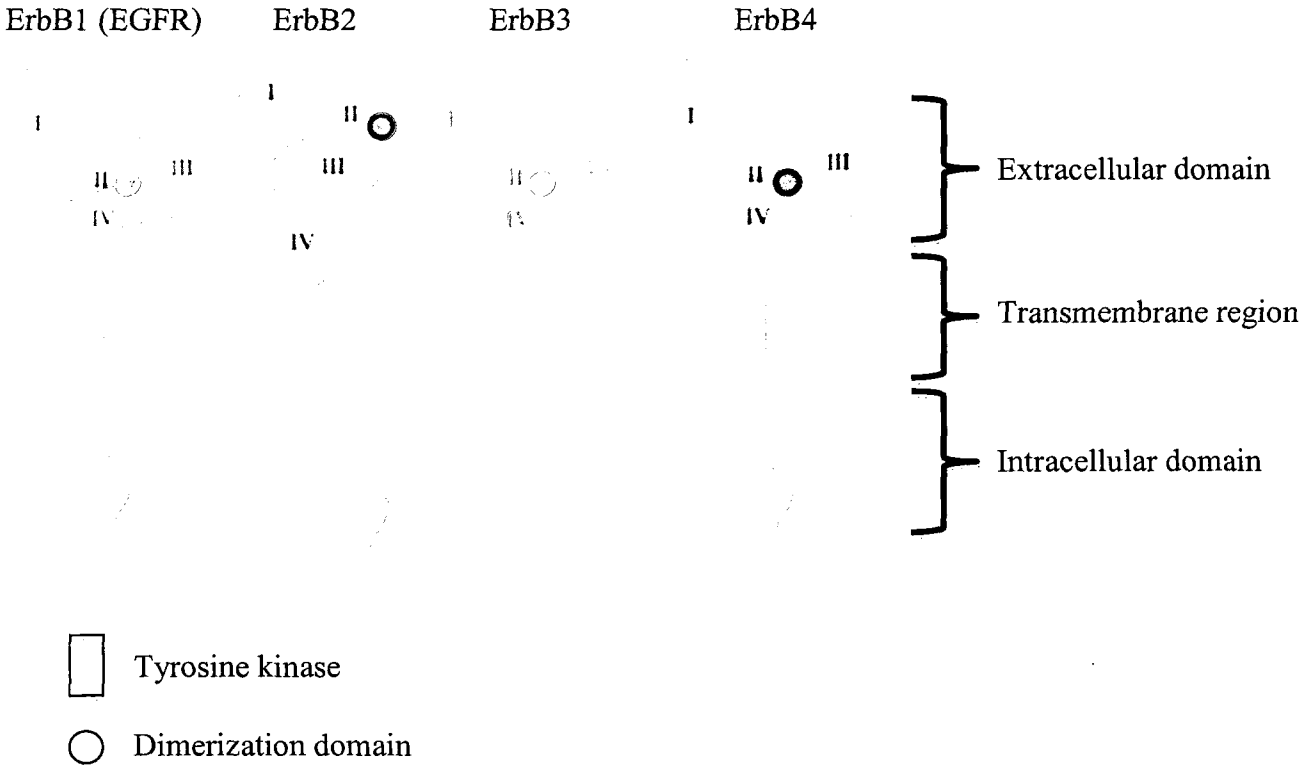
ErbB1 (EGFR)
ErbB2
ErbB3
ErbB4
I
II
III
IV
Extracellular domain
Transmembrane region
Intracellular domain
Tyrosine kinase
Dimerization domain

Figure 4. ErbB receptors. A, Distribution of the domains of the ErbB receptors. Sections 1-1V represent the extracellular domain, with section II being the dimerization domain that is responsible for interaction with other ErbB receptors. The intracellular domain consists of the tyrosine kinase domain and the carboxy terminus. L1, L2 – leucine rich region 1 and 2, CR1, CR2 – cysteine rich region 1 and 2, TM – transmembrane domain. The numbers show the amino acid position between the domains. **B**, There are four ErbB family members. Each has three functional domains: the extracellular ligand binding domain; the transmembrane domain; and the intracellular protein tyrosine kinase domain. ErbB2 has no known ligand and is always in the open position capable of dimerization. ErbB3 is missing a tyrosine kinase domain and just rely on other ErbB receptors for downstream signaling. Modified from Nair, 2005 and Baselga and Swain, 2009.

factor kappa-light-chain enhancer of activated B cells (NF-κB) pathway, and the phosphatidylinositol 3-kinase (PI3K)-V-akt murine thymoma viral oncogene homolog (Akt) pathway (Mosesson and Yarden, 2004) (Figure 5). P13K activation leads to expression of casein kinase 2 (CK2), which can phosphorylate an inhibitor of NF-κB (IκB) at serine residues in the proline (P), glutamic acid (E), serine (S), threonine (T) (PEST) domain (Figure 5) (Kato *et al.*, 2003). Activation of the MAPK signaling cascade can have a direct influence on cellular proliferation and migration. PI3K activity may result in inhibition of apoptosis in tumour cells. ErbB2-tyrosine kinase activity can also influence tumour angiogenesis by upregulation of VEGF and interleukin 8 (Nair, 2005). ErbB2 may work through activation of NF-κB inducing kinase (NIK), which preferentially activates the non-canonical NF-κB pathway (Chen *et al.*, 2003). NF-κB induction by ErbB2 has been shown in both breast cancer cell lines and in primary mouse tumours (Liu *et al.*, 2009).

In many cell lines, it has been shown that ligand-induced activation of ErbB2 leads to increased cellular proliferation (Beerli *et al.*, 1995). In cancer, the presence of ErbB2 enhances the ability of tumour cells to invade the extracellular matrix, allowing for cancer stem cell migration and metastasis (Spencer *et al.*, 2000). Thus, ErbB2 signaling can contribute to and increase cellular transformation capacity in a variety of ways.

1.5 NF-κB and breast cancer tumourigenesis

1.5.1 The NF-κB signaling pathway

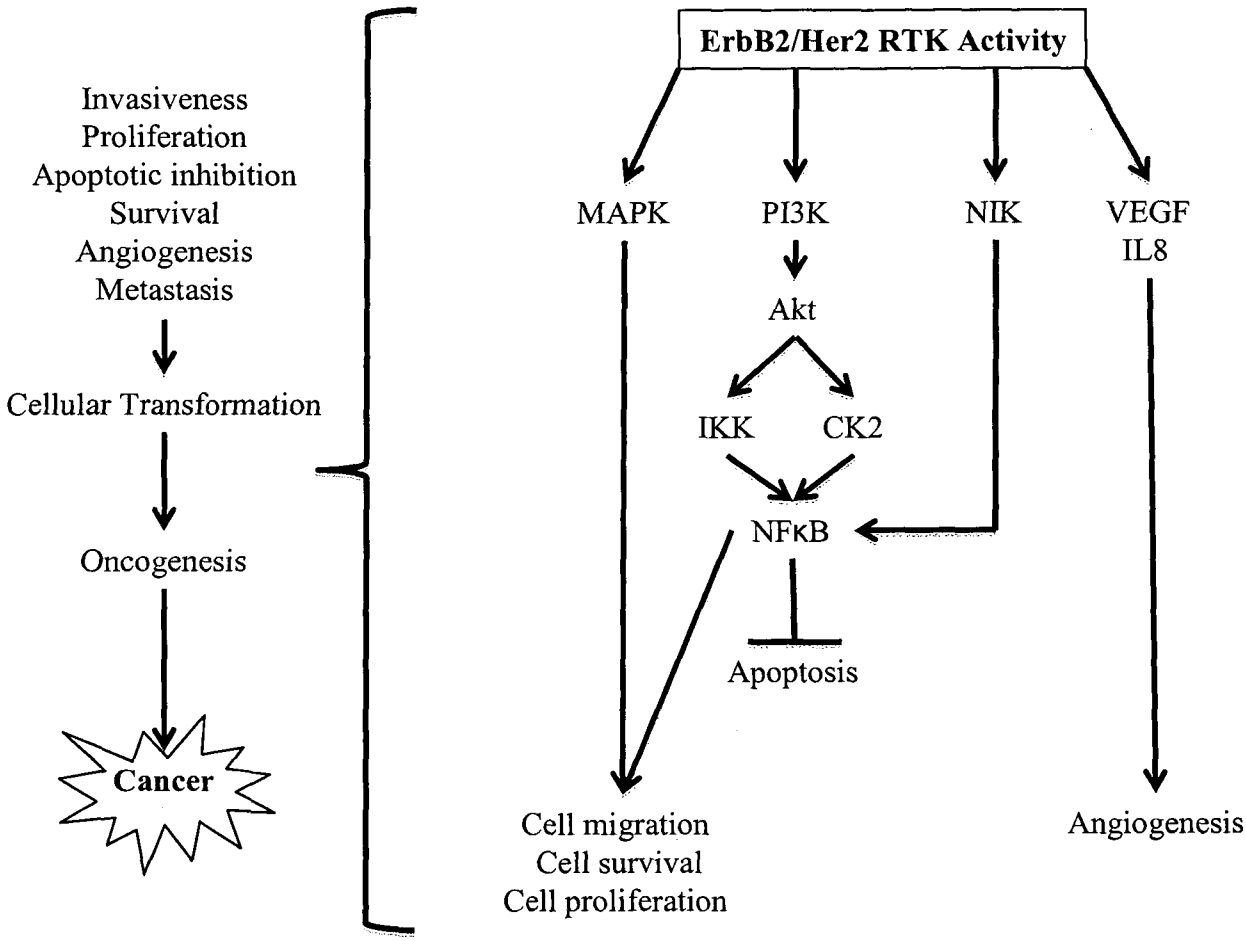
ErbB2/Her2 RTK Activity
MAPK
PI3K
NIK
VEGF
IL8
Akt
IKK
CK2
NFκB
Apoptosis
Cell migration
Cell survival
Cell proliferation
Angiogenesis
Invasiveness
Proliferation
Apoptotic inhibition
Survival
Angiogenesis
Metastasis
Cellular Transformation
Oncogenesis
Cancer

Figure 5. ErbB2 signaling. The activation of the ErbB2 (Her2/Neu) oncogene in cancer can lead to the initiation of signaling events that promote oncogenesis. Downstream signaling events may allow the cell to increase its invasiveness, proliferation, apoptotic evasion, survival, capacity to promote angiogenesis and the ability to metastasize. Adapted from Nair, 2005, Hynes and Lane, 2005 and Zhou *et al.*, 2000.

The NF-κB signaling pathway is often constitutively active during breast cancer tumour development, leading to the promotion of cellular survival, proliferation and uncontrolled growth. It is also an essential pathway needed for proper mammary gland development. NF-κB was first discovered in the lab of Nobel Prize Laureate David Baltimore through interaction with immunoglobulin κ enhancer sequences using electrophoretic mobility shift assays (Sen and Baltimore, 1986). NF-κB is a heterodimer of the Rel family of transcription factors that includes p50 (NF-κB1, produced as the precursor p105), p52 (NF-κB2, produced as the precursor p100), p65 (RelA), RelB and c-Rel (Baldwin, 2001; Cao and Karin, 2003; Chen *et al.*, 2001; Karin *et al.*, 2002). The NF-κB proteins all share a highly conserved 300-amino acid-long N-terminal Rel homology domain (RHD) that is responsible for DNA binding, dimerization and nuclear localization (Xiao *et al.*, 2006). NF-κB dimers are sequestered in the cytoplasm through direct interaction to ankyrin repeat domain (ARD)-containing members of inhibitory proteins called IκB, rendering them inactive (Ghosh *et al.*, 1998; Xiao *et al.*, 2006). There have been seven members of IκB proteins identified: IκBα, IκBβ, IκBε, IκBγ, B-cell CLL/lymphoma 3 (Bcl-3) and NF-κB1/p105 and NF-κB2/p100 precursor proteins. Signaling pathway activation can occur by many factors, including inflammatory cytokines, reactive oxygen species, and growth factor receptor signaling (like ErbB2), leading to, in the case of IκB, the phosphorylation and degradation of the inhibitory proteins, or the processing of precursor proteins and subsequent translocation of NF-κB to the nucleus, where it binds to response elements on the DNA, activating genes involved in inflammation, cell cycle progression, cellular invasion, tumour metastasis, angiogenesis and anti-apoptosis (Bhat-Nakshatri *et al.*, 2002; Brasier, 2006; Ghosh *et al.*,

1998; Gilmore, 1999; Gilmore, 2006; Karin and Ben-Neriah, 2000; Tian and Brasier, 2003).

All five NF-κB proteins bind to DNA motifs called κB sites, and they all have similar structural composition; however, the proteins can be classified into two groups based on how they are made and the structure and function of the C-terminal sequences (Perkins, 2000). Group 1 consists of Rel A/p65, RelB and c-Rel; these proteins contain transcriptional activation domains (TADs) at the C-terminus and are synthesized directly (Figure 6A). Group 2 includes NF-κB1/p50, and NF-κB2/p52 which are generated from the precursor proteins, p105 and p100 respectively (Xiao *et al.*, 2006) (Figure 6B). The C-terminal domains of p105 and p100 do not contain the TAD found in other NF-κB proteins. Instead, they contain the ARD characteristic of IκB proteins and function as inhibitors of NF-κB (Rice *et al.*, 1992; Mercurio *et al.*, 1993). The major, or canonical pathway leading to NF-κB pathway activation involves the IκB inducible degradation, allowing NF-κB dimers, mainly p65/p50, to accumulate in the nucleus and activate transcription. The processing of p100 and the translocation of p52-containing dimers to the nucleus is termed the alternative or non-canonical pathway (Xiao *et al.*, 2006)

1.5.2 Canonical NF-κB activation

The canonical NF-κB pathway can be rapidly activated by a wide variety of stimuli including MAPK, and DNA damage; these stimuli will lead to activation of a specific IκB kinase (IKK). IKK is a multiprotein complex that contains (at least) four subunits: two catalytic subunits termed IKKα and IKKβ, and two regulatory subunits, IKKγ (also known as NF-κB essential modular (NEMO); IKK associated protein 1

A

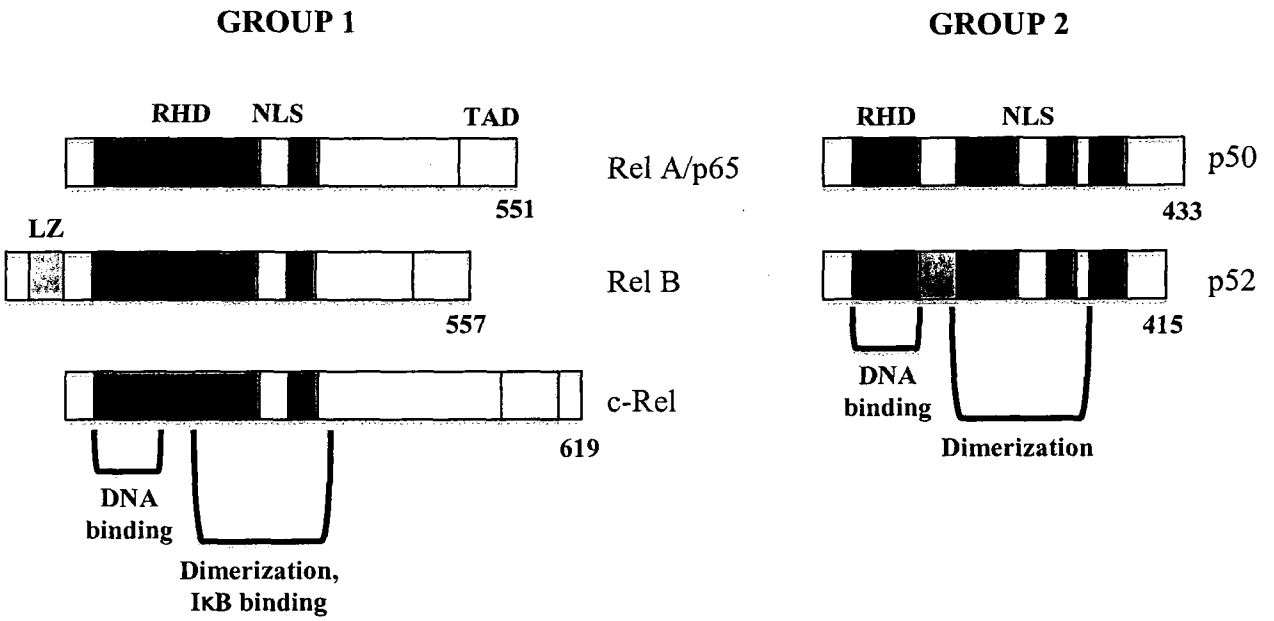
GROUP 1
GROUP 2
RHD
NLS
TAD
Rel A/p65
551
LZ
Rel B
557
c-Rel
619
DNA binding
Dimerization, IκB binding
RHD
NLS
p50
433
p52
415
DNA binding
Dimerization

B

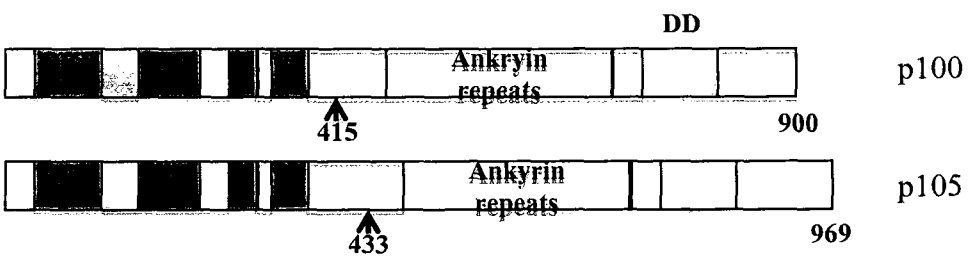
DD
Ankryin repeats
p100
415
900
Ankyrin repeats
p105
433
969

Figure 6. Schematic representation of the NF-κB proteins. **A**, The five NF-κB proteins are classified into two groups based on their synthesis and C-terminal sequence. The group 1 proteins RelA/p65, RelB and c-Rel are all synthesized directly and are inhibited by IκB proteins. The group 2 NF-κB proteins p50 and p52 are generated from large precursor proteins p105 and p100 respectively. The dimer p65/p50 and the dimer RelB/p52 represent the prototypically canonical and non-canonical pathway dimers, respectively. **B**, Full-length p100 and p105 must be processed to allow for the activation of p52 and p50, respectively. Abbreviations used: LZ – leucine zipper; RHD – Rel-homology domain; TAD – transactivation domain; DD – death domain. The brackets under the figures encompase the domain areas. Modified from Xiao *et al.*, 2006.

(IKKAP1)) and ERC1 (ELKS/Ras-related in the brain (RAB)-6/cytomatrix in the brain (CAZ)-associated structural protein (CAST) family member 1), currently known as ELKS (Xiao *et al.*, 2006; Ghosh *et al.*, 1998).

IKKα and IKKβ are functionally distinct; IKKβ is responsible IκB degradation in the canonical NF-κB pathway, while the functions of IKKα are more varied. Although IKKα induces degradation of IκB in some cases, it is also involved in keratinocyte differentiation, histone phosphorylation, termination of NF-κB activation and p100 phosphorylation (non-canonical signaling; see below) (Xiao *et al.*, 2006). The function of both IKKα and IKKβ depend heavily on IKKγ and ELKS. ELKS functions by recruiting downstream IκB proteins to the IKK complex for phosphorylation (Sigala *et al.*, 2004). IKKγ serves as a scaffolding protein, and also functions to recruit activators to the IKK complex, or to bring the IKK complex to active receptors, triggering the activation of IKKα and/or IKKβ by phosphorylation, or autotransphosphorylation (Xiao *et al.*, 2000). In canonical pathway signaling, once IKKβ has become active via phosphorylation, it is recruited to the NF-κB/IκB cytoplasmic complex, inducing degradation of the IκB protein by serine phosphorylation (Figure 7). Once the IκB protein has been phosphorylated, it is recognized by the beta-transducin repeat containing protein-Skp1-cullin-F-box protein (β-TrCP-SCF) E3 ubiquitin ligase, which causes polyubiquitination of IκB and degradation by the 26S proteasome. This step exposes the nuclear localization signal (NLS) of now free NF-κB dimers, allowing translocation to the nucleus, where it binds κB DNA sequences, activating genes involved in immunity, inflammation and cell survival. Prior to nuclear translocation, free NF-κB dimers may be

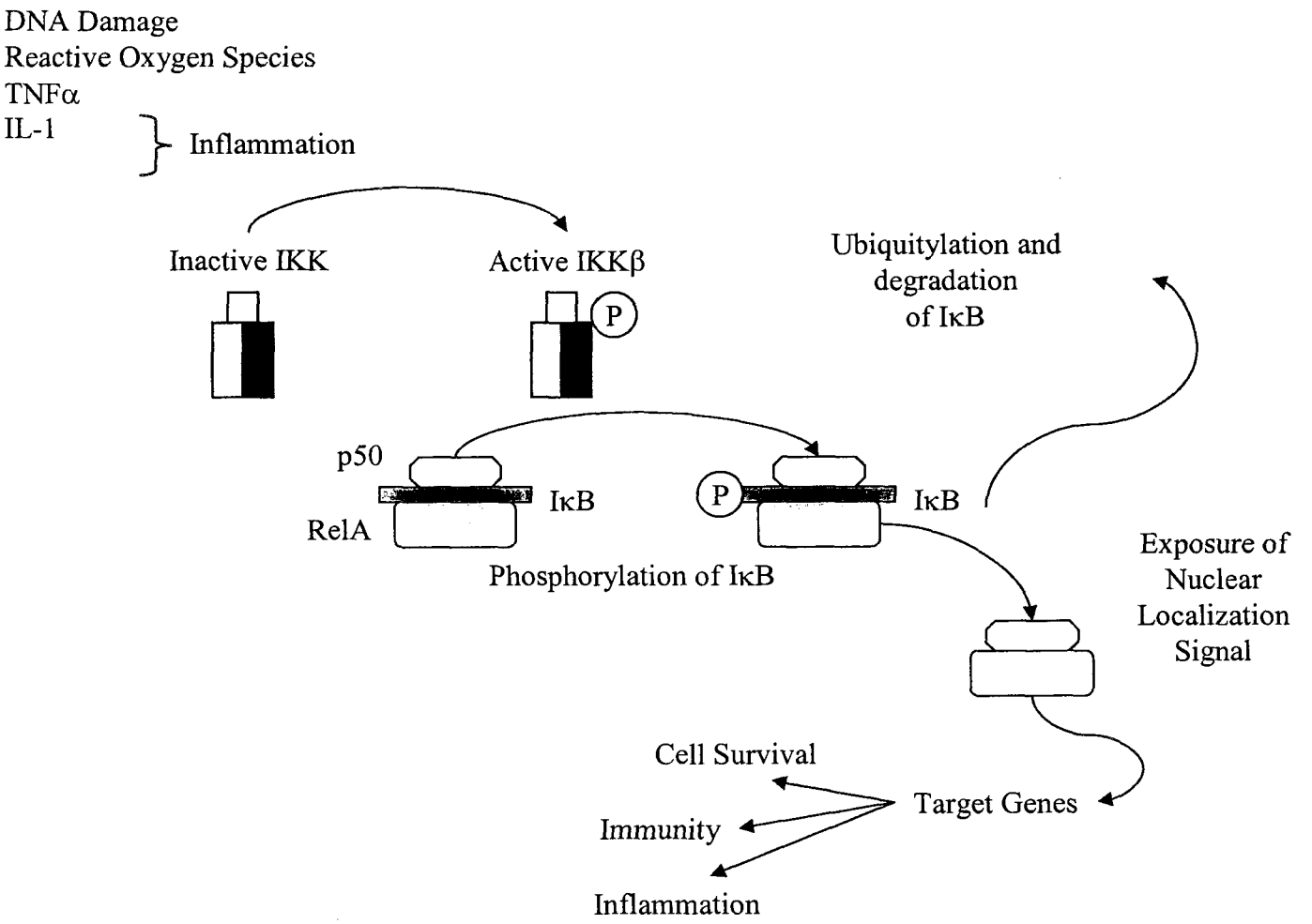
DNA Damage
Reactive Oxygen Species
TNFα
IL-1
Inflammation
Inactive IKK
Active IKKβ
P
Ubiquitylation and
degradation
of IκB
p50
RelA
IκB
P
IκB
Phosphorylation of IκB
Exposure of
Nuclear
Localization
Signal
Cell Survival
Immunity
Inflammation
Target Genes

Figure 7. Canonical NF-κB signaling. Activation of the canonical NF-κB pathway occurs from a variety of stimuli including DNA damage and reactive oxygen species. This stimulates the activation of IKKβ, and it is recruited to the NF-κB/IκB complex. IκB must be phosphorylated and degraded to allow for the activation of the NF-κB dimer and the exposure of its nuclear localization sequence. This step is achieved by the active IKKβ. Once active, the NF-κB canonical dimer consisting of p50/RelA can translocate to the nucleus where it activates the transcription of target genes. Modified from Xiao *et al.*, 2006, Baldwin, 2001 and Perkins, 2000.

further modified; RelA is modified by phosphorylation (Xiao *et al.*, 2006; Baldwin, 2001; Perkins, 2000).

The canonical NF-κB pathway is tightly controlled; persistent or aberrant activation can lead to fatal conditions, such as acute inflammation or septic shock (Baldwin, 2001). At a cellular level, prolonged NF-κB activation can lead to inappropriate cellular growth and survival, which can lead to cancer (Sun and Xiao, 2003). Active NF-κB also induces the expression of its inhibitors, including IκBα, which can terminate NF-κB signaling in an autoregulatory feedback loop. Other mechanisms are employed to ensure proper inhibition of the NF-κB pathway, including inactivation of the IKK complex, and deacetylation of the NF-κB subunits which allows IκB proteins to rebind NF-κB dimers. (Greene and Chen, 2004).

1.5.3 Non-canonical NF-κB activation

The non-canonical NF-κB pathway is based on the proteolytic processing of p100 and the activation of p52 containing dimers (Xiao *et al.*, 2006). As previously stated, the unprocessed NF-κB proteins p100 and p105 act in a similar manner to IκB. The processing of p100 is a extremely controlled phenomenon; active p52 protein is barely detected in the cell compared to its p100 counterpart (Xiao *et al.*, 2001). Non-canonical signaling begins via ligand binding to receptors such as the lymphotoxin beta receptor (LTβR), causing the activation and stabilization of the kinase NIK (Figure 8). Non-canonical pathway activation can also be triggered by other stimuli, including B-cell activating factor (BAFF), tumour necrosis factor-like weak inducer of apoptosis (TWEAK) and receptor activator for NF-κB ligand (RANKL) (Xiao *et al.*, 2006). The

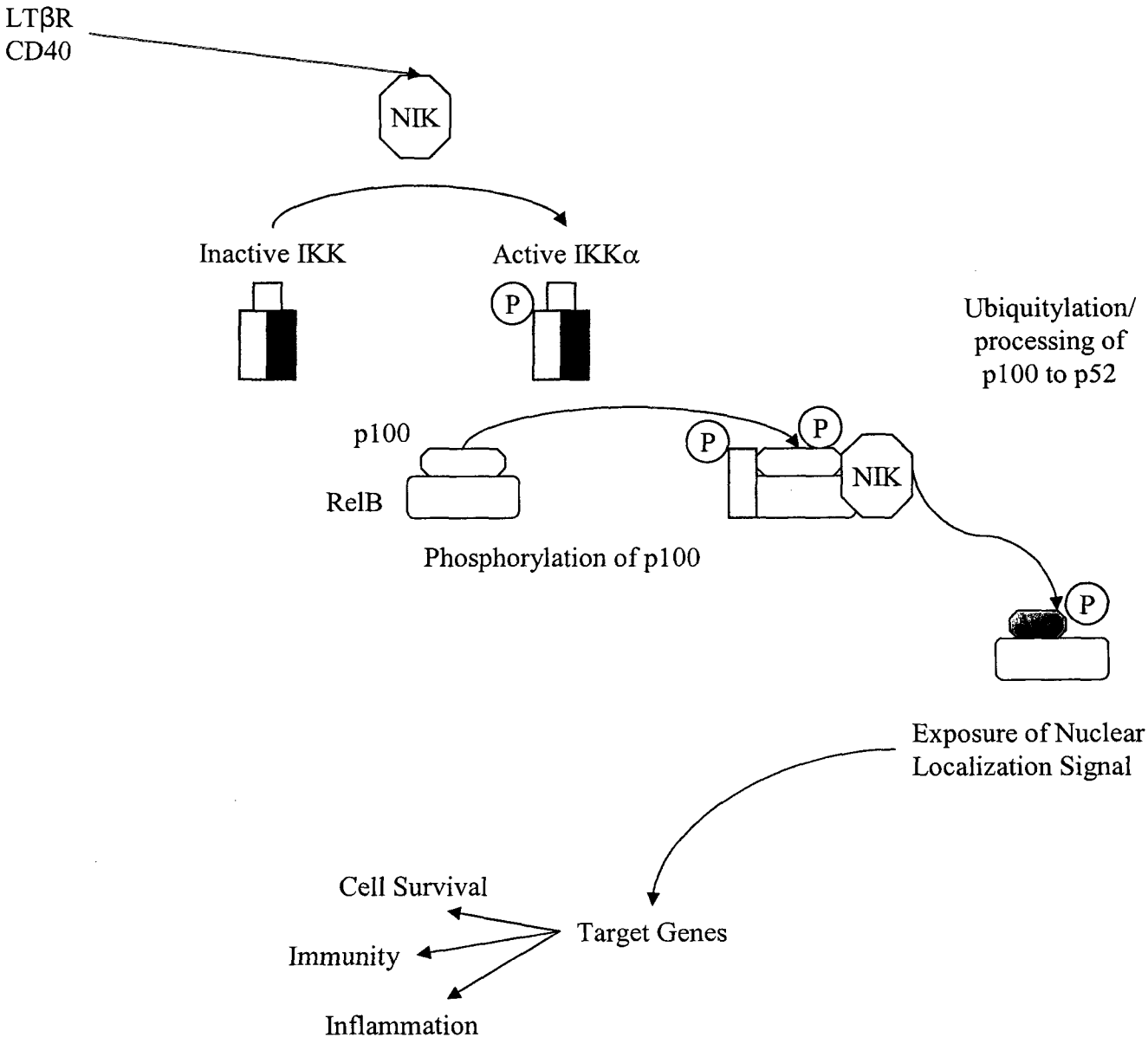
LTβR
CD40
NIK
Inactive IKK
Active IKKα
P
Ubiquitylation/
processing of
p100 to p52
p100
RelB
P
P
NIK
Phosphorylation of p100
P
Exposure of Nuclear
Localization Signal
Cell Survival
Target Genes
Immunity
Inflammation

Figure 8. Non-canonical NF-κB signaling. The non-canonical NF-κB signaling pathway is based on the proteolytic processing of p100. It begins via ligand binding to receptors such as lymphotoxin beta receptor (LTβR), causing the activation and stabilization of NIK. Active NIK is capable of activating the non-canonical kinase IKKα, bringing it in close proximity to the p100 complex. IKKα phosphorylates serines in the N- and C-terminal domains of p100, causing its partial degradation of generating p52. p52 is then capable of dimerizing with other NF-κB proteins, typically RelB; the dimer then enters the nucleus to regulate gene transcription. Adapted from Xiao *et al.*, 2001, Fong and Sun, 2002, and Xiao *et al.*, 2006.

stabilization of NIK may occur via association with other proteins, like tumour necrosis factor receptor associated factor (TRAF), which may act as mediators of upstream signaling events. However, it has also been reported that the TRAF3 protein physically associates with NIK via an N-terminal sequence motif, causing the degradation of NIK and downregulation of non-canonical signaling (Liao *et al.*, 2004). This is the only clearly understood mechanism of suppressing non-canonical signaling (Xiao *et al*, 2006).

Once active, NIK is capable of activating the non-canonical downstream kinase IKKα, and brings it in close proximity to the p100 complex. IKKα then phosphorylates serines located at both the N- and C-terminal of p100, triggering ubiquitination of p100 by β-TrCP and its partial proteasomal degradation (Fong and Sun, 2002). This generates active p52, which is then capable of forming dimers with other NF-κB proteins and enter the nucleus to regulate gene transcription (Xiao *et al.*, 2006).

1.6 NF-κB signaling

NF-κB proteins play a key role in the regulation of cellular responses to infection, and incorrect regulation has been linked to cancer, inflammatory autoimmune diseases, septic shock, viral infection and improper immune development (Liu *et al.*, 2009). Once NF-κB proteins are no longer sequestered in the cytoplasm, their translocation to the nucleus can cause induction of a number of key anti-apoptotic proteins, such as cellular inhibitor of apoptosis 1 and 2 (cIAP1, cIAP2), and B-cell CLL/lymphoma 2 (Bcl-2) (Weinberg, 2007). NF-κB also functions in a mitogenic fashion through induction of proteins like v-myc myelocytomatosis viral oncogene homolog (*myc*), and cyclin D1, components of cell-cycle machinery. Mice deficient in NF-κB proteins display a wide

variety of immune-related defects; these defects occur due to the function of NF-κB proteins in proper immune response and development, or in apoptotic inhibition in developing immune organs, such as the liver (Hayden and Ghosh, 2004). Non-canonical NF-κB signaling controls the expression of genes involved in B-cell function and lymphoid organogenesis, as well as processes typically controlled by canonical signaling, such as cell proliferation and survival (Xiao *et al.*, 2006).

1.6.1 NF-κB and mammary gland development

In addition to the role in immunity, the NF-κB family of transcription factors regulates growth, differentiation and apoptosis in embryonic limb, lung and liver, skin, and bone (Brantley *et al.*, 2001). Mammary gland development is highly regulated by NF-κB; p65 and p50 and the major inhibitory protein IκBα are expressed in the mammary epithelium of virgin, pregnant, and lactating mice, as well as those undergoing involution (Brantley *et al.*, 2000). The DNA-binding activity of dimer of NF-κB peaks during pregnancy, and diminishes, becoming undetectable during lactation; binding activity is re-established during involution (Cao and Karin, 2003). It is unknown if NF-κB activation plays a role in mammary stem cell proliferation, maintenance and survival.

During the period of mammary epithelial branching, NF-κB expression is needed to maintain normal epithelial architecture; abnormally high NF-κB expression can induce increased lateral branching and hyperplasia in mice lacking IκBα (Brantley *et al.*, 2001). NF-κB has also been shown to be essential for the proper development of milk-secreting units during pregnancy; mice with mutations in IKKα that abrogates its kinase activity, thus preventing pregnancy-induced NF-κB activation, display a severe lactation defect

(Cao *et al.*, 2001; Shillingford *et al.*, 2003). Mice that express a mutant form of IκB known as IκB super repressor ($IκB^{SR}$) also display this phenotype, confirming the necessity of NF-κB activation during pregnancy. $IκB^{SR}$ has serine to alanine mutations in its IKKβ phosphorylation sites (serines 32 and 36), blocking canonical NF-κB pathway activation (Cao *et al.*, 2001).

The role of NF-κB activation during involution is related to its role in apoptosis. Involution is characterized by extensive apoptosis and mammary epithelial remodeling. Although NF-κB plays a role as an anti-apoptotic protein, a balance between pro- and anti-apoptotic is needed during involution to insure that the process is properly regulated (Clarkson and Watson, 1999).

1.6.2 NF-κB and apoptosis

The role of NF-κB in anti-apoptotic signaling has been elucidated by studies in which NF-κB family genes or upstream kinases have been knocked out (Chen, Castranova and Shi, 2001). Significant hepatocyte apoptosis in mice lacking expression of RelA lead to an embryonic lethal phenotype (Beg *et al.*, 1995). Mouse embryos exhibiting either the IKK-β or double IKK-α/IKK-β gene knockout are not carried to term due to high levels of liver degeneration (Li *et al.*, 2000; Li *et al.*, 1999). Knockout of IKK-α results in embryo lethality; male mice lacking IKK-γ die due to massive lymphocytic apoptosis and liver degeneration, while female mice lacking this kinase display skin pigmentation that has resulted from keratinocyte apoptosis (Gerondakis *et al.*, 1999; Makris *et al.*, 2000). One of the ways in which NF-κB suppresses apoptosis is through the transcriptional activation of both cIAP1 and cIAP2. This allows for the

survival of genetically altered and mutated cells, giving rise to transformed progeny (Karin *et al.*, 2002). The promoter region of cIAP2 contains three NF-κB response elements, suggesting that cIAP2 is a potentially important target in tumourigenesis and progression (Hong *et al.*, 2000).

cIAP1 and cIAP2 belong to the inhibitor of apoptosis (IAP) family that has six other members in humans: X-linked IAP (XIAP), neuronal IAP (NAIP), melonoma IAP (ML-IAP), testis-specific IAP (Ts-IAP), BIR-containing ubiquitin conjugating enzyme (BRUCE) and survivin (Vaux and Silke, 2005; Hunter *et al.*, 2007). Both proteins were first identified in 1995 via their ability to bind both TRAF1 and TRAF2 (Rothe *et al.*, 1995). cIAP1 and cIAP2 are RING (Really Interesting New Gene)-domain containing ubquitin ligases that are capable of ubiquitinating themselves and many binding partners, including TRAF2 and TRAF3. cIAP1 and cIAP2 are also capable of ubiquitinating NIK, causing NIK degradation and downregulation of non-canonical NF-κB signaling; in cells where both cIAP1 and cIAP2 are not functional, NIK stabilization has been reported (Baud and Karin, 2009; Varfolomeev *et al.*, 2008; Vince *et al.*, 2007) (Figure 9).

In normal resting cells, NIK is rapidly degraded. This degradation is dependent on an association with TRAF3, which recruits NIK to a complex that consists of cIAP1/2 and TRAF2 (Baud and Karin, 2009). In this complex, cIAP1 and 2 are directly responsible for degradation of NIK via K48-linked polyubiquitylation ((Liao *et al.*, 2004). Thus, cIAP1 and 2, which are downstream of NF-κB activation, can negatively regulate NF-κB signaling. In cells where upstream receptors (eg. CD40) have been bound by ligand, TRAF3, 2 and cIAP1/2 are recruited to the receptor, leading to TRAF2 activation. Once active, TRAF2 is capable of ubiquitylating cIAP1/2, enhancing the E3

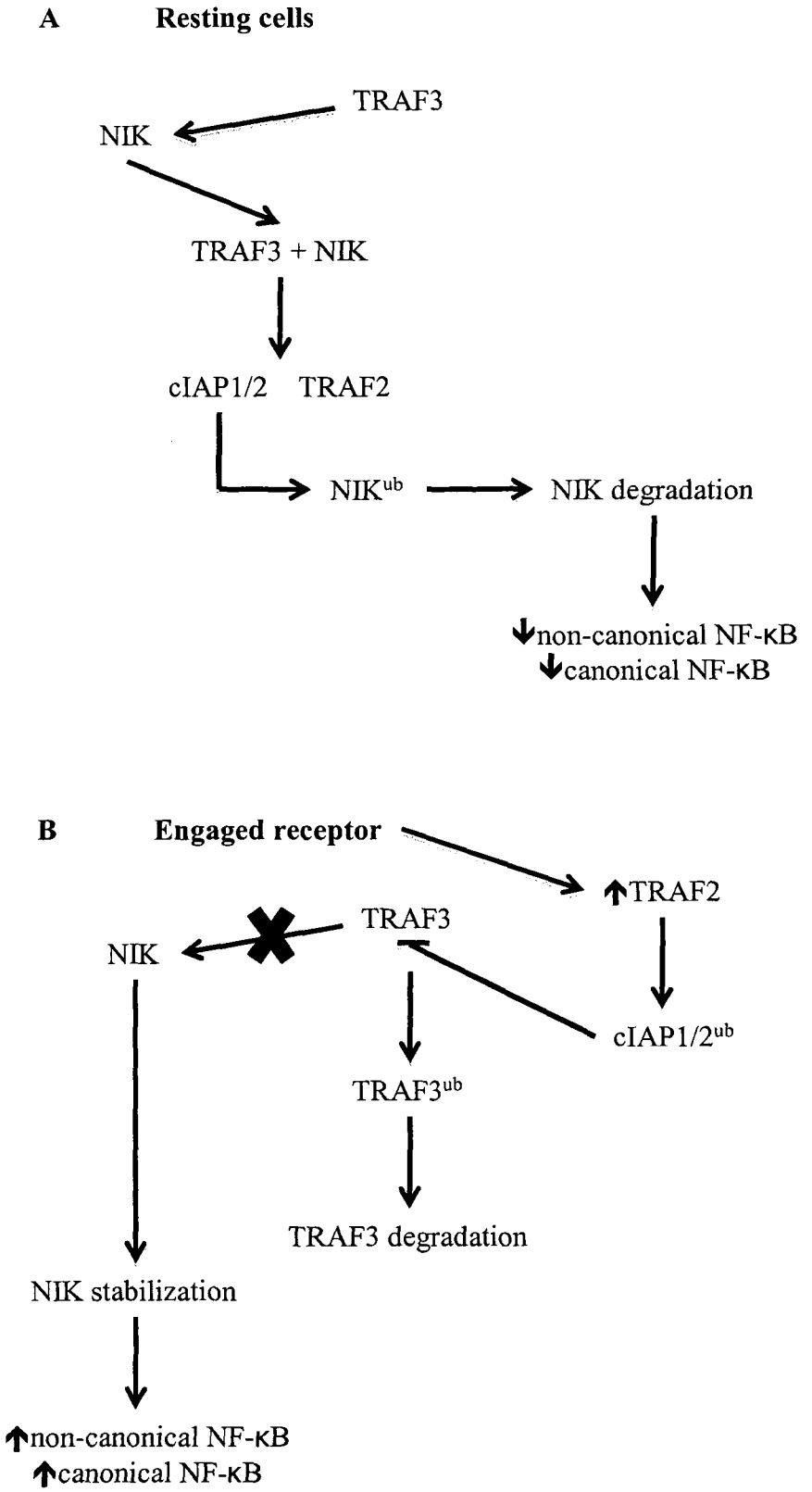
A
Resting cells
TRAF3
NIK
TRAF3 + NIK
cIAP1/2
TRAF2
NIK^ub
NIK degradation
↓non-canonical NF-κB
↓canonical NF-κB
B
Engaged receptor
↑TRAF2
TRAF3
NIK
cIAP1/2^ub
TRAF3^ub
TRAF3 degradation
NIK stabilization
↑non-canonical NF-κB
↑canonical NF-κB

Figure 9. NIK stabilization. **A,** In resting cells, newly synthesized NIK is rapidly degraded by a complex of TRAF2 and cIAP1/2 through its association with the adapter protein, TRAF3. **B**, In cells where a receptor has been engaged (eg. CD40), TRAF2 and cIAP1/2 are recruited to the active receptor, resulting in activation of TRAF2 and the ubiquitylation of cIAP1/2. Ubiquitylation (ub) of cIAP1/2 enhances ubiquitin ligase activity, which is now directed towards TRAF3. Once TRAF3 is degraded, NIK protein expression is stabilized, resulting in an increase in both canonical and non-canonical NF-κB signaling.

ubiquitin ligase activity of the cIAP1/2 complex, which is now directed at the degradation of TRAF3. Once TRAF3 is degraded, NIK is no longer capable of interacting with TRAF2 and cIAP1/2, leading to NIK protein stabilization, and its eventual autophosphorylation (Baud and Karin, 2009). Although NIK activation typically results in upregulation of non-canonical NF-κB signaling, it has been reported that its stabilization also increases canonical signaling (Annunziata *et al.*, 2007; Keats *et al.*, 2007).

When apoptosis is initiated, cIAP1 and cIAP2 are recruited to signaling complexes where they negatively modulate pro-caspase 8. Caspases are a family of cysteine-aspartate proteases produced as zymogens or inactive pro-caspases and are activated by proteolytic cleavage. Once active, caspase 8 is able to target apoptotic executioner caspases 3 and 7, which trigger the apoptotic signaling cascade (Baud and Karin, 2009) (see Appendix for outline of apoptotic signaling cascade). Although it has been reported in the literature that cIAP1 and cIAP2 are capable of ubiquitinating caspase 3 and 7, emerging evidence has shown that it may be only XIAP that is capable of directly inhibiting caspase activity (Eckelman and Salvesen, 2006); this research is even questioning the role of cIAP1 and cIAP2 in the modulation of pro-caspase 8, and mechanisms accounting for their pro-survival roles now remain uncertain. It has been shown, however, that chromosomal regions that make up the cIAP1 and cIAP2 genes are amplified in many forms of human cancer facilitating tumour progression, so understanding the function of these proteins in cancer cell survival is becoming a priority (Zender *et al.*, 2006).

1.6.3 NF-κB and cancer

It has been shown that NF-κB can become constitutively active in many cancers, especially breast cancer; a link between NF-κB, cellular transformation, oncogenesis, and metastasis has been recently discovered (Huber *et al.*, 2004). NF-κB activation can lead to downstream signaling events that can affect all known hallmarks of cancer; these hallmarks are self-sufficient proliferation and limitless replicative potential, evasion of apoptosis and insensitivity to inhibitory growth signals, and induction of angiogenesis, cellular invasion and metastasis (Baud and Karin, 2009; Hanahan and Weinberg, 2000). Due to its role in immune signaling, aberrant NF-κB is associated with various autoimmune diseases and lymphoid malignancies; in humans, constitutive processing of p100 due to *nfκb2* gene rearrangements resulting in partial loss of the p100 C-terminal domain is associated with many types of leukemia and lymphoma, including cutaneous T-cell lymphomas, B-cell-non Hodgkin lymphomas, and chronic lymphocytic leukemia and myeloma (Rayet and Gelinas, 1999; Sun and Xiao, 2003). In multiple myeloma, two research groups have recently shown that there is frequent activation of both canonical and non-canonical pathways due to gene mutations associated with both pathways (Annunziata *et al.*, 2007; Keats *et al.*, 2007). Using 155 multiple myeloma samples, both research groups showed that the most commonly occurring mutations lead to the inactivation of TRAF3, TRAF2, cylindromatosis (CYLD), and cellular inhibitor of apoptosis 1 and 2 (CIAP1/2), and activation of NF-κB1 and 2, CD40, LTβR, tachykinin precursor 1 (TAC1) and NIK, with the single most common abnormality being inactivation of TRAF3.

1.6.4 NF-κB and breast cancer

The role of NF-κB in normal mammary gland development has strengthened the idea that NF-κB plays a role in mammary tumourigenesis and breast cancer. Many studies have shown the presence of elevated NF-κB binding activity in mammary carcinoma cell lines and primary human breast cancer tissues (Cao and Karin, 2003). Rodent mammary tumours induced by DMBA exhibit high levels of NF-κB activation; elevated nuclear NF-κB activation was detected in the mammary gland even before a mammary tumour was detectable (Kim *et al.*, 2000). It is possible that early NF-κB activation promotes that survival of cells that have mutated and will eventually give rise to mammary tumours. The progression of mammary tumour cells from and ER positive to an ER negative state is accompanied by an increase in NF-κB activation and binding activity (Nakshatri *et al.*, 1997; Pratt *et al.*, 2003).

The NF-κB pathway also appears to play a role in inflammatory breast cancer (IBC), functioning as a tumour promoter (Lerebours *et al.*, 2008). IBC is a rare type of breast cancer that induces rapid breast cancer inflammation and the extreme tendency to metastasize. This subset of breast cancer has extremely poor prognosis; while the 3-year survival rate for non-inflammatory breast cancer is 85%, the rate for IBC is only 40%. Using real time quantitative PCR, Lerebours *et al.*, (2008) measured mRNA expression levels of 60 NF-κB related genes in 35 IBC samples, and 22 stage II and III non-inflammatory breast cancer samples to serve as poor prognosis controls. Thirty-five (58%) of the NF-κB related genes were upregulated in IBC compared to non-IBC controls; these genes including those directly coding for NF-κB proteins, apoptotic genes, immune response genes, proliferation genes and angiogenesis genes.

NF-κB upregulation and activation has also been reported in ER-negative/ErB2 positive tumour samples. Biswas *et al.* (2004) measured NF-κB activation in 31 human breast cancer samples and found that 86% of ER-negative and ErbB2 positive tumours contained active NF-κB expression. Increased nuclear p65 was detected by both electrophoretic mobility shift assay (EMSA) and immunofluorescence, substantiating the hypothesis that some breast cancer cell types rely on NF-κB for aberrant cellular proliferation and to avoid apoptosis. Many other investigators have substantiated these results. Sovak *et al.* (2004) demonstrated increased NF-κB activity in the study of *in vitro* human cell lines, *in vivo* rat breast cancer and clinical biopsies; Coswell *et al.* (2004) confirmed these findings, and also found elevated transcripts of NF-κB in breast tumours compared to adjacent normal tissues.

Despite a large body of evidence suggesting that NF-κB activation is implicated in mammary tumourigenesis, it is still unknown if deregulation in NF-κB signaling plays a causative role in the development of breast cancer. It also remains unclear if NF-κB upregulation is detected in the recently identified mammary TICs. Several oncogenes are known to activate NF-κB dimers and mediate their transforming potential, including Harvey-retrovirus associated DNA sequences (Ha-Ras), breakpoint cluster region-V-Abl Abelson murine leukemia viral oncogene homolog 1 (Bcr-Abl), and more recently, ErbB2 (Orlowski and Baldwin, 2002). NF-κB has been shown to enhance ErbB2-mediated mammary tumourigenesis through the promotion of both growth and survival signaling (Liu *et al.*, 2009). If NF-κB does play a causative role in mammary tumourigenesis, it could be an ideal a target for breast cancer treatment through its selective inhibition.

1.7. Objectives and Hypothesis

1.7.1 The role of cIAP2 in mammary tumourigenesis

The role of cIAP2 in carcinogen-induced mammary tumourigenesis was previously unknown. Dr. Pratt's lab previously conducted a study using DMBA and mice lacking cIAP2 expression in a carcinogen-induced mammary tumourigenesis model. In this study, it was found that mice lacking cIAP2 expression displayed an increase in tumour latency associated with a significant increase in the number of tumour cells undergoing apoptosis and mitosis. Using an antibody against CD68, it was also noted that the tumours lacking cIAP2 expression also exhibited an increase in tumours associated macrophages (TAMs). The presence of TAMs is often correlated with poor prognosis in cancer; TAMs are capable of secreting a vast diversity of growth factors, proteolytic enzymes, cytokines, and inflammatory mediators that can actually help to increase the growth of tumour cells and mediate tumour cell metastasis. In the carcinogen-induced model, the mechanism of tumourigenesis in the cIAP2 knockout mice was associated with inflammation and the delay in tumour growth was due to the increase in apoptotic cells associated with the loss of the inhibitor of apoptosis.

The research completed using cIAP2 knockout mice in a carcinogen-induced model has been recently applied by the Pratt lab to a transgenic mouse model where mammary tumourigenesis is induced by the mammary specific expression of the oncogene ErbB2. Previous studies have suggested that NF-κB signaling is important for breast cancer development, and that cIAP2 is a critical downstream target. By deleting this target protein, **it is hypothesized that the oncogenic effect of NF-κB may be**

eliminated and that the development of mammary tumours will be delayed.

1.7.2 The role of NF-κB activation in mouse MaSCs and TICs

Previous work from the Pratt lab has shown that the canonical NF-κB signaling pathway is needed for the formation of luminal mammary neoplasias (Pratt *et al.*, 2009). It had been previously hypothesized that inhibition of NF-κB activation might prevent tumour formation based on its role in both mammary differentations and cancer. This was investigated using a transgenic mouse expressing a dominant-negative inhibitor of κB called IκB super repressor ($IκB^{SR}$) expressed in the mammary gland under the control of MMTV. As stated in the introduction, $IκB^{SR}$ has serine to alanine mutations in its IKKα phosphorylation sites (serines 32 and 36), blocking canonical NF-κB pathway activation (Cao *et al.*, 2001). Mammary lesions produced in the presence of the $IκB^{SR}$ were squamous/basal in origin rather than luminal-type mammary adenomas; squamous/basal metaplasias were detected in both transgenic and control mice, while luminal tumours developed almost exclusively in control mice. Canonical p65/RelA NF-κB DNA-binding activity assessed by EMSA was detected in mammary luminal lesions, but rarely in squamous metaplasias.

Using the results obtained from the MMTV-$IκB^{SR}$ tumourigenesis study, it was **hypothesized that luminal mammary epithelial stem cells and tumour initiating cells identified by CD24 and CD44 staining, respectively, will contain nuclear NF-κB expression.**

1.7.3 Objectives

1. Investigate the effect on tumourigenesis induced by MMTV-ErbB2 in mice lacking cIAP2 expression.

.2. To determine is NF-κB expression is associated with CD24+ cell surface staining in luminal progenitor cells and is absent in CD49+ basal mammary stem cells using *cis*-NF-κB^{EGFP} reporter mice.

3. To determine if TICs labeled by CD44+ cell surface staining in tumour from MMTV-ErbB2 X *cis*-NF-κB^{EGFP} reporter mice are associated with NF-κB protein activation.

CHAPTER TWO

MATERIALS AND METHODS

2.1 Mice

2.1.1 Mouse genotyping

Male MMTV-ErbB2 (MMTV-Neu/NDL1) with an activated rat ErbB2 oncogene were bred with female friend virus B NIH Jackson (FVB/NJ) mice (Jackson Laboratories, Bar Harbour, Maine, USA) to generate male MMTV-ErbB2 heterozygous mice. The MMTV-ErbB2 transgenic mice carried an activated ErbB2 transgene via a Neu deletion mutation (NDL); these mice have been reported to develop mammary tumours at 182 ± 50 days (n=22) (Siegel *et al.*, 1999). Genotyping was confirmed by PCR using tail tip DNA and the forward primer (Neu-3) 5'TTTCCTGCAGCAGCCTAA-3' and the reverse primer (Neu-4) 5'-CGGAACCCACATCAGGC-3' generating a band of approximately 630 basepairs (bp) (Oshima *et al.*, 2004; Siegel *et al.*, 1999). At 4 weeks of age, a small section of mouse tail was removed and was placed in 500μL of tail tip digestion buffer (100mg/mL proteinase K, 5X TE, 1% SDS, 200mM NaCl) overnight at 65°C. Following incubation, the DNA was extracted using a phenol chloroform extraction method for mouse-tail tip DNA (Wang and Storm, 2006). The DNA was quantified and was used for PCR analysis or for Southern blot analysis. For the PCR reaction, the DNA was diluted to 0.1μg/μL and 1μL was used for the PCR reaction along with 12.5μL (1X) GoTaq Green PCR Master Mix (containing Green loading dye, $MgCl_2$, dNTPs and Taq DNA polymerase; Promega) and forward and reverse ErbB2 primers. PCR products were run on a 1.5% agarose gel and were visualized using ethidium bromide.

ErbB2 heterozygous mice were crossed with cIAP2 homozygous knockout female mice (a gift from Robert Korneluk, University of Ottawa) to generate 20 MMTV-ErbB2 heterozygous, cIAP2 knockout (test) and 20 MMTV-ErbB2, cIAP2 wildtype (control)

females. Genotyping for cIAP2 was done by Southern blot analysis of EcoRV digested genomic tail tip DNA hybridized with a radioactively labeled probe to exon 1 of the cIAP2 gene (Conte *et al.*, 2006). The digested DNA was run on a 1% agarose gel at 100 volts for 3 hours. The gel was stained with ethidium bromide to visualize the fragmented DNA. The gel was the washed in 0.5M HCl for 20 minutes, followed by two denaturing washes in 0.5M NaOH for 40 minutes. After this, the DNA was transferred onto a Hybond XL charged membrane (Amersham) overnight. Following the transfer, the membrane was washed in 6X SSC (NaCl, Na_3-citrate x 2 H_20) and was placed in a hybridization column. The membrane was pre-washed in 6X SSC Hyb buffer (6X SSC, Denhardt's, 20% SDS, Yeast RNA) with salmon sperm for 3 hours. A radioactively labelled probe to exon 1 of the cIAP2 gene was added to the Hyb column overnight at 65°C. To radioactively label the DNA probe, the DNA was diluted in TE buffer (10mM Tris HCl, pH 8.0, 1mM EDTA) and was denatured for 5 minutes at 100°C, and was quickly cooled. The denatured DNA was added to an Amersham reaction tube along with 5μL of Redivue [^{32}P] dCTP, and was incubated at 37°C for 10 minutes. The sample was then added to a G50 column, and centrifuged at 3000RPM for 2 minutes. The sample was boiled for 5 minutes, and cooled for 5 minutes. Following the overnight hybridization, the membrane was washed with 2X SSC with 0.1% SDS three times for 40 minutes, and was placed in an Autorad cassette at -80°C for two days with a blank film. The film was developed using a Kodak developer.

2.1.2 Stem cell analysis

For the mammary stem cell analysis experiments, *cis*-NF-κB^{EGFP}reporter mice (a gift from Dr. C. Jobin, were bred with wild type (WT) C57BL6 (Charles River Laboratories, USA) to generate WT female mice (control) or female heterozygous *cis*-NF-κB^{EGFP}reporter mice. This transgenic mouse expresses an X-linked enhanced green fluorescent protein (EGFP) under the transcriptional control of NF-κB *cis* regulatory elements (Magness *et al.*, 2004). The mouse genotype was confirmed by PCR on genomic tail tip DNA using the forward primer (EGFPFOR) 5'-GAGCTGAAGGGCATCGACTTCAAG-3' and the reverse primer (EGFPREV) 5'-GGACTGGGTGCTCAGGTAGTGG-3', which generated an amplicon of 256 bp. These mice were kept until 8-14 weeks of age.

2.1.3 TIC analysis

For analysis of TICs, male MMTV-ErbB2 mice were crossed with female *cis*-NF-κB^{EGFP}reporter mice to generate MMTV-ErbB2 heterozygous mice and MMTV-ErbB2 heterozygous, *cis*-NF-κB^{EGFP}reporter heterozygous mice. Genotyping was done as previously described.

2.2 Tumour development

2.2.1 Tumour collection

Mice were palpated 3 times a week until a detectable mammary tumour developed. At the first sign of a tumour, the tumour latency was recorded (the time in days from birth to tumour development) and the tumour was left to grow until it reached

an endpoint of 1.7cm in diameter. Mice were euthanized by carbon dioxide (CO_2) and the tumour area was washed with 70% ethanol. Tumours were excised and half was placed in a cryogenic tube and frozen immediately in dry ice or liquid nitrogen, and the other half was placed in 10% formalin to be paraffin embedded for preservation (for the cIAP2 study) or were processed as described below (CSC study).

2.2.2 Tumour and mammary gland cryosectioning

Frozen tumour halves were embedded in OCT (Optimal Cutting Temperature; VWR) compound and were sectioned to 8μm using a Microtome cryostat at -20°C. Sections were mounted onto charged Superfrost Plus slides (VWR); 4-5 sections were mounted per slide and 5 slides were done per tumour. The slides were stored at -80°C.

With some *cis*-NF-κB^{EGFP}reporter mice, mammary glands were ressected and were frozen for cryosectioning as previously stated with some modifications. These mice were sacrificed at 8-14 weeks of age when the mammary glands were fully developed. Mammary glands were sectioned at 10μm at -30 to -26°C and were placed 8-10 per slide. Due to the high fat content of mouse mammary glands, sectioning was done at a lower temperature and higher thickness to prevent fat melting.

2.3 Mammary stem cell analysis

2.3.1 Mammary gland dissociation

For the flow cytometry experiments, and primary cell culture on mouse mammary cells and stem cells, mammary glands were dissociated and a single cell suspension was made as described by Stem Cell Technologies and Stingl *et al.*, 2006. All solutions were

purchased from Stem Cell Technologies. The 4 inguinal mammary glands from 6-8 *cis*-NF-κB^{EGFP}reporter mice at ages 8-14 weeks, or 2-3 C57BL6 mice at the same age were ressected and transferred to a glass petri dish where they were minced into a paste with a sterile scalpel. The samples were transferred to centrifuge tubes containing 2-5 mL of a 1:9 mixture of 10X collagenase/hyaluronidase:complete Epicult® B mouse medium supplemented with 5% fetal bovine serum (FBS) for every 2 mammary glands followed by incubation at 37°C for 6-8 hours. Complete medium was made by adding the provided proliferation supplements plus 10ng/mL human epidermal growth factor (hEGF), 10 ng/mL recombinant human basic fibroblast growth factor (rh bFGF) and 4 μg/mL (0.0004%) heparin to Epicult® B mouse medium. Following incubation and centrifugation, the resulting cell pellet was incubated in a 1:4 mixture of Hank's balanced salt solution (HBSS) with 2% FBS followed by centrifugation.

2.3.2 Generation of a single cell suspension

To generate a single cell suspension, the cell pellet was incubated with pre-warmed trypsin-ethylenediaminetetraacetic acid (EDTA). Please note, after each incubation period, 10 mL of HBSS plus 2% FBS (now called HF) was added to the pellet followed by low speed centrifugation. 2 mL of pre-warmed dispase (5 mg/mL) plus 1 mL DNase was added to the cell pellet, followed by pipetting to dissociate clumps. The cell suspension (plus HF) was filtered through a 40μm cell strainer (BD Falcon), followed by centrifugation. The resulting cell pellet contained mammary epithelial cells to be used for cell culture or for flow cytometry.

2.3.3 Stem cell enrichment of mammary epithelial cells

The mammary single cell suspension (see previous) was diluted to 1 x 10^8 cells/mL in HF supplemented with 0.1 mg/mL DNase I. Stem cell enrichment (lineage negative (Lin-) cell enrichment) was done using the EasySep® negative selection procedure (Stem Cell Technologies). The negative selection cocktail was added at 50 μL/mL cells and incubated for 15 minutes, after which the EasySep® biotin cocktail at 100 μL/mL cells was added, followed by another 15 minute incubation. The negative selection cocktail contains biotinylated monoclonal antibodies directed against cell surface markers of hematopoetic and endothelial cells (CD45, TER119 and CD31), and together with the biotin selection cocktail and dextran iron nanoparticles, will deplete the suspension of contaminating cells. The provided nanoparticles were added (50 μL/mL cells) followed by incubation for 15 minutes. The resulting mixture was incubated with the EasySep® magnet for 5 minutes, and the desired fraction was poured off; this incubation was repeated and the desired fractions were pooled.

2.3.4 FACS analysis of mammary stem cells

The mammary single cell suspension was labeled with an anti-mouse CD24-Phycoerythrin (PE) antibody (10 μL/mL cells), and CD49f-Alexa Fluor®647 (80 μL/mL cells) for 15 minutes, followed by low speed centrifugation. The resulting cell pellet was resuspended at 5 x 10^8 cells/mL (or in at least 500 μL) and was subject to FACS at the Sprott Centre for Stem Cell Research using a DakoCytomation MoFlo Flow Cytometer. Paul Oleynik at the Ottawa Hospital Research Institute (OHRI) completed the flow cytometry and analysis.

2.4 TIC Analysis

2.4.1 Tumour dissociation

MMTV-ErbB2 induced tumours in *cis*-NF-κB^{EGFP}reporter and WT mice were dissociated into a single cell suspension using the method described by Liu *et al.* (2007). Briefly, half of the removed tumour was washed with PBS, and minced into a paste using a sterile razor. The resulting paste was washed in PBS and digested in 100 units/mL collagenase (Stem Cell Technologies) for 2 hours at 37°C. The samples were washed with 5 volumes of HF plus 2 mmol/L EDTA (HFE) and centrifuged at 450 x *g* for 5 minutes. The cell pellet was dissociated in 2 mL dispase (Stem Cell Technologies) for 3 minutes with continuous pipetting, diluted with 10 mL HFE and passed through a 40 μm cell strainer (BD Falcon).

2.4.2 TIC enrichment

The Lin- tumour cells were enriched using the EasySep® negative selection procedure as previously described.

2.4.3 FACS analysis of TICs

The Lin- tumour cells were labeled with a CD44 mouse monoclonal Alexa Fluor®647 antibody (Biolegend). In initial experiments, the concentration of antibody used was varied (no label, 0.5X, 1X and 2X where X=0.2μg/10^6 cells) to determine the optimal concentration for FACS analysis. The flow cytometry was carried out as previously stated.

2.5 Immunohistochemistry

2.5.1 Tumour immunohistochemistry

Frozen tumour sections were fixed following the antibody manufacturer instructions and were permeabilized with 0.3% Triton. Blocking was done with immunohistochemistry (IHC) blocking solution (1.0% bovine serum albumin (BSA), 10mM Tris buffer (pH 7.4) and 0.3% Triton). Slides were incubated with primary antibody for 2 hours in a humid chamber. The following antibodies were used: Relb (sc-28689), p65 (sc-109), Neu/ErbB2 (sc-284) (Santa Cruz Biotech, Santa Cruz, CA, USA); phospho-histone H3 (#H0412, Sigma, Oakville, ON, Canada); CD68 (Serotec, Raleigh, NC, USA); CD31 (ab25563), GFP (ab290) (Abcam, Cambridge, MA, USA). After washing 3 times in PBS-triton, antibody visualization was achieved using anti-mouse or rabbit cyanine-3 (CY3)-conjugated secondary antibodies (Jackson Immunoresearch, Westgrove, PA, USA) for 1 hour in a humid chamber in the dark. The slides were mounted with mounting medium containing 4'-6-diamidino-2-phenylindole (DAPI), and stored at -80°C in the dark until visualization using a fluorescent microscope.

For experiments using the CD31 antibody, 2-3 microscopic fields of view were analyzed from eight tumours with and eight tumours without cIAP2 expression to determine if there was a visual difference in CD31 staining. It was difficult to count the tumour blood vessels because of extensive branching, and due to the size of the vessels, so counting couldn't be completed for this study.

2.5.2 TUNEL assay

Frozen tumour sections were subject to apoptotic analysis by terminal deoxynucleotidyl transferase dUTP nick end labeling (TUNEL) using the ApopTag® Red *In Situ* Apoptotic Detection Kit (Millipore; previously Chemicon International). Briefly, frozen sections were fixed in ice-cold methanol, and were pretreated with proteinase K (20 μg/mL) for 15 minutes. The slides were washed twice with 1X phosphate buffered saline (PBS) for 2 minutes. After the wash, 75 μL/5 cm^2 of sample was added directly to the sample, followed by the application of 55 μL/5 cm^2 of working strength TdT solution and incubation in a humidified chamber for 1 hour at 37°C. The slides were then placed in a coplin jar with working strength stop/wash buffer and were agitated for 15 seconds, followed by 3 washes in 1X PBS. Room temperature anti-digoxigenin conjugate (rhodamine) was added to the slide at 65 μL/5 cm^2 and the slides were incubated in a humidified chamber in the dark for 30 minutes. After washing 3 times with 1X PBS, the slides were mounted with mounting medium containing DAPI. Mounted slides were stored at -80°C in the dark until visualization using a fluorescent microscope.

In order to determine if the loss of cIAP2 in the MMTV-ErbB2-induced tumours changed apoptotic levels, the number of apoptotic cells in the tumour sections was counted. TUNEL pictures of tumour sections from five cIAP2 wild type and five cIAP2 knockout mice were taken, and three representative fields of view were selected. The number of tumour cells undergoing apoptosis (as represented by positive TUNEL staining) in each field of view was counted and this was compared to the total number of tumour cells present. This data was used to calculate the percentage of tumour cells

undergoing apoptosis in each sample, and an average was generated for use in statistical analysis. Statistical significance was determined by Student's T-test.

2.5.3 Mammary gland immunohistochemistry

Frozen mammary gland sections were fixed with cold methanol, permeabilized in 0.3% Triton, and blocked in IHC blocking buffer. Antibodies were diluted in IHC blocking buffer and were incubated on the slides for 2 hours at room temperature in a humid chamber. The following antibodies were used: p65 (sc-109, Santa Cruz Biotech, Santa Cruz, CA, USA), and GFP (ab290, Abcam, Cambridge, MA, USA). Slides were washed with PBS-triton, and incubated with CY3 or fluorescein isothiocyanate (FITC)-conjugated secondary antibodies (Jackson Immunoresearch, Westgrove, PA, USA) for 1 hour at room temperature in a humid chamber in the dark. After washing 3 times with 1X PBS, the slides were mounted with mounting medium containing DAPI. Mounted slides were stored at -80°C in the dark until visualization using a fluorescent microscope.

2.5.4 Mammary stem cell immunohistochemistry

MRU and Ma-CFC stem cells that were sorted by FACS analysis were subject to immediate low-speed centrifugation onto glass slides using a Cytospin centrifuge. These cells were fixed with 4% paraformaldehyde (PFA) for 10 minutes and incubated with a p65 antibody (sc-109, Santa Cruz Biotech, Santa Cruz, CA, USA) for 1 hour at room temperature. Cells were carefully washed 3 times in PBS, following which visualization was achieved using a CY3 conjugated secondary antibody for 1 hour in the dark in a humid chamber on the same day; overnight incubation resulted in over 50% cell loss

(Pratt lab, unpublished observation). Slides were stored at 4°C for no more than 2 days in the dark to prior to visualization using a fluorescent microscope to ensure that the fluorescent signal was not lost.

2.6 Immunoblots and antibodies

Tumour tissue was pulverized under liquid nitrogen. Following the addition of RIPA buffer (25 mM Tris•HCl pH 7.6, 150 mM NaCl, 1% NP-40, 1% sodium deoxycholate, 0.1% SDS) with protease inhibitors, samples were sonicated and incubated for 30 min on ice, then centrifuged at 16 000 x *g* for 20 minutes to remove insoluble protein. Protein concentration was determined using the Lowry method (Lowry *et al.*, 1951). Protein (20 μg) was assessed by sodium dodecyl sulfate polyacrylamide gel electrophoresis (SDS-PAGE). Tumour protein was transferred onto polyvinylidene fluoride (PVDF) membrane (Immobilon-P, Millipore). The following antibodies were used: anti-phospho IKK-α/β (#2697), total IKK-β (#2370), p27 (#3688), phospho-Jnk/SAPK, phospho p44/p42, and phospho p38 from the phospho MAPK antibody sampler kit (#9910) (Cell Signaling, Cambridge, MA, USA); actin (#A-2066, Sigma, Oakville, ON, Canada); Neu/ErbB2 (sc-284), TRAF-1 (sc-1830) (Santa Cruz Biotech, Santa Cruz, CA, USA). The proteins were visualized using anti-mouse or rabbit horse radish peroxidase (HRP) secondary antibodies (Jackson Immunoresearch, Westgrove, PA, USA), ECL-Plus (enhanced chemiluminescence, GE Healthcare (formerly Amesham), UK), and film.

2.7 Electrophoretic mobility shift assay (EMSA)

EMSA was performed on nuclear extracts from tumours isolated as described by Osborn *et al.* (1989). NF-κB site oligonucleotides were obtained from Promega (E3291) and were end labeled with T4 polynucleotide kinase with [γ^{32}-p] ATP (Amesham). 5 micograms nuclear extracts were mixed with 5 μL DNA binding buffer (20 mM HEPES [pH 7.9], 0.2mM EDTA, 0.2mM EGTA and 2mM dithiothreitol in 50% glycerol), 5 μg poly (dI-dC) and 0,2 ng of labeled probe to a final volume of 20 μL and then incubated at room temperature for 25 minutes. Equivalence of extract loading was demonstrated with DNA fragment containing stable protein 1 (Sp1) binding site (Promega). Samples were loaded on 5% native polyacrylamide gel and run in non-denaturing Tris-glycine buffer.

CHAPTER THREE

RESULTS

3.1 The role of cIAP2 in ErbB2-induced mammary tumourigenesis

3.1.1 Knockout of cIAP2 increases mammary tumour latency

In order to generate cIAP2 knockout female mice carrying the ErbB2 transgene, the second generation of a cIAP2 knockout X MMTV-ErbB2 cross was genotyped using genomic tail tip DNA. Southern blot analysis of the genomic tail tip DNA using a probe to exon 1 of the cIAP2 gene confirmed that cIAP2 was knocked out; cIAP2 WT mice exhibited a 27kb band corresponding to the functional cIAP2 allele. A 15kb band was present in cIAP2 knockout mice (Figure 10A). The presence of the ErbB2 transgene was detected by PCR analysis; a 630kb PCR product was evident from the DNA of mice carrying the activated ErbB2 transgene.

The impact of cIAP2 knockout in mammary tumourigenesis was previously examined by subjecting 20 cIAP2 WT and 20 cIAP2 knockout mice to mammary tumourigenesis induced by the presence of an activated ErbB2 transgene (Pratt lab, unpublished data). Emma Tibbo, previously of the Pratt lab and myself completed these experiments. Animals were monitored for the formation of palpable masses as described in Materials and methods. Large variations in tumour latency for both groups of mice were observed; however, Kaplein-Meier analysis revealed a significant difference in the tumour latent period (Figure 10B). Mice with normal cIAP2 expression showed a mean latency of 283 days whereas knockout of the cIAP2 gene resulted in an increase in tumour latency to 399 days.

A

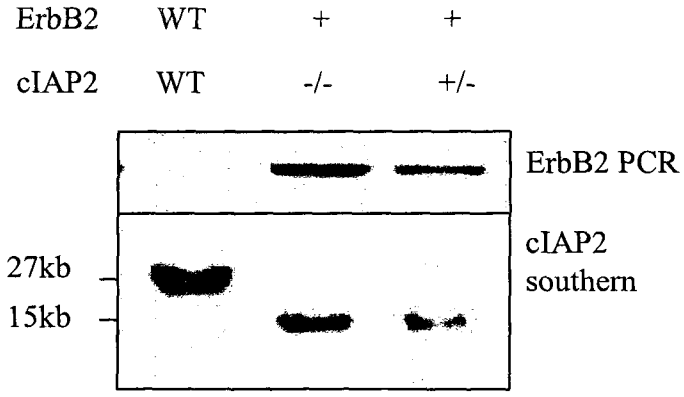

B

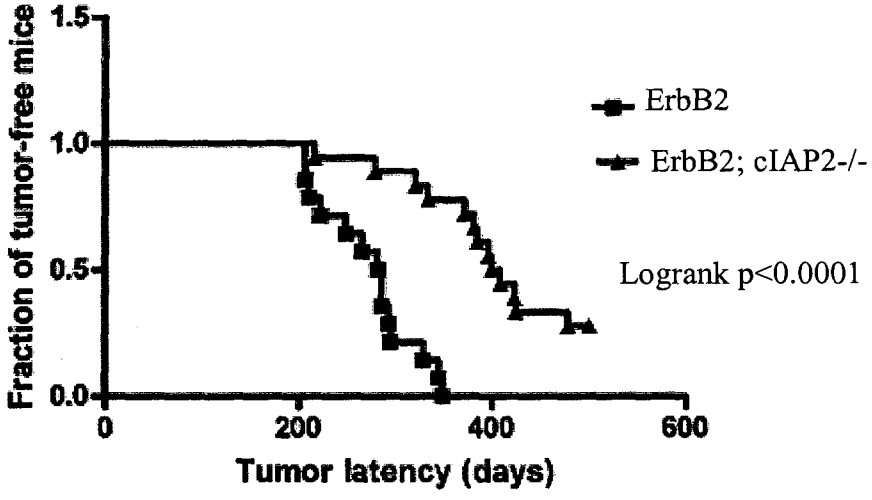

ErbB2;cIAP2$^{+/+}$ median latency =283 days
ErbB2;cIAP2 $^{-/-}$ median latency= 399 days

Figure 10. Generation of cIAP2 null mice expressing the ErbB2 transgene. A, Southern blot analysis of EcoRV-digested genomic DNA from mouse tail tips probed with sequences corresponding to exon 1 of the cIAP2 gene and PCR analysis of mouse genomic DNA using primers that amplify the ErbB2 transgene in order to identify cIAP2 knockout mice that express the ErbB2 transgene. **B**, Kaplan-Meier plot showing mammary tumour latency of ErbB2 mice with and without cIAP2 expression. Tumour latency was calculated as the number of days from birth to the first detection of a palpable mammary tumour. The mean latency of ErbB2 mice with cIAP2 expression was 283 days, while the mean tumour latency for the cIAP2 knockout ErbB2 mice was 399 days (Log rank $p<0.0001$).

3.1.2 Loss of cIAP2 leads to an increase in apoptotic cells

It was previously shown in the Pratt laboratory that, in a carcinogen-induced model, cIAP2 knockout resulted in a significant increase in the number of mammary tumour apoptotic cells. To determine if this was also the case in the ErbB2-induced model, tumour sections from mice with and without cIAP2 expression were subjected to TUNEL analysis (Figure 11A). The number of cells undergoing apoptosis in both groups of tumour sections was counted as described in the materials and methods. The results show that similar to the carcinogen-induced model, cIAP2 knockout significantly increased the number of tumour cells undergoing apoptosis (Figure 11B). In mice with normal cIAP2 expression, only 1.7% of the tumour cells were undergoing apoptosis, whereas in mice lacking cIAP2 expression, 8.14% of the tumour cells were apoptotic. The significance was determined using a Student's T-test.

3.1.3 The canonical and non-canonical NF-κB pathways are active in both types of mammary tumours

Previous work from the Pratt lab has shown that NF-κB nuclear activation is often variable depending on the type of tumour produced and that the canonical pathway is required for the formation of luminal mammary tumours (Pratt *et al.*, 2009). In the carcinogen-induced study, cIAP2 knockout resulted in variable activation of both the canonical and non-canonical pathways. We wanted to determine if loss of cIAP2 expression leads to differential activation of NF-κB canonical or non-canonical pathways when mammary tumours are induced by ErbB2; ErbB2 is thought to activate the non-

A

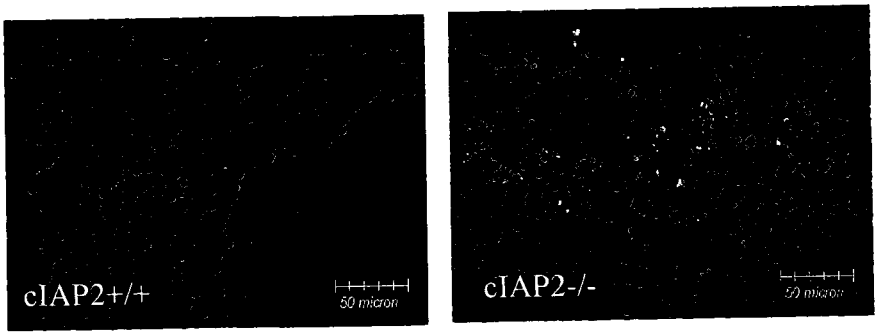
cIAP2+/+
50 micron
cIAP2-/-
50 micron

B

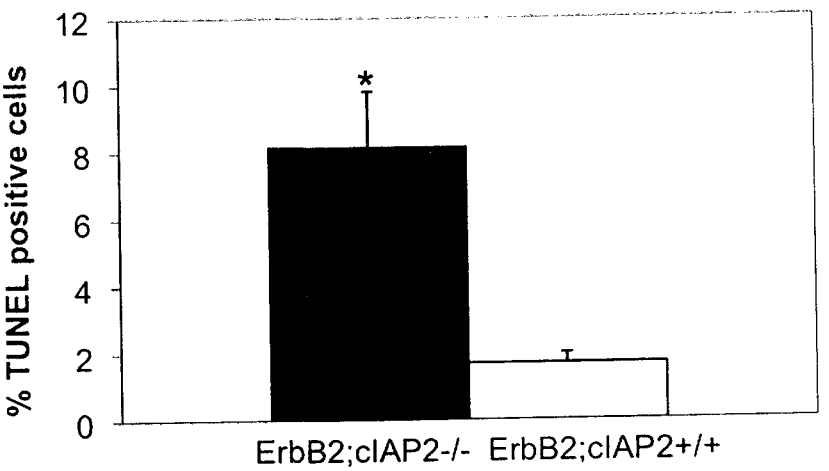
% TUNEL positive cells
12
10
8
6
4
2
0
*
ErbB2;cIAP2-/-
ErbB2;cIAP2+/+

Figure 11. TUNEL staining of apoptotic tumour cells from sectioned tumours. A, Frozen tumours from ErbB2 mice with or without cIAP2 gene expression were sectioned to 8μm with a cryostat and were subject to indirect TUNEL, utilizing an anti-digoxigenin antibody with a rhodamine fluorochrome, then counterstained with DAPI. Scale bar is 50 microns. **B,** Percentage of tumour cells showing apoptosis from frozen tumour sections of ErbB2 +/- mice with and without cIAP2 expression. Tumours with cIAP2 expression exhibited a mean percentage of apoptotic cells of 1.70 +/- 0.30 (n=14) whereas tumours lacking cIAP2 expression had a mean of 8.14 +/- 1.67 (n=14). Statistical significance was determined by Student's T test (*p=0.0008).

canonical NF-κB pathway through NIK (Chen *et al.*, 2003). To do this, tumour sections were subject to immunohistochemical analysis using antibodies against the canonical pathway protein p65 and the non-canonical pathway protein RelB. Although NF-κB activation was extremely variable, both the canonical and non-canonical pathways were active in tumours from mice with and without cIAP2 expression (Figure 12A). This variability in NF-κB activation (positive signal in the nucleus, not the cytoplasm) in the tumour sections was expected based on studies previously done in the lab.

To further assess NF-κB activation in mammary tumours, an electrophoretic mobility shift assay (EMSA) was performed using an NF-κB consensus sequence on nuclear extracts from representative tumours from MMTV-ErbB2 mice with and without cIAP2 expression (Figure 12B). Mouse mammary gland nuclear extract from MMTV-ErbB2 mice was used as a control. EMSA of the Sp1 probe was used as a relative loading control for the tumour nuclear extracts. Nuclear extract loading was not equivalent; however, NF-κB DNA binding activity was detected in samples with and without the expression of cIAP2. Thus, loss of cIAP2 did not lead to a significant difference in the two signaling pathways leading to NF-κB nuclear translocation and activation.

3.1.4 Characterization of cIAP2 knockout tumours

Previously, the Pratt lab found that when cIAP2 was knocked out in a carcinogen-induced mammary tumourigenesis model, the resulting tumours were mitotic and were associated with inflammation; this was measured by immunohistochemical staining of tumour sections using a phospho histone H3 antibody and an antibody to CD68,

A

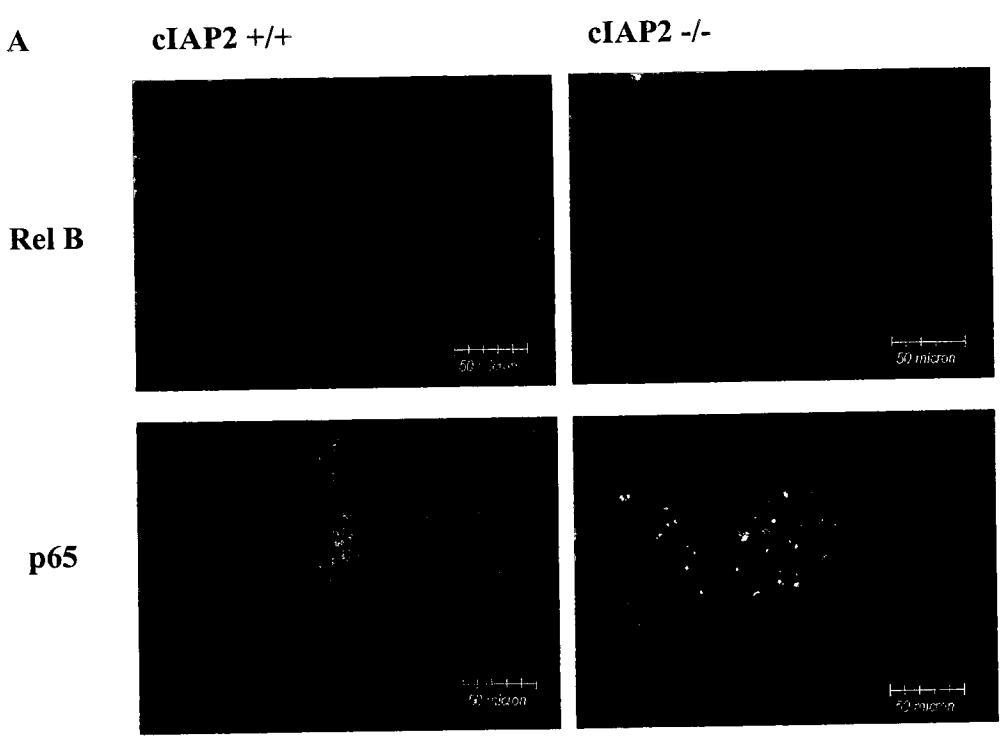

B

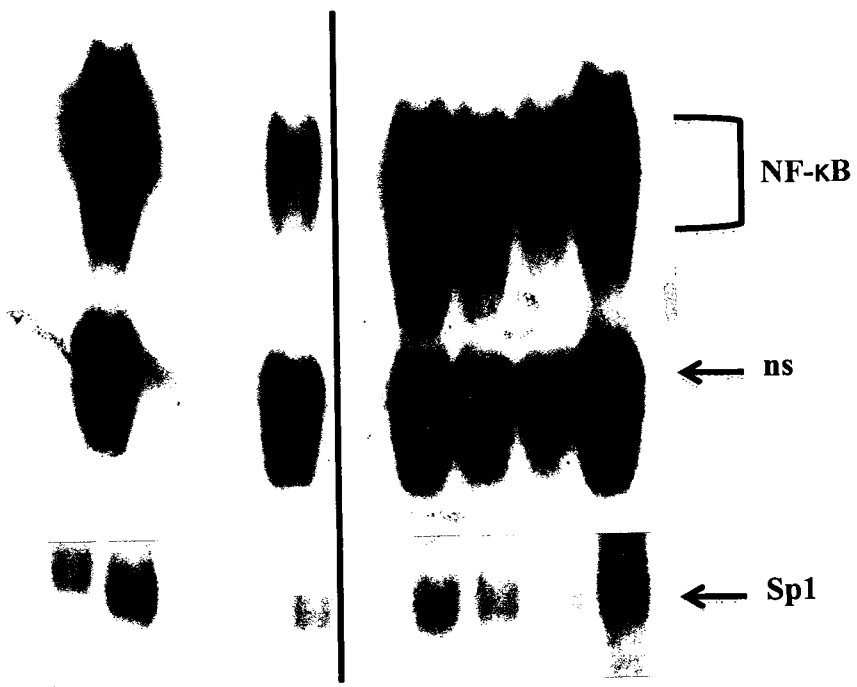

Figure 12. NF-κB activation in ErbB2-induced tumours in mice with and without cIAP2 expression. **A**, Immunohistochemical analysis of canonical (p65) and non-canonical (RelB) NF-κB expression of 8μm frozen tumour sections using anti p65 or RelB antibodies (CY3) then counterstained with DAPI. Scale bar is 50 microns. **B**, NF-κB DNA binding was assessed by EMSA using nuclear extracts from the mice with and without cIAP2 expression. Mouse mammary gland (MG) from MMTV-ErbB2 mice was used as a control. An Sp1 probe was used as a control for nuclear extract loading. ns – non specific binding.

respectively. To determine if knockout of cIAP2 resulted in the same outcome in the ErbB2-induced model, tumour sections from mice with and without cIAP2 were subject to immunohistochemical analysis using the same antibodies. During mitosis, histone proteins in the nucleosome become phosphorylated to allow for the condensation of DNA in the nucleus (Workman and Kingston, 1998). Staining with the antibody phospho-histone H3 can thus be used to measure the level of cellular growth or the cellular mitotic index. Unlike in the carcinogen induced model, tumours from mice with and without cIAP2 expression showed no difference in levels of cellular growth (See Appendix A.4; these sections were stained by Min Ying Niu, a Pratt Lab technician. I analyzed the results of this experiment). The increase in phospho histone H3 and cellular growth that was detected in the carcinogen-induced model was hypothesized to be a mechanism that the tumour cells acquired to overcome the increase in apoptotic cells resulting from loss of cIAP2 expression. This was not the case in the MMTV-ErbB2 induction model; however, to confirm this, tumour immunohistochemistry using an antibody to Ki67 could be performed (see discussion).

The antibody CD68 was used to determine the levels of TAM infiltration in the tumour sections; representative tumour from both cIAP2 wild type and knockout sections were stained and the staining was compared visually. Anti-CD68 stains for a transmembrane glycoprotein that is present at high levels in monocytes and tissue macrophages, which are often present at high levels in aggressive tumours (Leek and Harris, 2002). In the carcinogen-induced model, the tumours were highly inflammatory. The Pratt lab hypothesized that tumour inflammation was caused by the ROS production associated with the carcinogen DMBA (see introduction, based on the mechanism of

action of DMBA), leading to high levels of macrophage infiltration. The tumours that were induced by ErbB2 were not inflammatory and knockout of cIAP2 did not increase the amount of TAM infiltration (see Appendix A.4; the sections were stained by Min Ying Niu, a Pratt lab technician; I analyzed the results of this experiment). There was no significant difference in CD68 staining in either tumour type.

Since cIAP2 knockout tumours were able to form without increasing the amount of cellular growth, despite the fact that they were highly apoptotic, we thought that the resulting tumours may exhibit an increase in the number of tumour-associated blood vessels; the blood vessel infiltration would allow for tumour cells to have access to more nutrients to allow for mass formation. This was done using an antibody against CD31. CD31, also known as platelet endothelial cell adhesion molecule 1 (PECAM1), is a type I integral membrane glycoprotein and a member of the immunoglobulin superfamily of cell surface receptors. It is constitutively expressed on the surface of endothelial cells, and concentrated at the junction between them. CD31 can be used to measure angiogenesis in association with tumour recurrence (DeLisser *et al.*, 1997). In the current study, preliminary data suggests that cIAP2 knockout resulted in an increase in the number of blood vessels in the tumour compared to wild type. Representative staining is shown in Figure 13; 2-3 microscopic fields of view from eight sections from cIAP2 wildtype and eight sections from cIAP2 knockout mice were analyzed for CD31 staining. These data will need to assessed by pathology to determine if the increase in the number of tumour blood vessels is statistically significant; the blood vessels were difficult to count based on the branching and immature vessel structure present in the tumour sections.

A

cIAP2+/+

cIAP2-/-

CD31

Figure 13. ErbB2-induced tumours in mice lacking cIAP2 expression appear to exhibit an increase in vascularization. A, Immunohistochemical analysis of tumour sections to determine blood vessel infiltration using an anti-CD31 antibody (CY3), counterstained with DAPI. A representative image is shown. Scale bar is 100 microns.

In tumours from cIAP2 knockout mice, large blood vessels were visible under the microscope while wild type tumours exhibited smaller blood vessels overall.

The cIAP2 knockout tumours were further characterized by immunoblot analysis. As previously stated, it was found by immunohistochemistry that both the canonical and non-canonical NF-κB pathways were active regardless of the expression status of cIAP2 (Figure 12). To confirm these results, a Western blot on cIAP2 WT and knockout mammary tumour protein was done using an antibody to phospho-IKKα/β. Expression of phosphorylated IKK-α would suggest that the non-canonical NF-κB pathway has been activated during tumourigenesis, whereas expression of IKK-β would correspond to NF-κB activation through the canonical pathway. The Western blot analysis using the phospho-IKKα/β antibody confirmed the immunohistochemical analysis: both the canonical and non-canonical pathways were active in both types of mammary tumours and there was no difference in expression levels between cIAP2 WT and knockout tumour protein (Figure 14A). There was also no detectable difference between the levels of total IKK-β protein between the two sets of tumour protein samples, which confirmed that there was not an increase in phospho-IKKβ protein expression and activation of the canonical pathway.

The status of p27 protein expression was also analyzed by immunoblot analysis. The p27 protein is a member of the kinase inhibitor protein (kip) family that also includes p21 and p57; it is an inhibitor of cyclin dependent kinase (CDK). CDK proteins regulate cell cycle progression by integrating mitogenic and growth inhibitory signals, allowing the cell to progress through the various cell cycle checkpoints and to complete the cell

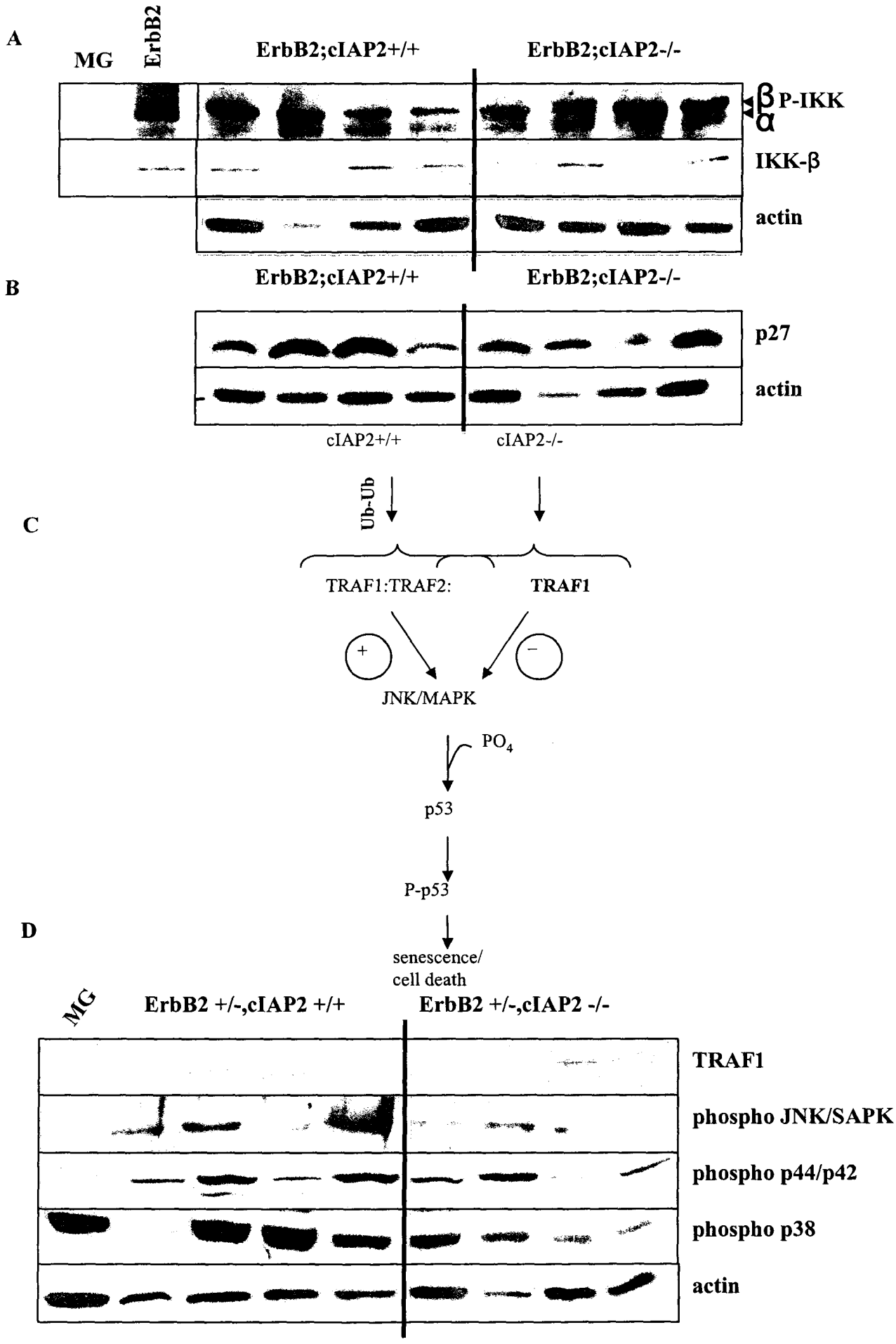
A
MG
ErbB2
ErbB2;cIAP2+/+
ErbB2;cIAP2-/-
β
α
P-IKK
IKK-β
actin
B
ErbB2;cIAP2+/+
ErbB2;cIAP2-/-
p27
actin
cIAP2+/+
cIAP2-/-
C
Ub-Ub
TRAF1:TRAF2:
TRAF1
+
−
JNK/MAPK
PO4
p53
P-p53
senescence/
cell death
D
MG
ErbB2 +/-,cIAP2 +/+
ErbB2 +/-,cIAP2 -/-
TRAF1
phospho JNK/SAPK
phospho p44/p42
phospho p38
actin

Figure 14. Western blot analysis of tumour protein from ErbB2-induced tumours with and without cIAP2 expression. Twenty μg of protein extracts from tumours were used for analysis. **A**, Protein extracts of tumours from (i) normal mammary gland (MG), (ii) ErbB2 normal mammary gland (ErbB2) and (iii) ErbB2 tumours with and without cIAP2 expression were immunoblotted with anti-phospho IKKα/β (top panel), anti-total IKK-β (middle panel) and anti-actin as a loading control. **B**, Protein extracts from ErbB2 tumours with and without cIAP2 expression were subject to immunoblot analysis using an anti-p27 antibody and anti-actin as a loading control. **C**, The ratio of TRAF1 and TRAF2 may alter kinase activity. cIAP2 interacts with TRAF1 protein, leading to an alteration in MAP kinase activity and changes in cellular survival. **D,** Twenty μg of protein extracts from (i) normal mammary gland (MG) and ErbB2 tumours from mice with and without protein expression were subject to immunoblot analysis using anti-TRAF1 (top panel), anti-phospho JNK/SAPK (second panel), anti-phospho p44/p42 (middle panel), anti-phospho p38 (fourth panel) and anti-actin (bottom panel) as a loading control.

cycle (Chiarle *et al.*, 2001). Loss of p27 has been shown in many tumour types; although rare in breast cancer, loss of p27 may increase mortality (Spirin *et al.*, 1996). The levels of p27 expression were evaluated to determine if loss of cIAP2 in the ErbB2-induced mammary tumourigenesis model could result in loss of p27 expression; if p27 protein expression is decreased or lost, this could provide evidence that the tumour cells have acquired an increase in aggressiveness via an increase in the rate of cell cycle progression. This, however, was not the case; p27 protein expression levels were unchanged regardless of cIAP2 expression status (Figure 14B). These results corroborate the immunohistochemical results using phospho-histone H3 (as previously stated, shown in appendix A4), which showed that the growth of both tumour types was similar.

Since the immunoblots done on the cIAP2 knockout mouse tumour protein were only partially informative, we decided to look at the expression of protein levels from other cIAP2 related pathways to determine other differences between cIAP2 WT and knockout tumours. The cIAP2 protein is involved in the TNFR signaling pathway through interaction with TRAF proteins; in the cell, the ratio of TRAF1 and TRAF2 can alter kinase activity resulting in cellular apoptosis. cIAP2 is capable of ubiquitylating the TRAF1 protein; when TRAF1 levels are low, TRAF2 can activate the phosphorylation of a number of MAP kinases, leading to apoptosis (Karin and Gallagher, 2009; Lee *et al.*, 2004). If cIAP2 expression is lost, there is a stabilization of the TRAF1 protein, leading to a decrease in MAP kinase expression and activity and an increase in cellular survival (Figure 14C). To determine if these series of events occurred during ErbB2-induced mammary tumourigenesis when cIAP2 was knocked out, immunoblots were done using anti-TRAF1 and TRAF2 antibodies. Unfortunately, TRAF2 Western blot analysis was

unsuccessful due to poor antibody quality. It was found that when cIAP2 was knocked out, there was no TRAF1 stabilization (Figure 14D). To determine if cIAP2 knockout resulted in a decrease in MAP kinase signaling, antibodies against phosphorylated p44/p42 (also known as extracellular signal related kinases (ERK) 1 and 2), and the stress activated kinases phospho-p38 and phospho-stress-activated protein kinase/c-Jun NH2-terminal kinase (SAPK/JNK) were used for Western blot analysis of tumour protein from cIAP2 WT and knockout mice. It was found that there was a decrease in the expression of activated SAPK/JNK, p42 and p38. Although that TRAF1 Western suggests that there is no TRAF1 stabilization, the results from the MAP kinase Westerns suggest that there should be since the activation of MAP kinases decreased when cIAP2 was knocked out. These results, however, cannot be fully verified since Western blot analysis of total protein was not completed. The decrease in phosphorylated proteins seen could be due to a decrease in the amount of total protein present in the tumour samples; if there were less total protein present, then less phosphorylated product would also be present. This could account for the discrepancy suggested by the TRAF1 Western.

3.2 The role of NF-κB activation in mouse MaSCs and TICs

3.2.1 NF-κB activation is limited to luminal cells in the normal mammary gland

In order to determine where NF-κB expression is localized in normal mouse mammary gland, NF-κB protein expression analysis via immunofluorescence was done on mammary gland sections from virgin female *cis*-NF-κB^{EGFP}reporter mice. Mammary gland sections from female mice were permeabilized and incubated an anti-NF-κB p65 primary antibody and a CY3 conjugated secondary antibody. Active (nuclear) NF-κB

p65 expression was localized to the inner luminal mammary cell layer, where the mammary luminal stem cell population is found (Figure 15, 2nd row of figures). The mammary gland sections were also incubated with an anti-EGFP antibody. In the *cis*-NF-κB^{EGFP}reporter mice, EGFP expression occurs in cells that have active NF-κB expression. Cells that were positive for EGFP expression were also limited to the mammary gland luminal cell layer (Figure 15, 4th row of figures). The luminal restricted expression of NF-κB in the mammary gland may be important to regulated cell survival; it is not known if NF-κB expression is needed for stem cell survival as well (Clarkson *et al.*, 2000).

3.2.2 Characterizing mammary stem cell populations

In a recently published study, Stingl *et al.* (2006) used a magnetic stem cell separation technique to isolate and characterize cell populations enriched for mammary progenitors and stem cells. Using CD24 and CD49f labeling and flow cytometry, they found two distinct populations in the mammary gland (as previously described): MRUs, characterized by CD24^{med}CD49f^{high} expression, and Ma-CFCs, with CD24^{high}CD49f^{low} staining. To determine if NF-κB expression is limited to one stem cell type, the technique used in the Stingl *et al.* (2006) paper was exploited using the EasySep® technique as described in the Materials and methods. The mammary gland stem cell populations were to be analyzed for EGFP expression to see what cell type showed NF-κB activation. The non-epithelial cells were removed from the single cell suspension,

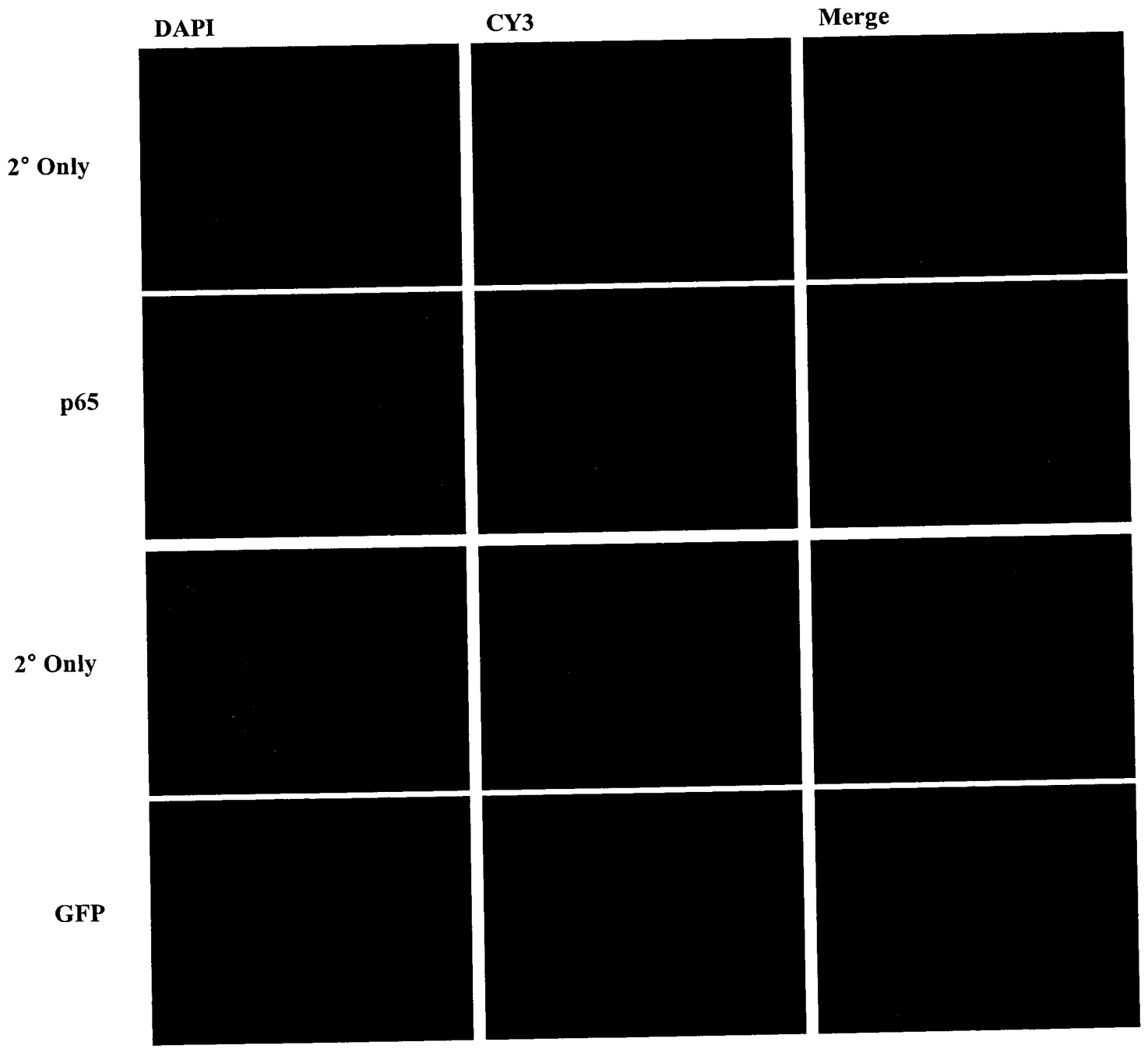
DAPI
CY3
Merge
2° Only
p65
2° Only
GFP

Figure 15. NF-κB expression is limited to luminal mouse mammary cells. Mammary glands from *cis*-NF-κB^{EGFP} reporter mice were cryosectioned to 8 microns, and using p65 and GFP antibodies, NF-κB expression was analyzed by immunofluorescence, and counterstained with DAPI. Staining was visualized with a CY3 conjugated secondary. As a control, mammary glands were incubated with the secondary antibody only. 40X magnification.

enriching the stem cell population, followed by labeling with CD49f AlexaFluor and CD24 PE antibodies. The CD49f antibody provided in the EasySep kit was FITC conjugated, which could not be used, as the emission and excitation wavelengths are the same as those for EGFP. Thus, a CD49f Alexa Fluor antibody was used instead. Since the antibody concentration needed for proper labeling was not known, the concentration of antibody was varied (titrated) and used in FACS analysis. The cells were incubated with no antibody (Figure 16A), 1X antibody (Figure 16B, 1X=10ul antibody/10^7 cells), 2X antibody (Figure 16C), 4X antibody (Figure 16D) and 8X antibody (Figure 16E). The 8X concentration of antibody was found to give the best separation of the three mammary stem cell populations, $CD49f^{high}$, $CD49f^{low}$ and $CD49f^{neg}$ without shifting the negative cell population, and was the concentration used for flow cytometry in the FACS analysis that followed.

3.2.3 NF-κB activation is limited to the Ma-CFC population

The mammary stem cell populations were separated bys FACS analysis based on the expression of CD24 and CD49f as described by Stingl *et al*, 2006. For the expression of CD24, the cells were labeled with no antibody (Figure 17A), and CD24 antibody at the concentration outlined in the Materials and methods (17B). The first box (R6) represents cells that are labeled low to medium with CD24, while the second box (R8) represents cells with high CD24 reactivity. The stem cells were also analyzed for CD49f expression; Figure 17C represents cells that were labeled with no CD49f antibody, and 17D cells that were labeled with 8X CD49f. The first box (R7) represents those cells with low reactivity with CD49f while the second box (R5) represents those with high

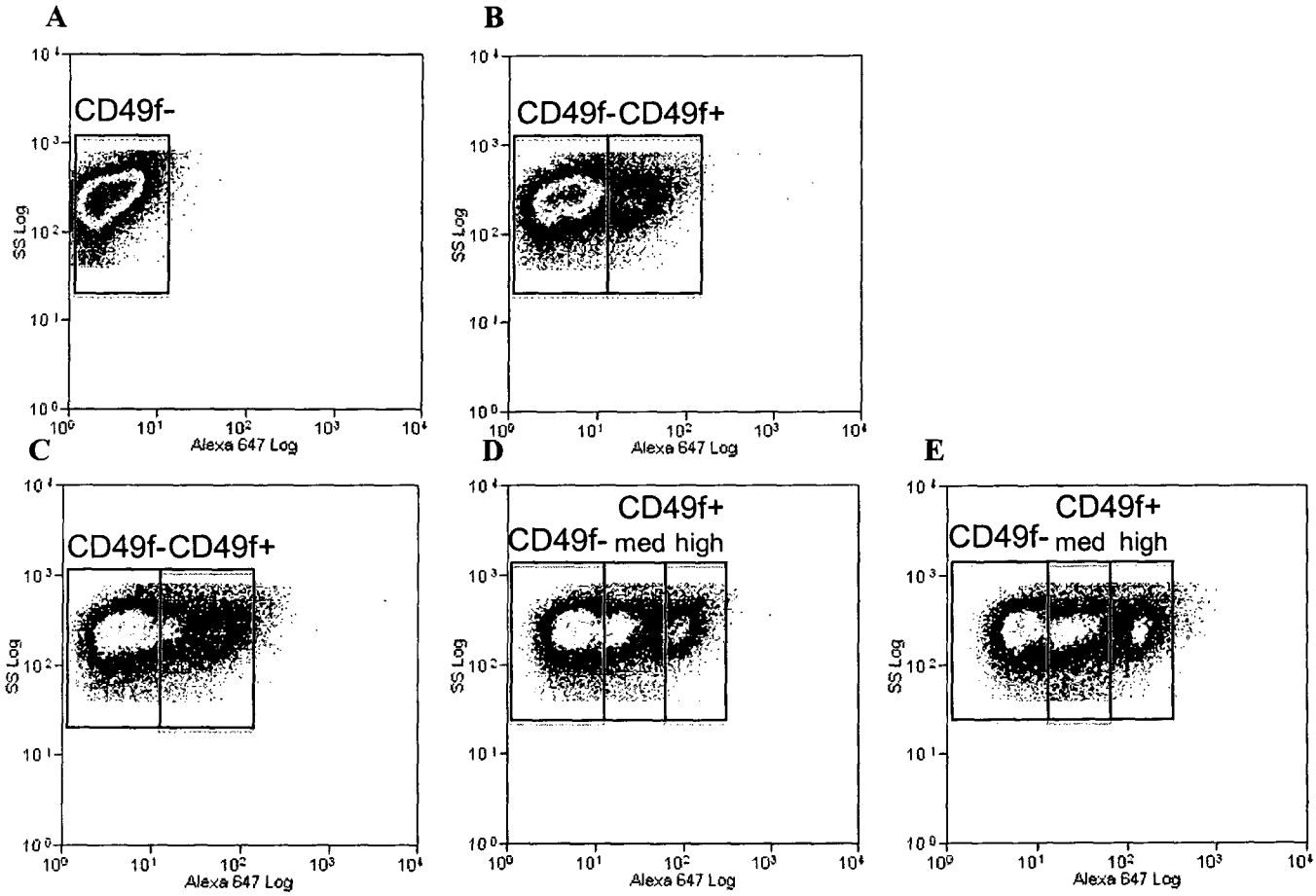
A
CD49f-
B
CD49f-CD49f+
C
CD49f-CD49f+
D
CD49f+
CD49f- med high
E
CD49f+
CD49f- med high
SS Log
Alexa 647 Log

Figure 16. Anti-CD49fAlexaFluor antibody titration using an enriched mammary stem cell fraction from *cis*NF-κB^{EGFP} normal mammary gland. Mammary epithelial cells from female mice were labeled with increasing amounts of anti-CD49fAlexaFluor to determine the best antibody concentration (note 1X=10ul antibody/10^7 cells). Labeled cells were analyzed by flow cytometry. **A**, No antibody label. **B**, 1X CD49f antibody. **C**, 2X CD49f antibody. **D**, 4X CD49f antibody. **E**, 8X CD49f antibody. The 8X antibody concentration gave the clearest separation of the populations of progenitor and stem cells expected after CD49fAlexaFluor staining (negative, low and high, based on Stingl *et al.*, 2006), without shifting the negative cell population.

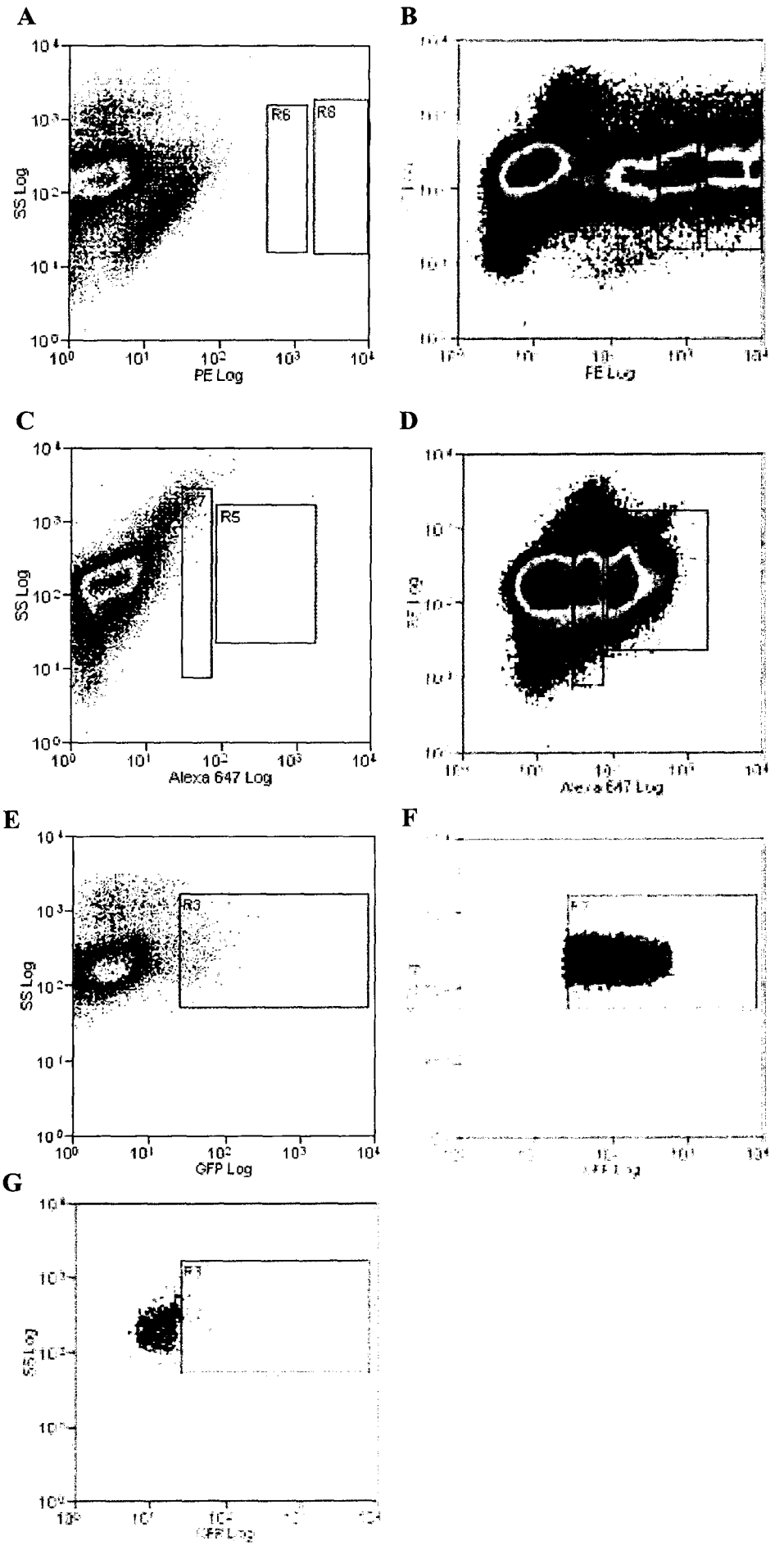
A
B
C
D
E
F
G
R6
R8
R7
R5
R3
SS Log
PE Log
Alexa 647 Log
GFP Log

H

Cell Type	Ma-CFC	MRU
Surface Antigen	$CD24^{high}$ $CD49f^{low}$ (R8+R7)	$CD24^{med}$ $CD49f^{high}$ (R6+R5)
Sorted Number	1.81E+04	9.44E+03
Sort Rate	5.67%	2.95%
Abort Rate	0.85%	0.36%
Total Sorted	3.19E+05	
GFP Positive	100%	6%

Figure 17. NF-κB expression is almost exclusively limited to the Ma-CFC mammary stem cell fraction. FACS analysis of mammary stem cell populations from *cis*-NF-κB^{EGFP} reporter mice labeled with CD24PE and CD49f AlexaFluor antibodies. **A**, Mammary stem cells unlabeled (CD24 sort). **B**, CD24 antibody labeling of mouse mammary stem cells. The first box (R6) represents cells that are labeled low to medium with CD24, while the second box (R8) represents cells with high CD24 reactivity. **C**, Mammary stem cells unlabeled (CD49f sort). **D**, CD49f labeling of mouse mammary stem cells. The first box (R7) are those cells with low reactivity with CD49f while the second box (R5) are those with high reactivity with the CD49f antibody. **E**, Analysis of the MRU fraction (R6 – CD24^{med}, R5 – CD49f^{high}) of the mouse mammary stem cell population for EGFP fluorescence. **F**, EGFP expression in the Ma-CFC fraction (R8 – CD24^{high}, R7 – CD49f^{low}) of the mouse mammary stem cell population. **G,** EGFP analysis of wild type mammary gland. **H**, Analysis of FACS sorted cells. Sort rate is the percentage of total sorted cell that labeled as Ma-CFC or MRUs. Abort rate is the percentage of cells that were unable to be sorted by flow cytometry. All of the Ma-CFCs (luminal-like progenitors) were positive for EGFP fluorescence, or active NF-κB., whereas only 6% of the MRUs (basal-like stem cells) were positive for EGFP fluorescence.

reactivity with the CD49f antibody. Based on the expression of CD24 and CD49f, the cells were separated into MRU fraction (R6 – $CD24^{med}$, R5 – $CD49f^{high}$), and the Ma-CFC fraction ((R8 – $CD24^{high}$, R7 – $CD49f^{low}$) an analyzed for EGFP expression (MRU, Figure 17E; Ma-CFC, Figure 17F). Mammary stem cells from WT mice were also analyzed for EGFP expression to ensure that no EGFP signal was detected and to establish a baseline of background fluorescence (Figure 17G). It was found that only 6% of the MRUs sorted were positive for EGFP, whereas 100% of the Ma-CFCs analyzed had EGFP fluorescence (Figure 17H), suggesting that active NF-κB is limited to the luminal stem cell population.

Attempts to repeat the FACS analysis of MRU and Ma-CFC populations in the NF-κB reporter mice were unsuccessful. The mammary stem and progenitor cells appeared to stop expressing the EGFP protein, thereby losing EGFP fluorescence (Appendix A.5). However, in the experiments that worked, the sorted MRU and Ma-CFC fractions were spun down onto glass slides using a Cytospin centrifuge and were incubated with anti-NF-κB p65 antibody. Visualization was done using a CY3 conjugated secondary antibody (Figure 18A). The luminal Ma-CFC fraction was positive for p65, while the MRU population did not have nuclear p65 expression, replicating the FACS analysis results. The number of cells that were positive for nuclear p65 expression in both populations was counted; Ma-CFCs exhibited nuclear NF-κB staining in 75.8% of cells whereas MRUs showed NF-κB staining in 9.4% of cells (Figure 18B, $p<0.001$ by Student's t test).

A

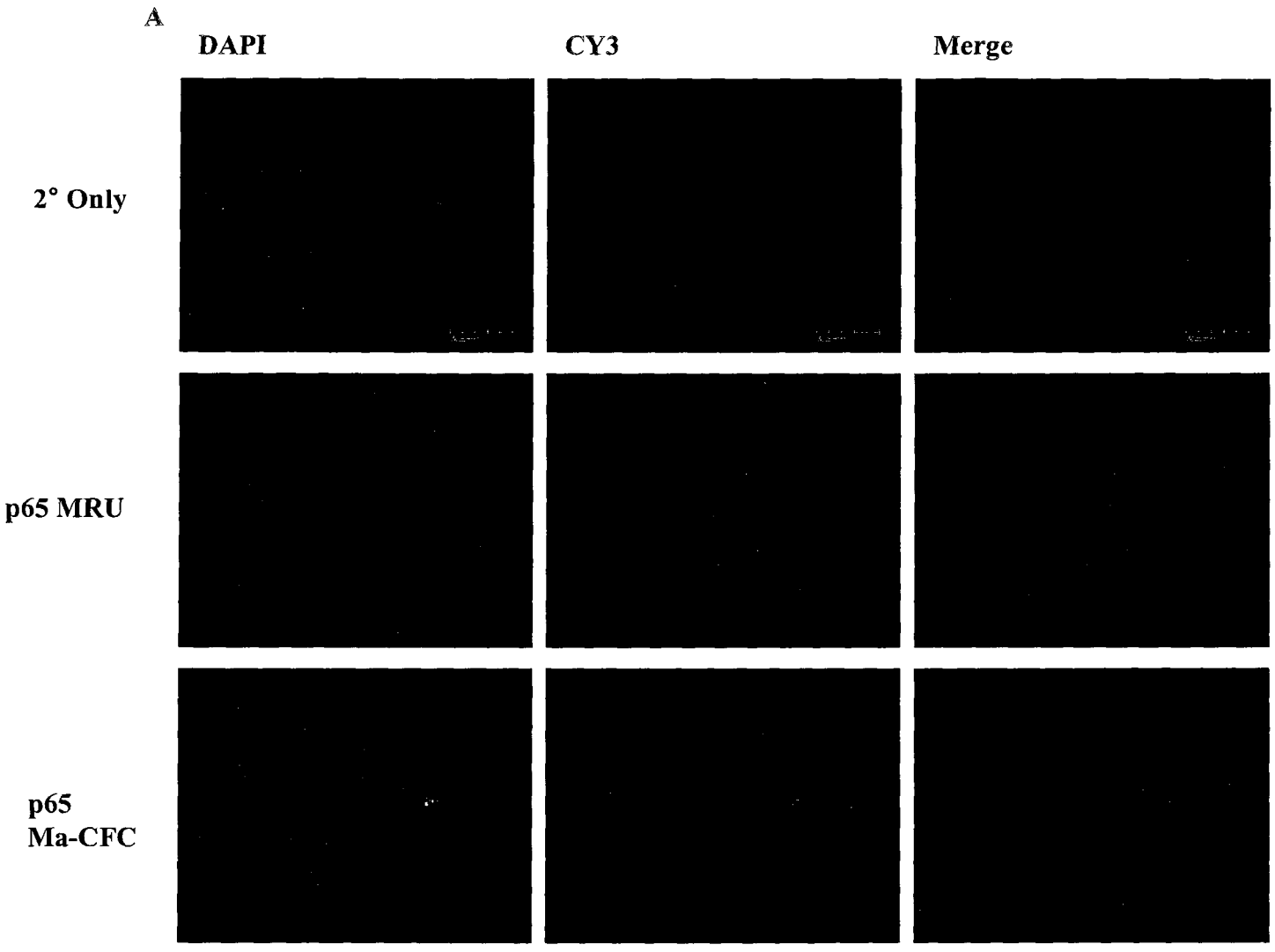
DAPI
CY3
Merge
2° Only
p65 MRU
p65
Ma-CFC

B

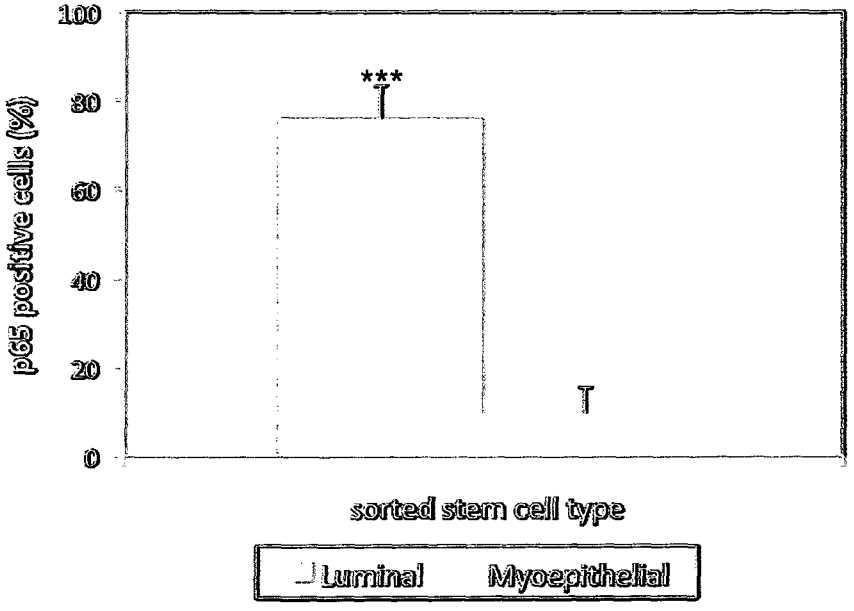
100
80
60
40
20
0
p65 positive cells (%)
***
sorted stem cell type
Luminal
Myoepithelial

Figure 18. Immunofluorescent analysis of FACS sorted mammary stem cells from *cis*-NF-κB^{EGFP}reporter mice. **A**, Cells spun onto glass slides using a cytospin centrifuge and p65 staining was visualized using a fluorescent microscope. p65 positive cells were visualized using a CY3 conjugated secondary antibody. As a control, cells were labeled with secondary antibody only. 40X magnification. **B**, p65 positive Ma-CFCs (luminal) and MRUs (myoepithelial) (those showing nuclear p65 staining) and those without NF-κB were counted. Ma-CFCs exhibited nuclear NF-κB staining in 75.8% (+/-7.5) of cells whereas MRUs showed NF-κB staining in 9.4% (+/-6.0) of cells. ***$p<0.001$ by Student's t test.

3.2.4 ErbB2-induced mammary tumours showed variable NF-κB expression

To look at the NF-κB expression status in CD44+ TICs, *cis*-NF-κB^{EGFP}reporter mice were crossed with MMTV-ErbB2 transgenic mice. These mice were palpated weekly until mammary tumour formation, which occurred around 8-12 months of age. Previous results from our lab have shown variable NF-κB expression in ErbB2-induced tumours. To confirm the NF-κB expression, sections from ErbB2-induced tumours from cis-NF-κB^{EGFP}reporter mice were incubated with anti-p65 antibody (Figure 19, arrows). The tumours were also incubated with an anti-ErbB2 antibody to confirm that presence of ErbB2; ErbB2 would be expressed on the surface of the cell membrane as it is a member of the EGFR family; its active form is typically assessed using a phospho-ErbB2 antibody. ErbB2 expression was variable; this has been previously reported (Figure 19). Transgenic MMTV-ErbB2 mice exhibit non-uniform transgene expression in the mammary gland epithelium (Muller *et al.*, 1996). It is unknown if the NF-κB positive cells were also CD44 positive, as the CD44 antibodies available are not compatible with frozen sections.

3.2.5 Analysis of CD44+ TICs

The remainder of the ErbB2 induced tumours was used to create a single cell suspension of the tumour cells, as described by Liu *et al.* (2007). This was done to determine if the NF-κB positive cells were also CD44 positive. The tumours were

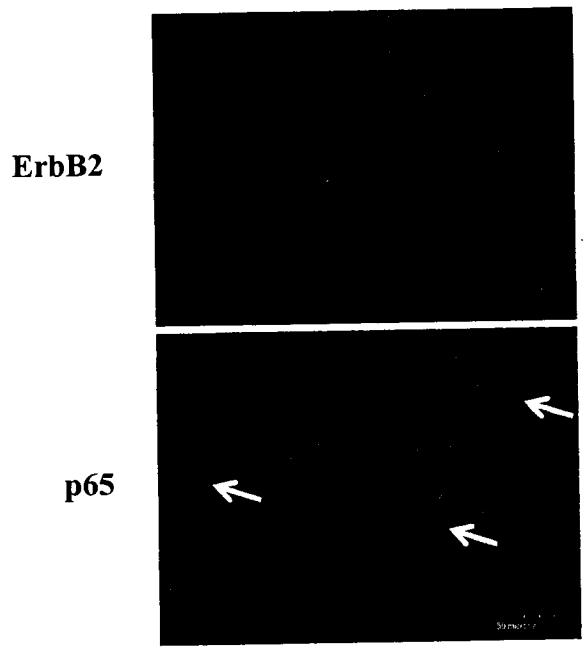
ErbB2
p65

Figure 19. Immunofluorescent analysis of ErbB2 induced tumours in *cis*-NF-κB^{EGFP}reporter mice. Mammary tumours were cryosectioned to 5 microns and NF-κB p65 nuclear activation and ErbB2 protein expression was analyzed using p65 and ErbB2 antibodies and CY3 conjugated secondary antibodies, and counterstained with DAPI. ErbB2 expression was variable, as was nuclear NF-κB (arrows). Magnification 40X.

dissociated for 2 hours at 37°C, and the Lin- cells were isolated using the EasySep® procedure followed by labeling with a CD44 AlexaFluor antibody and FACS analysis (Figure 20). The concentration of antibody used was varied to determine the optimal concentration: no label (Figure 20A), 0.5X (Figure 20B), 1X (Figure 20C) and 2X (Figure 20D; in all cases, X=0.2μg/10^6 cells). Unfortunately, all concentrations of antibody used were not optimal, but since a CD44 negative cell population was not used during labeling (like normal mammary cells), the correct cell antibody concentration could not be determined.

Despite the fact that the negative cells were also stained with the CD44 antibody, the positive cells were sorted (based on the R5 box represented CD44 positive cells) (Figure 20E). The positive cells were selected conservatively to limit the number of CD44 negative cells present. The CD44 positive cells were analyzed for EGFP expression (Figure 20F). Unfortunately, although the presence of the EGFP reporter gene was confirmed prior to the tumourigenesis study by genotyping, the presence of EGFP was not detected by FACS analysis; EGFP was only detected in 0.3% of sorted cells. Because of this problem, and because it was unclear if the CD44 positive cells were actually sorted correctly, the analysis of the CD44 positive population was not completed.

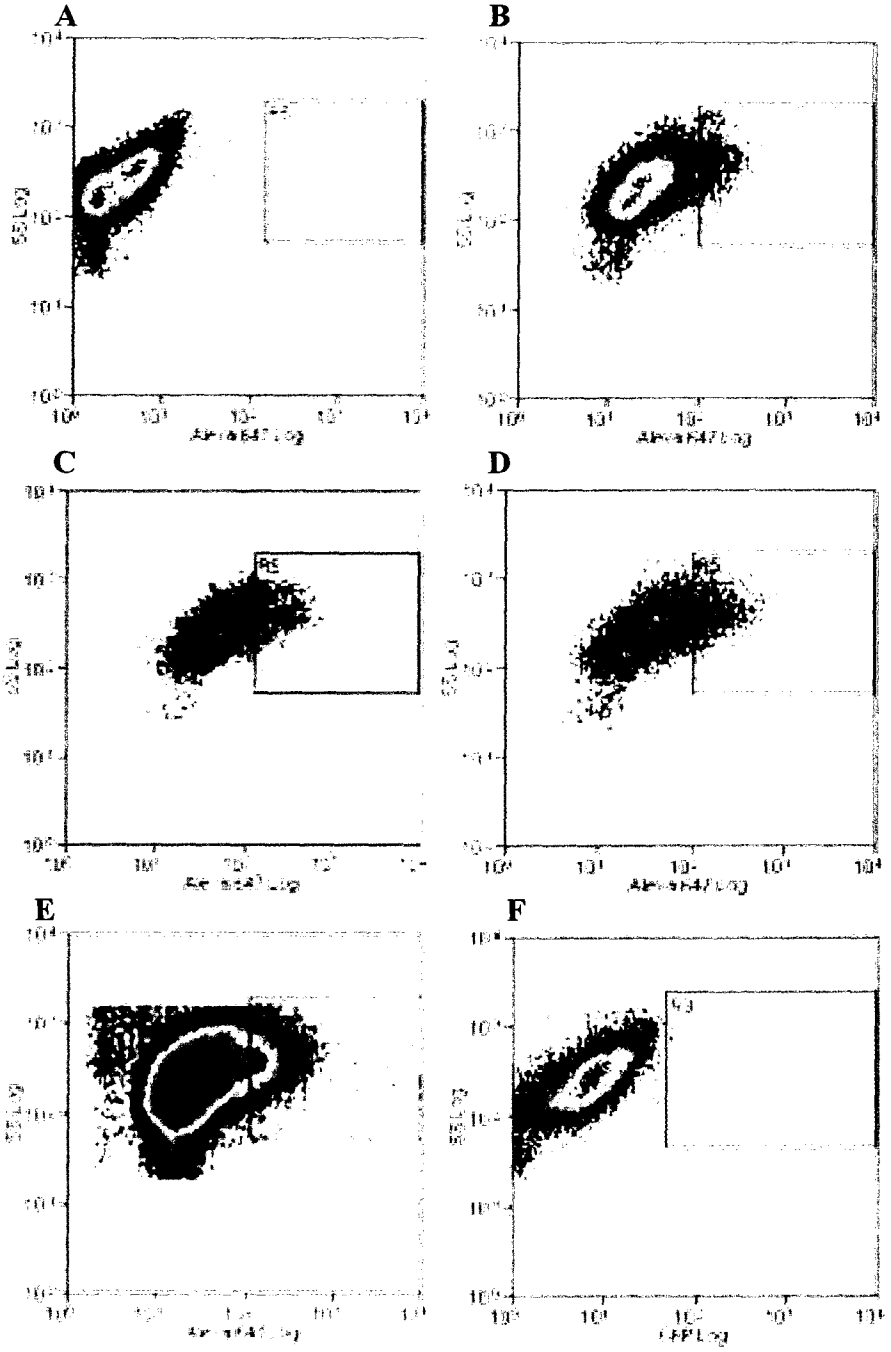
A
B
C
D
E
F

Figure 20. FACS analysis of ErbB2 induced tumours in *cis*-NF-κB^{EGFP}reporter mice using the TIC marker CD44. **A-D** CD44 Alexafluor antibody titration. **A**, Tumour cells with no label. **B**, Tumour cells labeled with 0.5X CD44 antibody (note 1X=10ul antibody/10^7 cells). **C**, Tumour cells labeled with 1X CD44 antibody. **D**, Tumour cells labeled with 2X CD44 antibody. **E**, EGFP analysis of CD44 sorted cells. EGFP was present in only 0.03% of CD44+ cells. **F**, CD44 positive cells sorted. Please note that in all panels, the R5 box represents the area where CD44 positive cells should be situated. This was based on previous flow cytometry experiments with CD44 positive breast cancer cells, such as that done by Shipitsin *et al.* in 2007. The R3 boxes in E and F are where EGFP positive cells should be. This box was selected based on previous FACS experiments done with mammary stem and progenitor cells.

CHAPTER FOUR

DISCUSSION

4.1 The role of cIAP2 in ErbB2-induced mammary tumourigenesis

Inappropriate apoptotic regulation contributes to a number of human diseases, and targeting proteins involved in apoptosis and cell growth regulation, such as IAPs and NF-κB, has recently become recognized as a potential disease therapy. A number of therapies based on the BIR-binding sequence of IAPs like cIAP1 and 2 have been shown to enhance the pro-apoptotic effects of other chemotherapeutic drugs, both *in vitro and in vivo* (Reed, 2000). Understanding the function of cIAP2 in mammary tumourigenesis may lead to appropriate therapies that are capable of reducing tumour growth through selective targeting of cIAP2 on its own.

It was difficult to ascertain exactly what occurred when cIAP2 was knocked out in mammary tumourigenesis. There appeared to be no change in either non-canonical or canonical NF-κB signaling when cIAP2 was knocked out in the ErbB2 transgenic mouse. As mentioned in the introduction, cIAP1 and cIAP2 have a role in the regulation of NF-κB signaling through a process involving the stabilizing of the kinase NIK (see Figure 9). In resting cells, NIK is degraded by cIAP1/2 mediated ubiquitination; it is recruited to a complex of cIAP1/2 and TRAF2 by TRAF3, and its degradation results in a decrease in NF-κB signaling (Baud and Karin, 2009). In cells where NF-κB signaling has been stimulated, cIAP1 and 2 no longer target NIK; instead, they target TRAF3 for degradation, leading to NIK stabilization and activation of both the non-canonical and canonical NF-κB pathways. In this study, knockout of cIAP2 did not alter NF-κB signaling; both cIAP1 and 2 have redundant roles in this type of NF-κB regulation. Since cIAP1 was not knocked out, the status of NF-κB expression was unchanged in the cIAP2 knockout tumours,

Both the IAP proteins cIAP1 and cIAP2 have also been implicated in TNFα-induced activation of NF-κB, even though cIAP2 upregulation can be downstream of NF-κB signaling (Mahoney *et al.*, 2008). TNFα is a cytokine involved in many biological processes, including the cellular response to inflammation and injury (Wajant, Pfizenmaier and Scheurich, 2003). TNFα signaling is achieved through binding to the TNFR-1, activating NF-κB and a proinflammatory signaling pathway. Upon TNFα binding, TNFR-1 recruits the TNFR-associated death domain (TRADD) protein and the receptor interacting protein 1 (Rip1). TRADD binding recruits TRAF2, forming a large complex at the cell membrane; this complex causes Rip1 to be modified with large polyubiquitin chains by an unknown E3 ligase (Ea *et al.*, 2006; Hsu *et al.*, 1996). The modification of Rip1 is essential for signal propagation; once this occurs, the IκB kinase heterocomplex and the transforming growth factor beta (TGF-β)-activated kinase 1 (Tak1) dock on Rip1. Tak1 phosphorylates IKKβ, which in turn leads to canonical NF-κB pathway activation; when this occurs, a number of prosurvival genes, including cIAP2, are activated (Micheau *et al.*, 2001). When NF-κB pathway activation does not occur, TNFR signaling can induce cell death via apoptosis. cIAP1 and cIAP2 both have the capacity to further activate NF-κB signaling and are required for the modification of Rip1. Thus, if cIAP2 is knocked out, there may be a modulation in amount of active (nuclear) NF-κB signal, leading to an increase in NF-κB signaling. This however was not the case in the current study. Since both cIAP1 and cIAP2 are capable of facilitating TNFα-mediated NF-κB activation, the presence of similar levels of NF-κB when cIAP2 is knocked out is probably due to the functional redundancy of cIAP1. A recent study suggests that cIAP1 may be the primary regulator of NF-κB activation by TNFα as it is

more abundantly and ubiquitously expressed in cells, and is less responsive to canonical NF-κB pathway activation (Mahoney *et al.*, 2008). cIAP2 may act as a back up when cIAP1 levels are too low. The cIAP2 antibodies currently available on the market do not distinguish between cIAP1 and cIAP2, thus it is unknown if there was an upregulation in cIAP1 upon cIAP2 loss.

Knockout of cIAP2 in a previous study using a carcinogen-induced tumourigenesis model resulted in an increase in tumour cell growth (or mitotic index) to compensate for the loss of cIAP2 signaling. In the current study, cIAP2 knockout in ErbB2-induced tumourigenesis resulted in no change in the levels of tumour cell growth. The results correlate with those obtained when the tumour was assessed for p27 expression levels. Loss of cIAP2 did not change the levels of p27 protein. Since p27 is a CDK inhibitor, a decrease in its expression would cause the cell to cycle through mitosis at a faster rate, increasing its growth and mitotic index (Toyoshima and Hunter, 1994). Deregulation and degradation of p27 is often seen in cancer, increasing the aggressiveness of the tumour cells (Chiarle *et al.*, 2001; Spirin *et al.*, 1996). The tumour cells lacking cIAP2 likely developed other mechanisms to compensate for the loss of cIAP2, most likely via the induction of angiogenesis as discussed below.

4.1.1. cIAP2 knockout increased tumour growth latency and apoptotic levels

In the current study, knockout of cIAP2 in the ErbB2-induced mammary tumourigenesis model lead to a significant increase in both cellular apoptotic levels as well as tumour growth latency. This increase in time to tumour appearance can be attributed to the fact that the cIAP2 null tumour cells are more likely to undergo

programmed cell death than cells with active cIAP2. However, tumour growth still did eventually occur, accompanied by an increase in both differentiated and poorly differentiated tumour-associated blood vessels. Upregulation of a number of other signaling pathways may have contributed to eventual tumour formation. EGFR (ErbB1) signaling through the oncogenic protein Ras has been shown to lead to upregulation of cIAP2 and another anti-apoptotic protein, X-linked inhibitor of apoptosis (XIAP) in intestinal epithelial cells (Liu *et al.*, 2005). XIAP and cIAP2 may work synergistically in ErbB2 positive tumours to promote tumour cell growth. Apoptotic inhibition by XIAP is similar to cIAP2 by reducing activation of caspase-3 and caspase-7 in the apoptotic signaling cascade (Deveraux *et al.*, 1997). Expression of XIAP has been associated with increased metastatic potential in primary cancer cells in culture and expression of XIAP in cancer cells may lead to the growth of more aggressive tumour cells (Liu *et al.*, 2005). XIAP upregulation may occur in tumours with and without cIAP2 expression; in the cIAP2 knockout tumours, upregulation of XIAP still may occur, but it is unable to work together with cIAP2 as expression of this protein has been lost. Upregulation of other anti-apoptotic proteins may account for the increased latency leading found in the current study that lead to eventual tumour growth.

A recent study has shown that upregulation of XIAP promotes NF-κB signaling and increased NF-κB activation through TGF-β (Neil *et al.*, 2009). Normally, TGF-β acts as a tumour suppressor; however, a number of cancers exhibit aberrant TGF-β signaling that leads to the conversion of TGF-β from a tumour suppressor to an oncogenic tumour promoter. In this study by Neil *et al.* (2009), metastatic 4T-1 breast cancer cells engineered to overexpress XIAP exhibited an increase is NF-κB activation

when stimulated with TGF-β; when cells without upregulation of XIAP were stimulated with TGF-β, a suppression of NF-κB activation occurred. XIAP was shown to interact with the TGF-β receptor, mediating a number of signaling events that lead to activation of p65/RelA, and the induction of a number of pro-metastatic genes (cyclooxygenase-2 and plasminogen activator inhibitor 1) and pro-survival genes (survivin). It would be interesting to know if the expression of XIAP and the pro-metastatic genes and pro-survival genes changes when cIAP2 is knocked out in the current study.

4.1.2 cIAP2 knockout and increased tumour angiogenesis

In this study, there is preliminary data suggesting that knockout of cIAP2 lead to an increase in the number of tumour blood vessels. During tumour formation and subsequent progression, malignant cells escape tissue control and resist anoikis, a form of apoptosis induced by anchorage-dependent cells detaching from the ECM (Chiarugi and Giannoni, 2008). A relationship develops between tumour cells and tumour stroma, which may exploit the host-immune response to promote angiogenesis and progression (Liotta and Kohn, 2001). The tumour cells secrete angiogenic factors that stimulate uncontrolled blood vessel formation to provide the tumour with much needed oxygen and nutrients, and favour increased tumour metastatic potential (Fox *et al.*, 2001). Changes within the tumour itself lead to resistance to anoikis (Simpson *et al.*, 2008); these changes may involve signaling through the PI3K signaling cascade, and through other host factors, including hepatocyte growth factor (HGF), and ERK signaling (Douma *et al.*, 2004; Galante *et al.*, 2008; Liotta and Kohn, 2004). Increased ErbB2 signaling, and subsequent NF-κB activation can also lead to increased blood vessel formation and

angiogenesis through stimulation of the cyclooxygenase-2 gene (COX-2), promoting increased tumour growth (Shishodia *et al.*, 2004). In the cIAP2 knockout mice, there may be an increase in the signaling events mediated by the tumour or the oncogene, leading to increased presence of angiogenic factors and blood vessel formation; these events are currently unknown, but further study will attempt to elucidate this novel pathway.

Tumour angiogenesis has significant prognostic value in many types of cancers, including breast cancer. Tumour angiogenesis is associated with poor prognosis and metastasis in a number of cancers, including invasive prostate carcinoma, early breast carcinoma, transitional cell carcinoma in the pelvis and ureter and melanoma (Craft and Harris, 1994; Inoue *et al.*, 2002; Weidner *et al.*, 1992; Weidner *et al.*, 1993). Targeting cIAP2 as a cancer therapy on its own may actually lead to a more aggressive tumour.

In previous studies in our lab, it was found that knockout of cIAP2 in a DMBA-induced tumourigenesis model lead to an increase in the levels of TAMs. TAMs are a major component of inflammatory infiltrate in many tumour types (Bingle *et al.*, 2002; Siveen and Kuttan, 2009; Yuan *et al.*, 2008). TAMs are a source of a number of growth-inducing cytokines, and can recruit angiogenic factors needed to allow for sufficient tumour cell growth. The presence of TAMs in the tumour environment is generally associated with poor prognosis in cancer because of their ability to promote tumour cell growth (al-Sarireh and Eremin, 2000). In the ErbB2-induced model presented herein, cIAP2 knockout was not associated with an increase in TAM production. These tumours have likely developed a signaling pathway promoting angiogenesis without the need for

TAM secretory factors. This pathway also appears to be independent of an increase in tumour cell growth.

To measure cellular mitotic index in this study, an antibody against phospho histone H3 was used. As outlined in the result section, histone proteins in the nucleosome become phosphorylated to allow for the condensation of DNA in the nucleus during mitosis (Workman and Kingston, 1998). Staining with the antibody phospho-histone H3 can thus be used to measure the level of cellular growth or the cellular mitotic index. Perhaps a more convincing way to measure cellular proliferation is to use an antibody against Ki67, a protein that is only associated with cellular proliferation (Scholzen and Gerdes, 2000). Expression of Ki67 is seen in the nucleus of cells in the G_1, S and G_2 phases of the cell cycle and is absent from cells in the G_0 phase Gerders *et al.*, 1984). Loss of cIAP2 in the oncogene-induced model presented here did not correspond to an increase is cellular proliferation as measured by phospho histone H3 staining. Loss of cIAP2 resulted in an increase in the number of apoptotic cells, although a tumour was still able to form. Staining with Ki67 would be beneficial to support the observations seen with the phospho histone H3 antibody.

4.1.3 cIAP2 knockout and ErbB2 signaling

Interestingly, preliminary data from this study suggests that knockout of cIAP2 resulted in a decrease in the number of cancer cells that express total ErbB2 and a corresponding decrease in the activation of the downstream protein, Akt as documented by Niu, M (2007), unpublished data (data not shown). Unlike other EGFRs, ErbB2 does not have a known activating ligand, but it can be activated via its own overexpression or

via transactivation by heregulin (Holmes *et al.*, 1992; Pierce *et al.*, 1991). Upon activation, ErbB2 becomes phosphorylated and bound to the sarcoma (Src) homology domain 2 (SH2) domain of the growth factor receptor bound protein-2 (Grb2), which binds to the guanine exchange factor, Son of Sevenless (Sos) (Bonfini *et al.*, 1992). This series of events activate expression of Ras, which leads to the stimulation of MAP-Erk kinase (MEK) and Erk1 and 2, and PI3K/Akt, kinases all responsible for mitogenesis (de Vries-Smits *et al.*, 1992; Downward, 1990; Howe *et al.*, 1992). Thus, Grb2 plays a vital role in the transduction of the mitogenic signals of overexpressed ErbB2 (Marais and Marshall, 1996). Inhibition of Grb2 protein expression leads to growth inhibition of cancer cells with high levels of ErbB2 overexpression (Lim *et al.*, 2000). Downregulation of Grb2 could therefore also lead to Akt inactivation in ErbB2 overexpressing cells. In our study, we have preliminary data suggesting that both ErbB2 and phospho-Akt were downregulated in mammary tumour samples lacking cIAP2 expression. The ErbB2 transgene is constitutively active in the MMTV-Neu/NDL1 transgenic; thus, analysis of total ErbB2 protein is sufficient to analyze ErbB2 activation. This downregulation could be due to a decrease in Grb2 expression levels; immunohistochemical analysis of tumour sections or immunoblot analysis of protein from both cIAP2 WT and knockout tumours could be used to detect the levels of Grb2 to determine if they change upon loss of cIAP2.

The decrease in ErbB2 expression and Akt activation in cIAP2 knockout cells could be directly related to the increase in apoptosis that occurred when cIAP2 was knocked out. The cells with high levels of ErbB2 could have been selected against, resulting in growth of tumour cells with relatively lower ErbB2 overexpression levels.

Immunohistochemical analysis using an anti-ErbB2 antibody to determine which cells have and do not have ErbB2 expression could provide further insight into what is occurring in ErbB2-induced mammary tumourigenesis when cIAP2 expression is knocked out.

The decrease in the expression of ErbB2 found in cIAP2 knockout mice could also be due to an age-dependent silencing of the transgene. In cIAP2 wildtype mice, the average tumour latency was 283 days. This latency increased to an average of 399 days in cIAP2 knockout mice. Tumours analyzed from wildtype mice were collected earlier than those from knockout mice, and it is possible that in cIAP2 knockout mice, an increase in transgene silencing occurred. In all mice in a given transgenic line, variegation in transgene expression is a frequently observed phenomenon (Robertson *et al.*, 1996). It has been documented that, with some transgenes, the proportion of cells expressing the transgene may decrease with time through a transgene silencing mechanism. In this study, the decrease in expression of MMTV-ErbB2 transgene observed in the cIAP2 knockout mice could be due to where the transgene inserted in the mouse genome; it is possible that there are repressor sites present near the MMTV promoter region or the decrease could be due to insertion of the transgene into a repressed promoter region. The transgene could also experience an increase in DNA methylation over time (resulting in a decrease in gene expression), or the transgene could be subject to X-inactivation (resulting in changes in gene expression between animals). The epigenetic effects of transgene expression could lead to transgene silencing over time (Palmiter and Brinster, 1986).

4.1.4 Summary and future directions

It is possible that when cIAP2 expression is knocked out, the tumour cells develop changes in TNFR and TRAF expression levels, leading to changes in expression of a number of kinases. The alteration in TRAF expression levels can lead to changes in tumour cells proliferation and survival. Although TRAF1 did not appear to be stabilized upon loss of cIAP2 protein expression, it appeared that this was the case as there was a decrease in phosphorylation of a number of kinases, including p44/p42 and SAPK/JNK. These conclusions can be made only after Western blots for total protein levels are completed, as the decrease in phosphorylated protein could be due to a decrease in total protein present. Assuming that the decrease is real, and to determine if this scenario is occurring when cIAP2 is knocked out, immunoblot analysis of TRAF2 expression levels in cIAP2 knockout and WT mice should be completed. Also, analysis of more tumour protein samples may provide insight into what exactly is occurring when cIAP2 is knocked out.

It is currently unclear as to what is occurring when cIAP2 expression is knocked out in ErbB2-induced mammary tumourigenesis. To determine the population of genes that are differentially expressed in these tumours, a microarray analysis may be beneficial. It is likely that a microarray analysis will provide some insight into differential gene expression when cIAP2 is knocked out, thus providing us with key information regarding the role of cIAP2 in mammary tumourigenesis. It may also provide information on other genes to be investigated as potential targets for cancer therapy.

The cIAP2 protein plays a critical role in cellular survival in oncogene-induced mammary tumourigenesis. Without it, tumour production is significantly delayed. cIAP2 knockout resulted in an increase in tumour cell apoptosis; however, the tumour cells eventually overcome this apoptotic increase, which may occur through a downregulation of ErbB2 and Akt signaling, a palpable mammary tumour forms. When cIAP2 is knocked out, it does appear that a significant increase in angiogenesis occurs without an increase in macrophage infiltration. It is hypothesized that tumours have developed a pathway to support cell growth through signaling resulting in the increase in angiogenesis observed; an increase in blood vessel infiltration would allow for the increased presence of growth and survival factors in the tumour environment, allowing for palpable tumour growth. Since cIAP2 activation is downstream of NF-κB, the NF-κB pathway plays a critical role in the development of mammary cancer by turning on key players in this cellular event. Its increased activation may be a molecular switch that can be exploited for screening of patients that are at high risk for mammary carcinoma, allowing patients an increased chance for survival, and better long term prognosis. Once the exact role of NF-κB in mammary tumourigenesis is determined, the value of it as a prognostic factor and as a potential therapeutic target will become clear.

4.2 The role of NF-κB activation in MaSCs

The Pratt lab has recently published a paper showing that mammary lesions induced by DMBA in mice that express a form of IκB that is unable to be phosphorylated ($IκB^{SR}$) were basal-like and developed without the need for NF-κB (Pratt *et al.*, 2009). Canonical NF-κB signaling may therefore be needed for luminal mammary

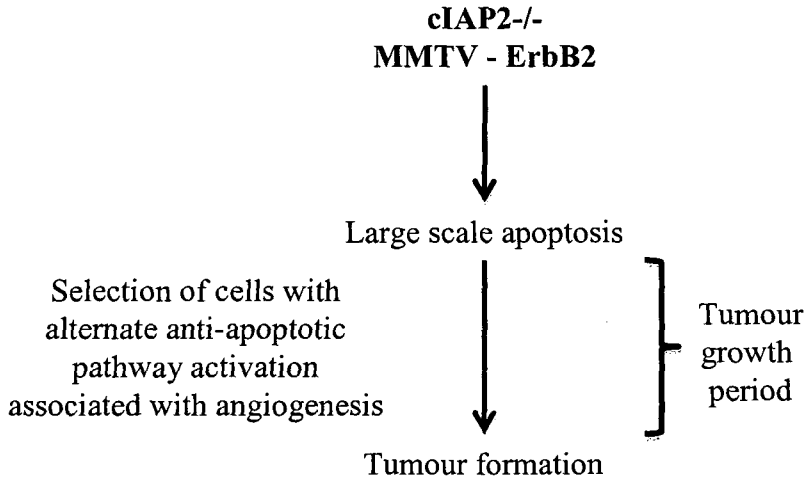
cIAP2-/-
MMTV - ErbB2
Large scale apoptosis
Selection of cells with alternate anti-apoptotic pathway activation associated with angiogenesis
Tumour growth period
Tumour formation

Figure 21. Proposed pathway of tumour formation in cIAP2 knockout mice induced by the presence of an activated ErbB2 oncogene. The presence of ErbB2 allowed for the growth of a palpable tumour in mice lacking cIAP2 expression.

tumourigenesis. This paper was used as the basis of the current study to determine the role of NF-κB activation in mouse MaSCs.

4.2.1 NF-κB activation is limited to luminal Ma-CFC

In order to determine the NF-κB activation status in the normal virgin mammary gland, immunohistochemical analysis was done on mammary gland sections from *cis*NF-κB^{EGFP} transgenic mice that express EGFP upon activation of NF-κB signaling using antibodies against both p65 and EGFP. In the virgin mammary gland, NF-κB signaling is kept relatively low, and increases during pregnancy, lactation and involution (Cao and Karin, 2003). During these three processes, NF-κB activation is limited to the luminal cell compartment and its signaling prevents luminal epithelial cell apoptosis, promoting luminal cell survival. In the current study, NF-κB activation was limited to the luminal cell compartment in the mammary gland of virgin mice that was not undergoing any developmental changes. These results suggest that NF-κB may help regulate the survival of the luminal epithelial cell compartment in virgin mouse mammary gland.

In order to determine the NF-κB activation status in the mammary stem cell and progenitor cell compartments, the method described by Stingl *et al.* (2006) was used. These authors determined that the mammary stem cells or MRUs and the progenitors, of Ma-CFCs differentially expressed the markers CD49f and CD24; the MRU cell fraction was limited to the CD49f^{high}CD24^{med} fraction, and the Ma-CFCs had CD49f^{low}CD24^{high} expression levels. We found that the Ma-CFC fraction, the more luminal cell type, was positive for NF-κB expression while the MRU basal like cells were mostly negative. NF-κB activation was limited to the luminal epithelial cell population and luminal stem cell

population, suggesting that NF-κB may also be active in only luminal progenitor cells, rendering them more susceptible to transformation and carcinogenesis (Pratt *et al.*, 2009). Indeed, luminal-type tumours are the most common tumour type (Sheridan *et al.*, 2006). NF-κB is not needed for the growth of basal/myoepithelial tumours; these tumours are negative for canonical pathway signaling and may rely on other pathways for their survival and subsequent oncogenic transformation (Pratt *et al.*, 2009; Stingl and Caldas, 2007). Interestingly, normal ErbB2 expression is typically found in the luminal cell compartment of the mouse mammary gland; ErbB2 overexpression is common in breast cancer and its transforming abilities rely on the expression of NF-κB.

4.2.2 CD44 as a TIC marker

The characterization of NF-κB activation in the TIC compartment of ErbB2-induced tumours was unsuccessful. Using the NF-κB reporter mouse and CD44 as a marker for TICs, FACS analysis of EGFP expressing cells was not useful in determining the NF-κB expression status. Using the limited results obtained from the FACS analysis of TICs, it appeared that there were too many cells positive for CD44. The use of CD44 as a TIC marker in human ErbB2-breast cancer has been recently questioned. In a recent study, it was found that there was no correlation between CD44 expression and ErbB2 status; surprisingly, in human breast cancer samples, ErbB2-positive tumour tissue exhibited a disproportionally high expression of CD44-/CD24+ cells (Honeth *et al.*, 2008). The CD44+ phenotype more often identified TICs in basal-like tumours, suggesting that it may not be a marker for TICs in all breast tumour types. There was also no correlation between CD44 expression and metastasis, prognosis and survival.

These results mirrored a number of other studies recently published. In 2006, a research group identified CD44+/CD24- as a marker for tumour cells with enhanced invasive properties (Sheridan *et al.*, 2006). The CD44 cell marker, which was initially identified in tumour cells capable of initiating tumour growth in nude mice, may actually be a marker for established cultured human cell lines with a metastatic phenotype (Al-Hajj *et al.*, 2003; Sheridan *et al.*, 2006). If CD44 is a marker for TICs, it may only be so in mice In the 2006 study (Sheridan *et al.*), it was found that CD44 expressing cell lines possessed three characteristics associated with metastasis: 1) expression of invasion/metastasis-associated genes, 2) the ability to invade surrounding tissue, and 3) the ability to home and proliferate to sites of metastasis. The CD44+/CD24- cells were those that stained positive for basal/myoepithelial cell markers. As in the 2008 study mentioned above, luminal cell types exhibited a higher than average cell surface expression of CD24. It has been postulated that CD44+ cells may represent TICs in mice, but not in humans. When CD44+ cells from human breast cancer tissue is injected into the mammary fat pad, the success of creating a tumour may be in part due to the mouse mammary gland microenvironment (Filmore and Kuperwasser, 2007). However, in the current study, it is unknown if CD44 staining of cells from MMTV-ErbB2-induced tumours represent the putative stem cell compartment since further study is needed, and the experiments presented herein were limited.

4.2.3 Summary and future directions

NF-κB activation was almost exclusively limited to the luminal epithelial cell compartment and the Ma-CFC compartment of the virgin mouse mammary gland. Using

an NF-κB reporter mouse and FACS analysis, close to 100% of Ma-CFCs characterized by $CD49f^{low}CD24^{high}$ cell surface staining was positive for active NF-κB expression; less than 10% of the $CD49f^{high}CD24^{med}$ MRU cell fraction contained active NF-κB. Primary mammary epithelial cells, most likely of the Ma-CFC lineage, were significantly affected by NF-κB inhibition.

Flow cytometric analysis of single cell suspensions using known surface markers provides an effective way of defining cell populations within a given tissue type. Although the technique described by Stingl *et al.* (2006) was successful, the use of the *cis*-NF-κB^{EGFP}reporter mouse was not. FACS analysis using the reporter mouse was only successful a limited number of times, after which EGFP expression was undetectable (as seen in the CD44+ FACS presented above, and experiments using FACS analysis of the Ma-CFC and MRU fractions as shown in the Appendix). In these cases, the presence of the EGFP transgene was detectable when genotyping the mouse population used in the studies by PCR (not shown). In order to determine why EGFP protein expression could not be detected in the mammary gland, genetic analysis of the mouse mammary gland in the *cis*-NF-κB^{EGFP}reporter mice should be completed. This may involve breeding the mice with wild type mice of a different genetic background, like an FVBN background to limit the inbreeding that inevitably occurs while setting up mouse studies. Also, to potentially further increase the intensity of the EGFP signal obtain, homozygous EGFP mice could be generated. The researchers that initially made the transgenic mice were unsure if there would be an increase in EGFP expression levels in the homozygous form. They found that, although the transgene was targeted to the X chromosome, they found that there were no differences is the number of peripheral blood mononuclear cells in

males and heterozygous females (after looking at 5 males and 5 females, they found the same number of positive mice), suggesting that the transgene is resistant to X-inactivation (Magness *et al.*, 2004). The *cis*-NF-κB^{EGFP}reporter mouse in a heterozygous form may not be a viable model to study NF-κB expression in the mouse mammary gland. While using this mouse, another University of Ottawa lab, the McBurney lab, noted that EGFP expression was unable to be detected during a skin tumourigenesis study.

The lab that created the EGFP transgenic mouse line found that it was possible to genotype the mice by looking at tail-tip blood under the microscope; mice expressing the EGFP transgene exhibited EGFP positive mononuclear cells. In the Pratt lab, genotyping by using tail-tip blood was somewhat unsuccessful; using the mouse founders obtained from the Jobin lab (the lab that generated the transgenic), it was difficult to visualize EGFP positive mononuclear cells using the microscopes available as red blood cells autofluoresce. Genotyping using blood identified "positive" mice that actually did not carry the EGFP transgene as determined by PCR. It would be possible to know the expression of EGFP in mice used for stem cell analysis using blood visualized under the microscope only if it were more conclusive (using the experimental equipment available at the time).

To specifically study the Ma-CFCs in cell culture (as they are the progenitor cells that have been shown to express NF-κB), the Ma-CFC assay should be completed. This assay is a commonly used method to quantify the number of progenitors, or colony forming cells in a given sample (Stingl *et al.*, 2006). In this assay, mammary cells are seeded at clonal density (less than 500 cells/cm^2) on a layer of pre-established irradiated

viable feeder cells. Irradiation is capable of halting cell division while not considerably affecting cellular metabolism. The irradiated cell layer can therefore provide growth factors to the media. Since all cells in a given tissue are provided with growth factors from surrounding stromal tissue, the use of fibroblast-like cells is often employed (Jessop and Hay, 1979). For the Ma-CFC assay, NIH 3T3 cells irradiated at $5X10^3$ Gray and seeded at $1X10^4$cells/cm^2 will be used. After a week in culture, Ma-CFCs will develop into discrete colonies that can be counted and analyzed for protein expression, like NF-κB. The effects of NF-κB inhibition will also be established. This will allow us to develop a better understanding of what happens when the Ma-CFCs lose NF-κB expression.

A 3D assay has been developed to study progenitor cells in a more natural environment. Often, when primary cells are cultured on tissue culture plastic, they lose important growth and homeostatic signals that are normally provided by surrounding extracellular matrix (ECM). Normal and malignant mammary cells can be cultured using a 3D ECM assay (Lee *et al.*, 2007). Normal mammary and tumour cells will be seeded in chilled basement membrane matrix (Matrigel). This assay allows for malignant and non-malignant cells to be phenotypically distinguished in culture: malignant cells will form large 3D masses of cells, whereas non-malignant cells will form small colonies (Lee *et al.*, 2007). The whole cell culture will be fixed, sectioned and immunostained to determine differential protein and cell surface expression between normal and malignant mammary cells, and to determine the effects of NF-κB inhibition on protein expression in the cells in culture. Some of these experiments were successfully completed in the Pratt lab and were included in a 2009 paper. The population associated with MRU activity and

containing almost no EGFP positive cells formed both amorphous and round colonies in Matrigel. The Ma-CFC enriched fraction with a high proportion of EGFP positive cells produced branching acinar structures in which one or two layers of epithelial cells surrounded by a lumen similar to formations described by Stingl *et al.* (2006).

NF-κB expression in CD44+ tumour initiating cells will be studied. Flow cytometric analysis of MMTV-ErbB2 tumours in EGFP reporter mice will be repeated using a titrated antibody concentration. The CD44 positive tumour cells will be isolated, and NF-κB expression will be assessed using the Cytospin centrifuge, and primary tumour culture (tumoursphere culture). The effects of NF-κB inhibition on these cells will also be studied.

The results from the experiments presented herein suggest that NF-κB is activated during differentiation in the luminal Ma-CFC progenitor population, but not in the stem cell enriched populations. It is possible that in the primitive mammary stem cell compartment, canonical NF-κB activation is needed for the development of the luminal cell progenitor cell population and not for the development of the multi-lineage progenitor that gives rise to basal and myoepithelial progenitor cell populations. ErbB2 overexpression in the luminal stem cell compartment further activates NF-κB signaling, leading to ErbB2 positive tumours that are sensitive to NF-κB inhibition (Pratt *et al.*, 2009; Stingl and Caldas, 2007). The myoepithelial progenitor cells are derived from a multi-lineage progenitor (MRU-like), and their development is not dependent upon canonical NF-κB signaling. When transformed, the myoepithelial lineage gives rise to the ErbB2-negative basal-like tumour.

With the success of the NF-κB EGFP reporter mouse in these experiments, it should serve as a valuable tool to study NF-κB upregulation and activation in many experiments involving mammary tumourigenesis models. Based on the literature, NF-κB targeting for therapeutics is becoming more attractive; in a recent paper by Cao *et al.*, (2007), it was shown that blocking activation of IKKα (the kinase involved in non-canonical pathway activation) significantly impaired the self-renewal of ErbB2 transformed mammary TICs, suggesting that NF-κB is needed for the survival of ErbB2 positive TICs. Knowing the NF-κB expression status in CD44 positive TICs (in an ErbB2-induced model) will provide insight into whether or not NF-κB targeting or inhibition during ErbB2 positive cancer treatment is a viable method for slowing or halting tumour cell proliferation.

5. REFERENCES

Acehan, D., Jiang, X., Morgan, D.G., Heuser, J.E., Wang, X., and Akey, C.W. (2002). Three-dimensional structure of the apoptosome: implications for assembly, procaspase-9 binding, and activation. Mol. Cell *9,* 423-432.

Aldaz, C.M., Liao, Q.Y., LaBate, M., and Johnston, D.A. (1996). Medroxyprogesterone acetate accelerates the development and increases the incidence of mouse mammary tumors induced by dimethylbenzathracene. Carcinogenesis *17,* 2069-2072.

Al-Hajj, M., Wicha, M.S., Benito-Hernandez, A., Morrison, S.J., and Clarke, M.F. (2003). Prospective identification of tumorigenic breast cancer cells. Proc. Natl. Acad. Sci. U. S. A. *100,* 3983-3988.

Allred, D.C., and Medina, D. (2008). The relevance of mouse models to understanding the development and progression of human breast cancer. J. Mammary Gland Biol. Neoplasia *13,* 279-288.

al-Sarireh, B., and Eremin, O. (2000). Tumour-associated macrophages (TAMS): disordered function, immune suppression and progressive tumour growth. J. R. Coll. Surg. Edinb. *45,* 1-16.

Andres, A.C., and Strange, R. (1999). Apoptosis in the estrous and menstrual cycles. J. Mammary Gland Biol. Neoplasia *4,* 221-228.

Annunziata, C.M., Davis, R.E., Demchenko, Y., Bellamy, W., Gabrea, A., Zhan, F., Lenz, G., Hanamura, I., Wright, G., Xiao, W. *et al.* (2007). Frequent engagement of the classical and alternative NF-kappaB pathways by diverse genetic abnormalities in multiple myeloma. Cancer. Cell. *12,* 115-130.

Aravind, L., and Koonin, E.V. (2000). SAP - a putative DNA-binding motif involved in chromosomal organization. Trends Biochem. Sci. *25,* 112-114.

Asch, H.L., and Asch, B.B. (1985). Expression of keratins and other cytoskeletal proteins in mouse mammary epithelium during the normal developmental cycle and primary culture. Dev. Biol. *107,* 470-482.

Baldwin, A.S.,Jr. (2001). Series introduction: the transcription factor NF-kappaB and human disease. J. Clin. Invest. *107,* 3-6.

Baud, V., and Karin, M. (2009). Is NF-κB a good target for cancer therapy? Hopes and pitfalls. Nature Rev. Drug Discovery *8,* 33-40.

BD Biosciences. (2000). Introduction to Flow Cytometry: A Learning Guide (San Jose, California: Becton, Dickinson and Company).

Beerli, R.R., Graus-Porta, D., Woods-Cook, K., Chen, X., Yarden, Y., and Hynes, N.E. (1995). Neu differentiation factor activation of ErbB-3 and ErbB-4 is cell specific and displays a differential requirement for ErbB-2. Mol. Cell. Biol. *15,* 6496-6505.

Beg, A.A., Sha, W.C., Bronson, R.T., Ghosh, S., and Baltimore, D. (1995). Embryonic lethality and liver degeneration in mice lacking the RelA component of NF-kappa B. Nature *376,* 167-170.

Behbod, F., and Rosen, J.M. (2005). Will cancer stem cells provide new therapeutic targets? Carcinogenesis *26,* 703-711.

Bhat-Nakshatri, P., Sweeney, C.J., and Nakshatri, H. (2002). Identification of signal transduction pathways involved in constitutive NF-kappaB activation in breast cancer cells. Oncogene *21,* 2066-2078.

Bingle, L., Brown, N.J., and Lewis, C.E. (2002). The role of tumour-associated macrophages in tumour progression: implications for new anticancer therapies. J. Pathol. *196,* 254-265.

Biswas, D.K., Shi, Q., Baily, S., Strickland, I., Ghosh, S., Pardee, A.B., and Iglehart, J.D. (2004). NF-κB activation in human breast cancer specimens and its role in cell proliferation and apoptosis.

Bjerkvig, R., Tysnes, B.B., Aboody, K.S., Najbauer, J., and Terzis, A.J. (2005). Opinion: the origin of the cancer stem cell: current controversies and new insights. Nat. Rev. Cancer. *5,* 899-904.

Bolander, F.F.,Jr. (1990). Differential characteristics of the thoracic and abdominal mammary glands from mice. Exp. Cell Res. *189,* 142-144.

Bonfini, L., Karlovich, C.A., Dasgupta, C., and Banerjee, U. (1992). The Son of sevenless gene product: a putative activator of Ras. Science *255,* 603-606.

Brantley, D.M., Chen, C.L., Muraoka, R.S., Bushdid, P.B., Bradberry, J.L., Kittrell, F., Medina, D., Matrisian, L.M., Kerr, L.D., and Yull, F.E. (2001). Nuclear factor-kappaB (NF-kappaB) regulates proliferation and branching in mouse mammary epithelium. Mol. Biol. Cell *12,* 1445-1455.

Brantley, D.M., Yull, F.E., Muraoka, R.S., Hicks, D.J., Cook, C.M., and Kerr, L.D. (2000). Dynamic expression and activity of NF-kappaB during post-natal mammary gland morphogenesis. Mech. Dev. *97,* 149-155.

Brasier, A.R. (2006). The NF-kappaB regulatory network. Cardiovasc. Toxicol. *6,* 111-130.

Bredemeyer, A.L., Huang, C.Y., Walker, L.M., Bassing, C.H., and Sleckman, B.P. (2008). Aberrant V(D)J recombination in ataxia telangiectasia mutated-deficient lymphocytes is dependent on nonhomologous DNA end joining. J. Immunol. *181,* 2620-2625.

Brown, K.D., Claudio, E., and Siebenlist, U. (2008). The roles of the classical and alternative nuclear factor-kappaB pathways: potential implications for autoimmunity and rheumatoid arthritis. Arthritis Res. Ther. *10,* 212.

Calmels, S., Hainaut, P., and Ohshima, H. (1997). Nitric oxide induces conformational and functional modifications of wild-type p53 tumor suppressor protein. Cancer Res. *57,* 3365-3369.

Cao, Y., Bonizzi, G., Seagroves, T.N., Greten, F.R., Johnson, R., Schmidt, E.V., and Karin, M. (2001). IKKalpha provides an essential link between RANK signalling and cyclin D1 expression during mammary gland development. Cell *107,* 763-775.

Cao, Y., and Karin, M. (2003). NF-kappaB in mammary gland development and breast cancer. J. Mammary Gland Biol. Neoplasia *8,* 215-223.

Cao, Y., Luo, J-L., and Karin, M. (2003). IκB kinase α kinase activity is required for self-renewal of ErbB2/Her2-transformed mammary tumour-initiating cells. PNAS *104,* 15852-15857.

Chaga, G., Bochkariov, D.E., Jokhadze, G.G., Hopp, J., and Nelson, P. (1999). Natural poly-histidine affinity tag for purification of recombinant proteins on cobalt(II)-carboxymethylaspartate crosslinked agarose. J. Chromatogr. A *864,* 247-256.

Chen, D., Xu, L.G., Chen, L., Li, L., Zhai, Z., and Shu, H.B. (2003). NIK is a component of the EGF/heregulin receptor signalling complexes. Oncogene *22,* 4348-4355.

Chen, F., Castranova, V., and Shi, X. (2001). New insights into the role of nuclear factor-kappaB in cell growth regulation. Am. J. Pathol. *159,* 387-397.

Chiarle, R., Pagano, M., and Inghirami, G. (2001). The cyclin dependent kinase inhibitor p27 and its prognostic role in breast cancer. Breast Cancer Res. *3,* 91-94.

Chiarugi, P., and Giannoni, E. (2008). Anoikis: a necessary death program for anchorage-dependent cells. Biochem. Pharmacol. *76,* 1352-1364.

Christen, S., Hagen, T.M., Shigenaga, M.K., and Ames, B.N. (1999). Chronic Infection and Inflammation Lead to Mutation and Cancer. In Microbes and Malignancy: Infection as a Cause of Cancer Parsonnet, J., and Horning, S. eds., (New York: Oxford University Press) pp. 35-88.

Clarke, C., Sandle, J., and Lakhani, S.R. (2005). Myoepithelial cells: pathology, cell separation and markers of myoepithelial differentiation. J. Mammary Gland Biol. Neoplasia *10,* 273-280.

Clarkson, R.W., Heeley, J.L., Chapman, R., Aillet, F., Hay, R.T., Wyllie, A., and Watson, C.J. (2000). NF-kappaB inhibits apoptosis in murine mammary epithelia. J. Biol. Chem. *275,* 12737-12742.

Clarkson, R.W., and Watson, C.J. (1999). NF-kappaB and apoptosis in mammary epithelial cells. J. Mammary Gland Biol. Neoplasia *4,* 165-175.

Cobbs, C.S., Samanta, M., Harkins, L.E., Gillespie, G.Y., Merrick, B.A., and MacMillan-Crow, L.A. (2001). Evidence for peroxynitrite-mediated modifications to p53 in human gliomas: possible functional consequences. Arch. Biochem. Biophys. *394,* 167-172.

Cohen, G.M. (1997). Caspases: the executioners of apoptosis. Biochem. J. *326 (Pt 1),* 1-16.

Conte, D., Holcik, M., Lefebvre, C.A., Lacasse, E., Picketts, D.J., Wright, K.E., and Korneluk, R.G. (2006). Inhibitor of apoptosis protein cIAP2 is essential for lipopolysaccharide-induced macrophage survival. Mol. Cell. Biol. *26,* 699-708.

Coswell, P.C., Guttridge, D.C., Funkhouser, W.K., and Baldwin, A.S. Jr. (2000). Selective activation of NF-κB subunits in human breast cancer: potential roles for NF-κB2/p52 and for Bcl-3. Oncogene *19,* 1123.

Craft, P.S., and Harris, A.L. (1994). Clinical prognostic significance of tumour angiogenesis. Ann. Oncol. *5,* 305-311.

Daniel, C.W., De Ome, K.B., Young, J.T., Blair, P.B., and Faulkin, L.J.,Jr. (1968). The in vivo life span of normal and preneoplastic mouse mammary glands: a serial transplantation study. Proc. Natl. Acad. Sci. U. S. A. *61,* 53-60.

de Murcia, J.M., Niedergang, C., Trucco, C., Ricoul, M., Dutrillaux, B., Mark, M., Oliver, F.J., Masson, M., Dierich, A., LeMeur, M. *et al.* (1997). Requirement of poly(ADP-ribose) polymerase in recovery from DNA damage in mice and in cells. Proc. Natl. Acad. Sci. U. S. A. *94,* 7303-7307.

de Vries-Smits, A.M., Burgering, B.M., Leevers, S.J., Marshall, C.J., and Bos, J.L. (1992). Involvement of p21ras in activation of extracellular signal-regulated kinase 2. Nature *357,* 602-604.

DeLisser, H.M., Christofidou-Solomidou, M., Strieter, R.M., Burdick, M.D., Robinson, C.S., Wexler, R.S., Kerr, J.S., Garlanda, C., Merwin, J.R., Madri, J.A., and Albelda, S.M.

(1997). Involvement of endothelial PECAM-1/CD31 in angiogenesis. Am. J. Pathol. *151,* 671-677.

Deome, K.B., Faulkin, L.J.,Jr, Bern, H.A., and Blair, P.B. (1959). Development of mammary tumors from hyperplastic alveolar nodules transplanted into gland-free mammary fat pads of female C3H mice. Cancer Res. *19,* 515-520.

Deveraux, Q.L., and Reed, J.C. (1999). IAP family proteins--suppressors of apoptosis. Genes Dev. *13,* 239-252.

Deveraux, Q.L., Takahashi, R., Salvesen, G.S., and Reed, J.C. (1997). X-linked IAP is a direct inhibitor of cell-death proteases. Nature *388,* 300-304.

Dick, J.E. (2003). Breast cancer stem cells revealed. Proc Natl Acad Sci U S A *100,* 3547-3549.

Dizdaroglu, M. (1994). Chemical determination of oxidative DNA damage by gas chromatography-mass spectrometry. Methods Enzymol. *234,* 3-16.

Dominguez-Bendala, J., Masutani, M., and McWhir, J. (2006). Down-regulation of PARP-1, but not of Ku80 or DNA-PKcs', results in higher gene targeting efficiency. Cell Biol. Int. *30,* 389-393.

Douma, S., Van Laar, T., Zevenhoven, J., Meuwissen, R., Van Garderen, E., and Peeper, D.S. (2004). Suppression of anoikis and induction of metastasis by the neurotrophic receptor TrkB. Nature *430,* 1034-1039.

Downs, J.A., and Jackson, S.P. (2004). A means to a DNA end: the many roles of Ku. Nat. Rev. Mol. Cell Biol. *5,* 367-378.

Downward, J. (1990). The ras superfamily of small GTP-binding proteins. Trends Biochem. Sci. *15,* 469-472.

Ea, C.K., Deng, L., Xia, Z.P., Pineda, G., and Chen, Z.J. (2006). Activation of IKK by TNFalpha requires site-specific ubiquitination of RIP1 and polyubiquitin binding by NEMO. Mol. Cell *22,* 245-257.

Earnshaw, W.C., Martins, L.M., and Kaufmann, S.H. (1999). Mammalian caspases: structure, activation, substrates, and functions during apoptosis. Annu. Rev. Biochem. *68,* 383-424.

Eckelman, B.P., and Salvesen, G.S. (2006). The human anti-apoptotic proteins cIAP1 and cIAP2 bind but do not inhibit caspases. J. Biol. Chem. *281,* 3254-3260.

Eisenhauer, E.A. (2001). From the molecule to the clinic--inhibiting HER2 to treat breast cancer. N. Engl. J. Med. *344,* 841-842.

Enari, M., Sakahira, H., Yokoyama, H., Okawa, K., Iwamatsu, A., and Nagata, S. (1998). A caspase-activated DNase that degrades DNA during apoptosis, and its inhibitor ICAD. Nature *391,* 43-50.

Fajac, A., Benard, J., Lhomme, C., Rey, A., Duvillard, P., Rochard, F., Bernaudin, J.F., and Riou, G. (1995). c-erbB2 gene amplification and protein expression in ovarian epithelial tumors: evaluation of their respective prognostic significance by multivariate analysis. Int. J. Cancer *64,* 146-151.

Fillmore, C., and Kuperwasser, C. (2007). Human breast cancer stem cell markers CD44 and CD24: enriching for cells with functional properties in mice or in man? Breast Cancer Res. *9*, 303.

Fong, A., and Sun, S.C. (2002). Genetic evidence for the essential role of β-transducin repeat-containing protein in the inducible processing of NF-κB2/p100. J. Biol. Chem. *277*, 22111-22114.

Fox, S.B., Gasparini, G., and Harris, A.L. (2001). Angiogenesis: pathological, prognostic, and growth-factor pathways and their link to trial design and anticancer drugs. Lancet Oncol. *2,* 278-289.

Furth, P.A. (1999). Introduction: mammary gland involution and apoptosis of mammary epithelial cells. J. Mammary Gland Biol. Neoplasia *4,* 123-127.

Galante, J.M., Mortenson, M.M., Bowles, T.L., Virudachalam, S., and Bold, R.J. (2008). ERK/BCL-2 Pathway in the Resistance of Pancreatic Cancer to Anoikis. J. Surg. Res.

Gao, Y., Ferguson, D.O., Xie, W., Manis, J.P., Sekiguchi, J., Frank, K.M., Chaudhuri, J., Horner, J., DePinho, R.A., and Alt, F.W. (2000). Interplay of p53 and DNA-repair protein XRCC4 in tumorigenesis, genomic stability and development. Nature *404,* 897-900.

Gellert, M. (2002). V(D)J recombination: RAG proteins, repair factors, and regulation. Annu. Rev. Biochem. *71,* 101-132.

Gerdes, J., Lemke, H., Baisch, H., Wacker, H-H., Schwab, U, and Stein, H. (1984). Cell cycle analysis of a cell proliferation-associated human nuclear antigen defined by the monoclonal antibody Ki-67. J. Immunol. *133*, 1710-1715.

Gerondakis, S., Grossmann, M., Nakamura, Y., Pohl, T., and Grumont, R. (1999). Genetic approaches in mice to understand Rel/NF-kappaB and IkappaB function: transgenics and knockouts. Oncogene *18,* 6888-6895.

Ghobrial, I.M., Witzig, T.E.m and Adjei, A.A. (2005). Targeting apoptosis pathways in cancer therapy. Cancer J. Clin. *55*, 178-194.

Ghosh, S., May, M.J., and Kopp, E.B. (1998). NF-kappa B and Rel proteins: evolutionarily conserved mediators of immune responses. Annu. Rev. Immunol. *16,* 225-260.

Gilmore, T.D. (2006). Introduction to NF-kappaB: players, pathways, perspectives. Oncogene *25,* 6680-6684.

Gilmore, T.D. (1999). The Rel/NF-kappaB signal transduction pathway: introduction. Oncogene *18,* 6842-6844.

Givan, A.L. (2000). The basics of staining for cell surface proteins. In In Living Color: Protocols in Flow Cytometry and Cell Sorting, Diamond, R., and DeMaggio, S. eds., (Berlin: Springer) pp. 142-164.

Givan, A.L. (2004). Flow cytometry: an introduction. Methods Mol. Biol. *263,* 1-32.

Grady, W.M., and Markowitz, S.D. (2002). Genetic and epigenetic alterations in colon cancer. Annu. Rev. Genomics Hum. Genet. *3,* 101-128.

Graus-Porta, D., Beerli, R.R., Daly, J.M., and Hynes, N.E. (1997). ErbB-2, the preferred heterodimerization partner of all ErbB receptors, is a mediator of lateral signalling. EMBO J. *16,* 1647-1655.

Greene, W.C. and Chen, L.F. (2004). Regulation of NF-κB action by reversible acetylation. Novartis Found. Symp. *259*, 208-217.

Gullo, C., Au, M., Feng, G., and Teoh, G. (2006). The biology of Ku and its potential oncogenic role in cancer. Biochim. Biophys. Acta *1765,* 223-234.

Hanahan, D., and Weinberg, R.A. (2000). The hallmarks of cancer. Cell *100*, 57-70.

Hayden, M.S., and Ghosh, S. (2004). Signalling to NF-kappaB. Genes Dev. *18,* 2195-2224.

Herzenberg, L.A., and De Rosa, S.C. (2000). Monoclonal antibodies and the FACS: complementary tools for immunobiology and medicine. Immunol. Today *21,* 383-390.

Holmes, W.E., Sliwkowski, M.X., Akita, R.W., Henzel, W.J., Lee, J., Park, J.W., Yansura, D., Abadi, N., Raab, H., and Lewis, G.D. (1992). Identification of heregulin, a specific activator of p185erbB2. Science *256,* 1205-1210.

Honeth, G., Bendahl, P.O., Ringner, M., Saal, L.H., Gruvberger-Saal, S.K., Lovgren, K., Grabau, D., Ferno, M., Borg, A., and Hegardt, C. (2008). The CD44+/CD24- phenotype is enriched in basal-like breast tumors. Breast Cancer Res. *10,* R53.

Hong, S.Y., Yoon, W.H., Park, J.H., Kang, S.G., Ahn, J.H., and Lee, T.H. (2000). Involvement of two NF-kappa B binding elements in tumor necrosis factor alpha -, CD40-, and epstein-barr virus latent membrane protein 1-mediated induction of the cellular inhibitor of apoptosis protein 2 gene. J. Biol. Chem. *275,* 18022-18028.

Howe, L.R., Leevers, S.J., Gomez, N., Nakielny, S., Cohen, P., and Marshall, C.J. (1992). Activation of the MAP kinase pathway by the protein kinase raf. Cell *71,* 335-342.

Hsu, H., Shu, H.B., Pan, M.G., and Goeddel, D.V. (1996). TRADD-TRAF2 and TRADD-FADD interactions define two distinct TNF receptor 1 signal transduction pathways. Cell *84,* 299-308.

Huber, M.A., Beug, H., and Wirth, T. (2004). Epithelial-mesenchymal transition: NF-kappaB takes center stage. Cell. Cycle *3,* 1477-1480.

Humphreys, R.C., Krajewska, M., Krnacik, S., Jaeger, R., Weiher, H., Krajewski, S., Reed, J.C., and Rosen, J.M. (1996). Apoptosis in the terminal endbud of the murine mammary gland: a mechanism of ductal morphogenesis. Development *122,* 4013-4022.

Hunter, A.M., LaCasse, E.C., and Korneluk, R.G. (2007). Inhibitors of apoptosis (IAPs) as cancer targets. Apoptosis *12,* 1543-1568.

Huntly, B.J., and Gilliland, D.G. (2004). Blasts from the past: new lessons in stem cell biology from chronic myelogenous leukemia. Cancer. Cell. *6,* 199-201.

Hynes, N.E., and Lane, H.A. (2005). ERBB receptors and cancer: the complexity of targeted inhibitors. Nat. Rev. Cancer. *5,* 341-354.

Ibrahim, S.F., and van den Engh, G. (2007). Flow cytometry and cell sorting. Adv. Biochem. Eng. Biotechnol. *106,* 19-39.

Inoue, K., Kamada, M., Slaton, J.W., Fukata, S., Yoshikawa, C., Tamboli, P., Dinney, C.P., and Shuin, T. (2002). The prognostic value of angiogenesis and metastasis-related genes for progression of transitional cell carcinoma of the renal pelvis and ureter. Clin. Cancer Res. *8,* 1863-1870.

Jaattela, M. (1999). Escaping cell death: survival proteins in cancer. Exp. Cell Res. *248,* 30-43.

Jessop, N.W., and Hay, R.J. (1979). Preparation, preservation, recovery and use of irradiated feeder layers in cell culture research. Methods Cell Science *5,* 1137-1139.

Kaklamani, V.G., and Gradishar, W.J. (2006). Gene expression in breast cancer. Curr. Treat. Options Oncol. *7,* 123-128.

Karin, M., and Ben-Neriah, Y. (2000). Phosphorylation meets ubiquitination: the control of NF-[kappa]B activity. Annu. Rev. Immunol. *18,* 621-663.

Karin, M., Cao, Y., Greten, F.R., and Li, Z.W. (2002). NF-kappaB in cancer: from innocent bystander to major culprit. Nat. Rev. Cancer. *2,* 301-310.

Karin, M., and Gallagher, E. (2009). TNFR signalling: ubiquitin-conjugated TRAFfic signals control stop-and-go for MAPK signalling complexes. Immunol. Rev. *228,* 225-240.

Karin, M., and Lin, A. (2002). NF-kappaB at the crossroads of life and death. Nat. Immunol. *3,* 221-227.

Kato, T.,Jr, Delhase, M., Hoffmann, A., and Karin, M. (2003). CK2 Is a C-Terminal IkappaB Kinase Responsible for NF-kappaB Activation during the UV Response. Mol. Cell *12,* 829-839.

Kay, R., Rosten, P.M., and Humphries, R.K. (1991). CD24, a signal transducer modulating B cell activation responses, is a very short peptide with a glycosyl phosphatidylinositol membrane anchor. J. Immunol. *147,* 1412-1416.

Keats, J.J., Fonseca, R., Chesi, M., Schop, R., Baker, A., Chng, W.J., Van Wiler, S., Tiedemann, R., Shi, C.X., Sebag, M., *et al.* (2007). Promiscuous mutations activate the canonical NF-κB pathway in multiple myeloma. Cancer Cell *12,* 131-144.

Kim, D.W., Sovak, M.A., Zanieski, G., Nonet, G., Romieu-Mourez, R., Lau, A.W., Hafer, L.J., Yaswen, P., Stampfer, M., Rogers, A.E., Russo, J., and Sonenshein, G.E. (2000). Activation of NF-kappaB/Rel occurs early during neoplastic transformation of mammary cells. Carcinogenesis *21,* 871-879.

Korsching, E., Jeffrey, S.S., Meinerz, W., Decker, T., Boecker, W., and Buerger, H. (2008). Basal carcinoma of the breast revisited: an old entity with new interpretations. J. Clin. Pathol. *61,* 553-560.

LaCasse, E.C., Baird, S., Korneluk, R.G., and MacKenzie, A.E. (1998). The inhibitors of apoptosis (IAPs) and their emerging role in cancer. Oncogene *17,* 3247-3259.

Lee, G.Y., Kenny, P.A., Lee, E.H., and Bissell, M.J. (2007). Three-dimensional culture models of normal and malignant breast epithelial cells. Nat. Methods *4,* 359-365.

Lee, J.S., Hong, U.S., Lee, T.H., Yoon, S.K., and Yoon, J.B. (2004). Mass spectrometric analysis of tumor necrosis factor receptor-associated factor 1 ubiquitination mediated by cellular inhibitor of apoptosis 2. Proteomics *4,* 3376-3382.

Leek, R.D., and Harris, A.L. (2002). Tumor-associated macrophages in breast cancer. J. Mammary Gland Biol. Neoplasia *7,* 177-189.

Lerebours, F., Vacher, S., Andrieu, C., Espie, M., Marty, M., Lidereau, R., and Bieche, I. (2008). NF-kappa B genes have a major role in inflammatory breast cancer. BMC Cancer *4*, 41.

Li, Q., Estepa, G., Memet, S., Israel, A., and Verma, I.M. (2000). Complete lack of NF-kappaB activity in IKK1 and IKK2 double-deficient mice: additional defect in neurulation. Genes Dev. *14*, 1729-1733.

Li, Z.W., Chu, W., Hu, Y., Delhase, M., Deerinck, T., Ellisman, M., Johnson, R., and Karin, M. (1999). The IKKbeta subunit of IkappaB kinase (IKK) is essential for nuclear factor kappaB activation and prevention of apoptosis. J. Exp. Med. *189*, 1839-1845.

Liao, G., Zhang, M., Harhaj, E.W., and Sun, S.C. (2004). Regulation of the NF-kappaB-inducing kinase by tumor necrosis factor receptor-associated factor 3-induced degradation. J. Biol. Chem. *279*, 26243-26250.

Lieber, M.R. (1999). The biochemistry and biological significance of nonhomologous DNA end joining: an essential repair process in multicellular eukaryotes. Genes Cells *4*, 77-85.

Lieber, M.R., Ma, Y., Pannicke, U., and Schwarz, K. (2004). The mechanism of vertebrate nonhomologous DNA end joining and its role in V(D)J recombination. DNA Repair (Amst) *3*, 817-826.

Lim, S.J., Lopez-Berestein, G., Hung, M.C., Lupu, R., and Tari, A.M. (2000). Grb2 downregulation leads to Akt inactivation in heregulin-stimulated and ErbB2-overexpressing breast cancer cells. Oncogene *19*, 6271-6276.

Liotta, L.A., and Kohn, E. (2004). Anoikis: cancer and the homeless cell. Nature *430*, 973-974.

Liotta, L.A., and Kohn, E.C. (2001). The microenvironment of the tumour-host interface. Nature *411*, 375-379.

Liston, P., Fong, W.G., and Korneluk, R.G. (2003). The inhibitors of apoptosis: there is more to life than Bcl2. Oncogene *22*, 8568-8580.

Liu, J.C., Deng, T., Lehal, R.S., Kim, J., and Zacksenhaus, E. (2007). Identification of tumorsphere- and tumor-initiating cells in HER2/Neu-induced mammary tumors. Cancer Res. *67*, 8671-8681.

Liu, M., Ju, X., Willmarth, N.E., Casimiro, M.C., Ojeifo, J., Sakamaki, T., Katiyar, S., Jiao, X., Popov, V.M., Yu, Z. *et al.* (2009). Nuclear factor-kappaB enhances ErbB2-induced mammary tumorigenesis and neoangiogenesis in vivo. Am. J. Pathol. *174*, 1910-1920.

Liu, Y., and West, S.C. (2002). Distinct functions of BRCA1 and BRCA2 in double-strand break repair. Breast Cancer Res. *4,* 9-13.

Liu, Z., Li, H., Derouet, M., Filmus, J., LaCasse, E.C., Korneluk, R.G., Kerbel, R.S., and Rosen, K.V. (2005). ras Oncogene triggers up-regulation of cIAP2 and XIAP in intestinal epithelial cells: epidermal growth factor receptor-dependent and -independent mechanisms of ras-induced transformation. J. Biol. Chem. *280,* 37383-37392.

Lodish, H., Berk, A., Matsudaira, P., Kaiser, C.A., Krieger, M., Scott, M.P., Zipursky, L., and Darnell, J. (2003). Molecular Cell Biology (New York, NY: W.H. Freeman).

Lowry, O.H., Rosebrough, N.J., Farr, A.L., and Randall, R.J. (1951). Protein measurement with the Folin phenol reagent. J. Biol. Chem. *193,* 265-275.

Madrid, L.V., Wang, C.Y., Guttridge, D.C., Schottelius, A.J., Baldwin, A.S.,Jr, and Mayo, M.W. (2000). Akt suppresses apoptosis by stimulating the transactivation potential of the RelA/p65 subunit of NF-kappaB. Mol. Cell. Biol. *20,* 1626-1638.

Magness, S.T., Jijon, H., Van Houten Fisher, N., Sharpless, N.E., Brenner, D.A., and Jobin, C. (2004). In vivo pattern of lipopolysaccharide and anti-CD3-induced NF-kappa B activation using a novel gene-targeted enhanced GFP reporter gene mouse. J. Immunol. *173,* 1561-1570.

Mahaney, B.L., Meek, K., and Lees-Miller, S.P. (2009). Repair of ionizing radiation-induced DNA double-strand breaks by non-homologous end-joining. Biochem. J. *417,* 639-650.

Mahoney, D.J., Cheung, H.H., Mrad, R.L., Plenchette, S., Simard, C., Enwere, E., Arora, V., Mak, T.W., Lacasse, E.C., Waring, J., and Korneluk, R.G. (2008). Both cIAP1 and cIAP2 regulate TNFalpha-mediated NF-kappaB activation. Proc. Natl. Acad. Sci. U. S. A. *105,* 11778-11783.

Makris, C., Godfrey, V.L., Krahn-Senftleben, G., Takahashi, T., Roberts, J.L., Schwarz, T., Feng, L., Johnson, R.S., and Karin, M. (2000). Female mice heterozygous for IKK gamma/NEMO deficiencies develop a dermatopathy similar to the human X-linked disorder incontinentia pigmenti. Mol. Cell *5,* 969-979.

Marais, R., and Marshall, C.J. (1996). Control of the ERK MAP kinase cascade by Ras and Raf. Cancer Surv. *27,* 101-125.

Martinou, J.C., and Green, D.R. (2001). Breaking the mitochondrial barrier. Nat. Rev. Mol. Cell Biol. *2,* 63-67.

Marx, J. (2003). Cancer research. Mutant stem cells may seed cancer. Science *301,* 1308-1310.

Maurer, C.A., Friess, H., Kretschmann, B., Zimmermann, A., Stauffer, A., Baer, H.U., Korc, M., and Buchler, M.W. (1998). Increased expression of erbB3 in colorectal cancer is associated with concomitant increase in the level of erbB2. Hum. Pathol. *29,* 771-777.

McClellan, H.L., Miller, S.J., and Hartmann, P.E. (2008). Evolution of lactation: nutrition v. protection with special reference to five mammalian species. Nutr. Res. Rev. *21,* 97-116.

Medina, D. (2000). The preneoplastic phenotype in murine mammary tumorigenesis. J. Mammary Gland Biol. Neoplasia *5,* 393-407.

Mercurio, F., DiDonato, J.A., Rosette, C., and Karin, M. (1993). p105 and p98 precursor proteins play an active role in NF-κB-mediated signal transduction. Genes Dev. *7,* 705-718.

Micheau, O., Lens, S., Gaide, O., Alevizopoulos, K., and Tschopp, J. (2001). NF-kappaB signals induce the expression of c-FLIP. Mol. Cell. Biol. *21,* 5299-5305.

Miller, E.C. (1978). Some current perspectives on chemical carcinogenesis in humans and experimental animals: Presidential Address. Cancer Res. *38,* 1479-1496.

Molyneux, G., Regan, J., and Smalley, M.J. (2007). Mammary stem cells and breast cancer. Cell Mol. Life Sci. *64,* 3248-3260.

Mosesson, Y., and Yarden, Y. (2004). Oncogenic growth factor receptors: implications for signal transduction therapy. Semin. Cancer Biol. *14,* 262-270.

Moulder, J.E. (1998). Power-frequency fields and cancer. Crit. Rev. Biomed. Eng. *26,* 1-116.

Moynagh, P.N. (2005). The NF-kappaB pathway. J. Cell. Sci. *118,* 4589-4592.

Muller, W.J., Arteaga, C.L., Muthuswamy, S.K., Siegel, P.M., Webster, M.A., Cardiff, R.D., Meise, K.S., Li, F., Halter, S.A., and Coffey, R.J. (1996). Synergistic interaction of the Neu proto-oncogene product and transforming growth factor alpha in the mammary epithelium of transgenic mice. Mol. Cell. Biol. *16,* 5726-5736.

Nakshatri, H., Bhat-Nakshatri, P., Martin, D.A., Goulet, R.J.,Jr, and Sledge, G.W.,Jr. (1997). Constitutive activation of NF-kappaB during progression of breast cancer to hormone-independent growth. Mol. Cell. Biol. *17,* 3629-3639.

Neil, J.R., Tian, M., and Schiemann, W.P. (2009). X-linked Inhibitor of Apoptosis Protein and Its E3 Ligase Activity Promote Transforming Growth Factor-{beta}-mediated Nuclear Factor-{kappa}B Activation during Breast Cancer Progression. J. Biol. Chem. *284,* 21209-21217.

Ohshima, H., Tatemichi, M., and Sawa, T. (2003). Chemical basis of inflammation-induced carcinogenesis. Arch. Biochem. Biophys. *417,* 3-11.

Oshima, R.G., Lesparance, J., Munoz, V., Hebbard, L., Ranshct, B., Sharan, N., Muller, W.J., Hauser, C.A. and Cardiff, R.D. (2004). Angiogenic acceleration of Neu induced mammary tumour progression and metastasis. Cancer Res. *64*, 169-179.

Olayioye, M.A. (2001). Update on HER-2 as a target for cancer therapy: intracellular signaling pathways of ErbB2/HER-2 and family members. Breast Cancer Res. *3,* 385-389.

Olivier, M., Eeles, R., Hollstein, M., Khan, M.A., Harris, C.C., and Hainaut, P. (2002). The IARC TP53 database: new online mutation analysis and recommendations to users. Hum. Mutat. *19,* 607-614.

O'Mahony, A., Lin, X., Geleziunas, R., and Greene, W.C. (2000). Activation of the heterodimeric IkappaB kinase alpha (IKKalpha)-IKKbeta complex is directional: IKKalpha regulates IKKbeta under both basal and stimulated conditions. Mol. Cell. Biol. *20,* 1170-1178.

Orlowski, R.Z., and Baldwin, A.S.,Jr. (2002). NF-kappaB as a therapeutic target in cancer. Trends Mol. Med. *8,* 385-389.

Osako, T., Miyahara, M., Uchino, S., Inomata, M., Kitano, S., and Kobayashi, M. (1998). Immunohistochemical study of c-erbB-2 protein in colorectal cancer and the correlation with patient survival. Oncology *55,* 548-555.

Osborn, L., Kunkel, S., and G.J. Nabel. (1989). Tumor necrosis factor alpha and interleukin 1 stimulate human immunodeficiency virus enhancer by activation of the nuclear factor kappa B. Proc. Natl. Acad. Sci. USA. *86.* 2236-2340.

Palmister, R.D., and Brinster, R.L. (1986). Germ-line transformation of mice. Ann. Rev. Genet. *20.*, 465-499.

Pardal, R., Clarke, M.F., and Morrison, S.J. (2003). Applying the principles of stem-cell biology to cancer. Nat. Rev. Cancer. *3,* 895-902.

Pierce, J.H., Arnstein, P., DiMarco, E., Artrip, J., Kraus, M.H., Lonardo, F., Di Fiore, P.P., and Aaronson, S.A. (1991). Oncogenic potential of erbB-2 in human mammary epithelial cells. Oncogene *6,* 1189-1194.

Perkins, N.D. (2001). The Rel/NF-κB family: friend and foe. TIBS. *25*, 434-440.

Pignatelli, B., Bancel, B., Plummer, M., Toyokuni, S., Patricot, L.M., and Ohshima, H. (2001a). Helicobacter pylori eradication attenuates oxidative stress in human gastric mucosa. Am. J. Gastroenterol. *96,* 1758-1766.

Pignatelli, B., Li, C.Q., Boffetta, P., Chen, Q., Ahrens, W., Nyberg, F., Mukeria, A., Bruske-Hohlfeld, I., Fortes, C., Constantinescu, V., Ischiropoulos, H., and Ohshima, H. (2001b). Nitrated and oxidized plasma proteins in smokers and lung cancer patients. Cancer Res. *61,* 778-784.

Pomerantz, J.L., and Baltimore, D. (2002). Two pathways to NF-kappaB. Mol. Cell *10,* 693-695.

Ponti, D., Costa, A., Zaffaroni, N., Pratesi, G., Petrangolini, G., Coradini, D., Pilotti, S., Pierotti, M.A., and Daidone, M.G. (2005). Isolation and in vitro propagation of tumorigenic breast cancer cells with stem/progenitor cell properties. Cancer Res. *65,* 5506-5511.

Pratt, MA., Bishop, T.E., White, D., Yasvinki, G., Menard, M., Niu, M.Y., and Clarke, R. (2003). Estrogen withdrawal-induced NF-κB activity and Bcl-3 expression in breast cancer: roles in growth and hormone independence. Mol. Cell. Biol. *23,* 6887-6900.

Pratt, M.A., Tibbo, E., Robertson, S.J., Jansson, D., Hurst, K., Perez-Iratxeta, C., Lau, R., and Niu, M.Y. (2009). The canonical NF-kappaB pathway is required for formation of luminal mammary neoplasias and is activated in the mammary progenitor population. Oncogene *28,* 2710-2722.

Radice, G.L., Ferreira-Cornwell, M.C., Robinson, S.D., Rayburn, H., Chodosh, L.A., Takeichi, M., and Hynes, R.O. (1997). Precocious mammary gland development in P-cadherin-deficient mice. J. Cell Biol. *139,* 1025-1032.

Raval, P., Kriatchko, A.N., Kumar, S., and Swanson, P.C. (2008). Evidence for Ku70/Ku80 association with full-length RAG1. Nucleic Acids Res. *36,* 2060-2072.

Reed, J.C. (2000). Mechanisms of apoptosis. Am. J. Pathol. *157,* 1415-1430.

Rayet, B., and Gelinas, C. (1999). Aberrant *rel/nfκb* genes and activity in human cancer. Onogene *18,* 6938-6947.

Richardson, K.C. (1949). Contractile tissues in the mammary gland, with special reference to myoepithelium in the goat. Proc. R. Soc. Lond. B. Biol. Sci. *136,* 30-45.

Rice, N.R., KacKichan, M.L., and Israel, A. (1992). The precursor NF-κB p50 has IκB-like functions. Cell. *71,* 243-253.

Richert, M.M., Schwertfeger, K.L., Ryder, J.W., and Anderson, S.M. (2000). An atlas of mouse mammary gland development. J. Mammary Gland Biol. Neoplasia *5,* 227-241.

Rivera-Calzada, A., Spagnolo, L., Pearl, L.H., and Llorca, O. (2007). Structural model of full-length human Ku70-Ku80 heterodimer and its recognition of DNA and DNA-PKcs. EMBO Rep. *8,* 56-62.

Robertson, G.,Garrick, D., Wilson, M., Martin, D.I.K., Whitelaw, E. (1996). Age-dependent silencing of globin transgenes in the mouse. Nuc. Acids. Res. *24*, 1465-1471.

Robinson, G.W., McKnight, R.A., Smith, G.H., and Hennighausen, L. (1995). Mammary epithelial cells undergo secretory differentiation in cycling virgins but require pregnancy for the establishment of terminal differentiation. Development *121,* 2079-2090.

Rothe, M., Pan, M.G., Henzel, W.J., Ayres, T.M., and Goeddel, D.V. (1995). The TNFR2-TRAF signalling complex contains two novel proteins related to the baculoviral inhibitor of apoptosis proteins. Cell *83*, 1243-1252.

Rothkamm, K., Kruger, I., Thompson, L.H., and Lobrich, M. (2003). Pathways of DNA double-strand break repair during the mammalian cell cycle. Mol. Cell. Biol. *23,* 5706-5715.

Russo, I.H., and Russo, J. (1996). Mammary gland neoplasia in long-term rodent studies. Environ. Health Perspect. *104,* 938-967.

Saffari, B., Jones, L.A., el-Naggar, A., Felix, J.C., George, J., and Press, M.F. (1995). Amplification and overexpression of HER-2/neu (c-erbB2) in endometrial cancers: correlation with overall survival. Cancer Res. *55,* 5693-5698.

Sakakura, T., Kusano, I., Kusakabe, M., Inaguma, Y., and Nishizuka, Y. (1987). Biology of mammary fat pad in fetal mouse: capacity to support development of various fetal epithelia in vivo. Development *100,* 421-430.

Salomon, D.S., Normanno, N., Ciardiello, F., Brandt, R., Shoyab, M., and Todaro, G.J. (1995). The role of amphiregulin in breast cancer. Breast Cancer Res. Treat. *33,* 103-114.

Salvesen, G.S., and Duckett, C.S. (2002). IAP proteins: blocking the road to death's door. Nat. Rev. Mol. Cell Biol. *3,* 401-410.

Sancar, A., Lindsey-Boltz, L.A., Unsal-Kacmaz, K., and Linn, S. (2004). Molecular mechanisms of mammalian DNA repair and the DNA damage checkpoints. Annu. Rev. Biochem. *73,* 39-85.

Sawchuk, D.J., Mansilla-Soto, J., Alarcon, C., Singha, N.C., Langen, H., Bianchi, M.E., Lees-Miller, S.P., Nussenzweig, M.C., and Cortes, P. (2004). Ku70/Ku80 and DNA-dependent protein kinase catalytic subunit modulate RAG-mediated cleavage: implications for the enforcement of the 12/23 rule. J. Biol. Chem. *279,* 29821-29831.

Schimmer, A.D. (2004). Inhibitor of apoptosis proteins: translating basic knowledge into clinical practice. Cancer Res. *64,* 7183-7190.

Schlozen, T., and Gerdes, J. (2000). The Ki-67 protein: from the known to the unknown. J. Cell. Phys. *182*, 311-322.

Sen, R., and Baltimore, D. (1986). Multiple nuclear factors interact with the immunoglobulin enhancer sequences. Cell. *48*, 705-716.

Shackleton, M., Vaillant, F., Simpson, K.J., Stingl, J., Smyth, G.K., Asselin-Labat, M.L., Wu, L., Lindeman, G.J., and Visvader, J.E. (2006). Generation of a functional mammary gland from a single stem cell. Nature *439,* 84-88.

Sheridan, C., Kishimoto, H., Fuchs, R.K., Mehrotra, S., Bhat-Nakshatri, P., Turner, C.H., Goulet, R.,Jr, Badve, S., and Nakshatri, H. (2006). CD44+/CD24- breast cancer cells exhibit enhanced invasive properties: an early step necessary for metastasis. Breast Cancer Res. *8,* R59.

Shillingford, J.M., Miyoshi, K., Robinson, G.W., Bierie, B., Cao, Y., Karin, M., and Hennighausen, L. (2003). Proteotyping of mammary tissue from transgenic and gene knockout mice with immunohistochemical markers: a tool to define developmental lesions. J. Histochem. Cytochem. *51,* 555-565.

Shishodia, S., Koul, D., and Aggarwal, B.B. (2004). Cyclooxygenase (COX)-2 inhibitor celecoxib abrogates TNF-induced NF-kappa B activation through inhibition of activation of I kappa B alpha kinase and Akt in human non-small cell lung carcinoma: correlation with suppression of COX-2 synthesis. J. Immunol. *173,* 2011-2022.

Siegel, P.M., Ryan, E.D., Cardiff, R.D., and Muller, W.J. (1999). Elevated expression of activated forms of Neu/ErbB2 and ErbB3 are involved in the induction of mammary tumours in transgenic mice: implication for human breast cancer. EMBO J. *18*, 2149-2164.

Sigala, J.L, Bottero, V., Young, D.B. Shevchenko, A., Mercurio, F., and Verma, I.M. (2004). Activation of the transcription factor NF-κB requires ELKS, and IκB inhibitory subunit. Science *304*, 1963-1967.

Silberstein, G.B., and Daniel, C.W. (1987). Reversible inhibition of mammary gland growth by transforming growth factor-beta. Science *237,* 291-293.

Simpson, C.D., Anyiwe, K., and Schimmer, A.D. (2008). Anoikis resistance and tumor metastasis. Cancer Lett. *272,* 177-185.

Sims, A.H., Howell, A., Howell, S.J., and Clarke, R.B. (2007). Origins of breast cancer subtypes and therapeutic implications. Nat. Clin. Pract. Oncol. *4,* 516-525.

Singh, S.K., Clarke, I.D., Terasaki, M., Bonn, V.E., Hawkins, C., Squire, J., and Dirks, P.B. (2003). Identification of a cancer stem cell in human brain tumors. Cancer Res. *63,* 5821-5828.

Siveen, K.S., and Kuttan, G. (2009). Role of macrophages in tumour progression. Immunol. Lett. *123,* 97-102.

Sleeman, K.E., Kendrick, H., Ashworth, A., Isacke, C.M., and Smalley, M.J. (2006). CD24 staining of mouse mammary gland cells defines luminal epithelial, myoepithelial/basal and non-epithelial cells. Breast Cancer Res. *8,* R7.

Smalley, M.J., Titley, J., and O'Hare, M.J. (1998). Clonal characterization of mouse mammary luminal epithelial and myoepithelial cells separated by fluorescence-activated cell sorting. In Vitro Cell. Dev. Biol. Anim. *34,* 711-721.

Smith, G.H. (1996). Experimental mammary epithelial morphogenesis in an in vivo model: evidence for distinct cellular progenitors of the ductal and lobular phenotype. Breast Cancer Res. Treat. *39,* 21-31.

Sonnenberg, A., Linders, C.J., Modderman, P.W., Damsky, C.H., Aumailley, M., and Timpl, R. (1990). Integrin recognition of different cell-binding fragments of laminin (P1, E3, E8) and evidence that alpha 6 beta 1 but not alpha 6 beta 4 functions as a major receptor for fragment E8. J. Cell Biol. *110,* 2145-2155.

Sotirou, C., and Pusztai, L. (2009). Gene-expression signatures in breast cancer. N. Engl. J. Med. *360,* 790-800.

Sovak, M.A., Bellas, R.E., Kim, D.W., Zanieski, G.J., Rogers, A.E., Traish, A.M., and Sonenshein, G.E. (1997). Aberrant nuclear factor-κB/Rel expression and the pathogenesis of breast cancer. J. Clin. Invest. *100,* 2952.

Spencer, K.S., Graus-Porta, D., Leng, J., Hynes, N.E., and Klemke, R.L. (2000). ErbB2 is necessary for induction of carcinoma cell invasion by ErbB family receptor tyrosine kinases. J. Cell Biol. *148,* 385-397.

Spirin, K.S., Simpson, J.F., Takeuchi, S., Kawamata, N., Miller, C.W., and Koeffler, H.P. (1996). p27/Kip1 mutation found in breast cancer. Cancer Res. *56,* 2400-2404.

Stephens, P., Hunter, C., Bignell, G., Edkins, S., Davies, H., Teague, J., Stevens, C., O'Meara, S., Smith, R., Parker, A. *et al.* (2004). Lung cancer: intragenic ERBB2 kinase mutations in tumours. Nature *431,* 525-526.

Stingl, J. (2009). Detection and analysis of mammary gland stem cells. J. Pathol. *217,* 229-241.

Stingl, J., and Caldas, C. (2007). Molecular heterogeneity of breast carcinomas and the cancer stem cell hypothesis. Nat. Rev. Cancer. *7,* 791-799.

Stingl, J., Eaves, C.J., Kuusk, U., and Emerman, J.T. (1998). Phenotypic and functional characterization in vitro of a multipotent epithelial cell present in the normal adult human breast. Differentiation *63,* 201-213.

Stingl, J., Eirew, P., Ricketson, I., Shackleton, M., Vaillant, F., Choi, D., Li, H.I., and Eaves, C.J. (2006). Purification and unique properties of mammary epithelial stem cells. Nature *439,* 993-997.

Sun, S.C., and Xiao, G. (2003). Deregulation of NF-κB and its upstream kinases in cancer. Cancer Metastasis Rev. *22,* 405-422.

Tan, B.T., Park, C.Y., Ailles, L.E., and Weissman, I.L. (2006). The cancer stem cell hypothesis: a work in progress. Lab. Invest. *86,* 1203-1207.

Thompson, H.J. (2000). Methods for induction of mammary carcinogenesis in the rat using either 7,12-dimethylbenz(a)anthracene or 1-methyl-1-nitrosurea. In Methods in Mammary Gland Biology and Cancer Research, Ip, M. M., and Asch, B. B. eds., (New York: Springer) pp. 19-31.

Tian, B., and Brasier, A.R. (2003). Identification of a nuclear factor kappa B-dependent gene network. Recent Prog. Horm. Res. *58,* 95-130.

Tonegawa, S. (1983). Somatic generation of antibody diversity. Nature *302,* 575-581.

Topper, Y.J., and Freeman, C.S. (1980). Multiple hormone interactions in the developmental biology of the mammary gland. Physiol. Rev. *60,* 1049-1106.

Toyoshima, H., and Hunter, T. (1994). p27, a novel inhibitor of G1 cyclin-Cdk protein kinase activity, is related to p21. Cell *78,* 67-74.

Van Antwerp, D.J., Martin, S.J., Kafri, T., Green, D.R., and Verma, I.M. (1996). Suppression of TNF-alpha-induced apoptosis by NF-kappaB. Science *274,* 787-789.

van Gent, D.C., and van der Burg, M. (2007). Non-homologous end-joining, a sticky affair. Oncogene *26,* 7731-7740.

Varfolomeev, E., Goncharov, T., Federova, A.V., Dynek, J.N., Kobel, K., Deshayes, K, Fairbrother, W.J., and Vucic, D. (2008). c-IAP1 and c-IAP2 are critical mediators of tumor necrosis factor alpha (TNFalpha)-induced NF-kappaB activation. J. Biol. Chem. *283*, 24295-24299.

Vaux, D.L., and Silke, J. (2005). IAPs, RINGs and ubiquitylation. Nat. Rev. Mol. Cell Biol. *6,* 287-297.

Vince, J.E., Wong, W.W., Khan, N., Feltham, R., Chau, D., Ahmed, A.U., Benetatos, C.A., Chunduru, S.K., Condon, S.M., McKinlay, M., Brink, R., Leverkus, M., Tergaonkar, V., Schneider, P., Callus, B.A., Koentgen, F., Vaux, D.L. and Silke, J. (2007). IAP antagonists target cIAP1 to induce TNF alpha-dependent apoptosis. Cell *131*, 682-693.

Wajant, H., Pfizenmaier, K., and Scheurich, P. (2003). Tumor necrosis factor signaling. Cell Death Differ. *10*, 45-65.

Walker, J.R., Corpina, R.A., and Goldberg, J. (2001). Structure of the Ku heterodimer bound to DNA and its implications for double-strand break repair. Nature *412*, 607-614.

Wang, Y., Ghosh, G., and Hendrickson, E.A. (2009). Ku86 represses lethal telomere deletion events in human somatic cells. Proc. Natl. Acad. Sci. U. S. A. *106*, 12430-12435.

Wang, Z., and Storm, D.R. (2006). Extraction of DNA from mouse tails. BioTechniques *41*, 410, 412.

Ward, J.M. and Parsoneault, E. (2006). Virtual Mouse Necropsy.*2008*,

Waris, G., and Ahsan, H. (2006). Reactive oxygen species: role in the development of cancer and various chronic conditions. J. Carcinog. *5*, 14.

Weidner, N., Carroll, P.R., Flax, J., Blumenfeld, W., and Folkman, J. (1993). Tumor angiogenesis correlates with metastasis in invasive prostate carcinoma. Am. J. Pathol. *143*, 401-409.

Weidner, N., Folkman, J., Pozza, F., Bevilacqua, P., Allred, E.N., Moore, D.H., Meli, S., and Gasparini, G. (1992). Tumor angiogenesis: a new significant and independent prognostic indicator in early-stage breast carcinoma. J. Natl. Cancer Inst. *84*, 1875-1887.

Weinberg, R.A. (2007). The Biology of Cancer (New York, NY: Garland Science, Taylor and Francis Group, LLC).

Weterings, E., and Chen, D.J. (2008). The endless tale of non-homologous end-joining. Cell Res. *18*, 114-124.

Williams, J.M., and Daniel, C.W. (1983). Mammary ductal elongation: differentiation of myoepithelium and basal lamina during branching morphogenesis. Dev. Biol. *97*, 274-290.

Workman, J.L., and Kingston, R.E. (1998). Alteration of nucleosome structure as a mechanism of transcriptional regulation. Annu. Rev. Biochem. *67*, 545-579.

World Health Organization. (2009). Cancer, Fact Sheet Number 297.*2009*, 1.

Xiao, G., Harhaj, E.W. and Sun, S.C. (2000). Domain-specific interaction with IκB kinase (IKK) regulatory subunit IKKγ is an essential step in Tax-mediated activation of IKK. J. Biol. Chem. *275*, 34060-34067.

Xiao, G., Harhaj, E.W., and Sun, S.C. (2001). NF-κB-inducing kinase regulates the processing of NF-κB2 p100. Mol. Cell. *7*, 401-409.

Xiao, G., Rabson, A.B., Young, W., Qing, G., and Qu, Z. (2006). Alternative pathways of NF-kappaB activation: a double-edged sword in health and disease. Cytokine Growth Factor Rev. *17,* 281-293.

Yasuda, M., Nakano, K., Yasumoto, K., and Tanaka, Y. (2002). CD44: functional relevance to inflammation and malignancy. Histol. Histopathol. *17,* 945-950.

Yoo, S., Kimzey, A., and Dynan, W.S. (1999). Photocross-linking of an oriented DNA repair complex. Ku bound at a single DNA end. J. Biol. Chem. *274,* 20034-20039.

Yu, D., and Hung, M.C. (2000). Role of erbB2 in breast cancer chemosensitivity. Bioessays *22,* 673-680.

Yu, J.H., Kim, K.H., and Kim, H. (2007). Nuclear loss of DNA repair Ku proteins and c-myc expression in apoptosis of cerulein-stimulated pancreatic acinar cells. Inflammopharmacology *15,* 282-287.

Yuan, A., Chen, J.J., and Yang, P.C. (2008). Pathophysiology of tumor-associated macrophages. Adv. Clin. Chem. *45,* 199-223.

Zender, L., Spector, M.S., Xue, W., Flemming, P., Cordon-Cardo, C., Silke, J., Fan, S.T., Luk, J.M., Wigler, M., and Hannon, G.J., *et al.* (2006). Identification and validation of oncogenes in liver cancer using integrative oncogenomic approach. Cell *125.*, 1253-1267.

Zhang, Z., Zhu, L., Lin, D., Chen, F., Chen, D.J., and Chen, Y. (2001). The three-dimensional structure of the C-terminal DNA-binding domain of human Ku70. J. Biol. Chem. *276,* 38231-38236.

A. APPENDICES

A.1 Flow cytometry

Flow cytometry is a method that allows for the multi-parameter measurement and analysis of particle characteristics, typically cells, as they pass through a beam of light while suspended in a stream of liquid (Ibrahim, and van den Engh, 2007). The size and complexity of the particle can be assessed, as well as the relative fluorescence intensity (Givan, 2004). A flow cytometer is composed of three main systems that allow for particle analysis (BD Biosciences, 2000). The fluidics system allows for the transport of particles one at a time in a stream to a laser beam in the optics system for analysis. The laser beam of the optic system passes a beam of light onto each particle; each particle will scatter the laser in a unique way depending on their size and complexity. The scattered light is then directed to detectors in the electronic system (BD Biosciences, 2000). A number of detectors are placed either in front of the particle to measure forward scatter (FSC) or perpendicular to the particle to measure side scatter (SSC) (Givan, 2000; Givan, 2004). The electronic system is responsible for converting the directed light signal (FSC or SSC) into electronic signals that can be amplified and analyzed by a computer. If the flow cytometer is equipped with a method for sorting particles, the electronic system also charges and deflects the particles to initiate the sorting (BD Biosciences, 2000). FSC data correlates with the cell volume or size, and SSC data is converted to information about the particle's inner complexity, which encompasses everything from the size of the nucleus to membrane roughness (BD Biosciences, 2000; Herzenberg and De Rosa, 2000).

A.2 Fluorescent activated cell sorting

Fluorescence activated cell sorting (FACS) analysis is a specialized type of flow cytometry that allows for the sorting of a heterogeneous mixture of cells into separate containers, one cell at a time, based on light scattering and fluorescent characteristics of a cells (Herzenberg and De Rosa, 2000). FACS can sort a single cell suspension of heterogeneous cells that naturally fluoresce or those labeled with fluorescently conjugated antibodies for a variety of cell surface markers or a fluorescent dye (Givan, 2000).

FACS analysis works on the same principle as flow cytometry (Herzenberg and De Rosa, 2000). A single cell suspension containing cells labeled with a fluorescent dye is introduced into the flow cytometer where it is passed in a into a nozzle that vibrates, breaking the stream into tiny droplets, some of which may contain a cell. A laser beam directed at the droplets excites the fluorescent dye on the cell and becomes scattered; the emitting fluorescent wavelength is then detected by a photocell. If the emitting signal meets the criteria for sorting (i.e. the correct emitting wavelength) an electric charge is assigned to the stream and the cells are sorted into separate containers. Uncharged droplets that do not meet sorting criteria are separated and discarded (Givan, 2000). FACS analysis in this manner allows for the precise sorting of up to 300,000 cells per minute, leaving behind the desired cell fraction for further analysis (Herzenberg and De Rosa, 2000). This application has been used to advance the understanding of many cell types in a number of scientific fields including molecular biology, immunology, pathology and marine biology, and has been especially useful in characterizing normal and cancerous cell populations.

A.3 Apoptosis

A.3.1 Intrinsic apoptosis

The mitochondria, cellular organelles essential for life, are found at the centre of the intrinsic apoptotic cascade (Weinberg, 2007). The outer mitochondrial membrane processes various apoptotic and survival signals through channels located in the membrane; cellular survival signals keep the channels closed, while pro-apoptotic signals can cause them to open (Reed, 2000). Once the channels are open, two pro-apoptotic proteins, cytochrome C and SMAC are released (Martinou and Green, 2001). Cytochrome C molecules aggregate with apoptotic peptidase activating factor 1 (APAF-1) to form the apoptosome, a seven-spoked wheel in which APAF-1 forms the spokes of the wheel and cytochrome C forms the spoke tips (Acehan *et al.*, 2002). Formation of the apoptosome attracts pro-caspase 9, processing it into the active caspase 9. In turn, caspase 9 activates pro-caspase 3, which activates a series of executioner caspases (3, 6, and 7) in the apoptotic cascade (Earnshaw *et al.*, 1999). Mitochondrial release of SMAC allows for SMAC-mediated degradation of IAPs, which also allows for the progression of apoptosis (Salvesen and Duckett, 2002). Executioner caspases cleave various death substrates, including lamins, and cytoskeletal proteins, leading to the characteristics of the apoptotic program: nuclear shrinkage, chromatin condensation, and the formation of apoptotic bodies (Cohen, 1997; Enari *et al.*, 1998).

A.3.2 Extrinsic apoptosis

The extrinsic pathway begins outside the cell through the activation of specific pro-apoptotic receptors on the cell surface. These receptors are activated by specific

molecules known as pro-apoptotic ligands, which include Apo2L/TRAIL and CD95L/FasL and bind their cognate receptors DR4/DR5 and CD95/Fas, respectively (Ashkenazi, 2002). Ligand binding induces receptor clustering and the recruitment of adaptor proteins and the initiator or pro-caspases 8 and 10, which together form the death inducing signaling complex (Boldin *et al*, 1995). The formation of the signaling complex brings pro-caspases into close proximity, facilitating autocatalytic processes and cytoplasmic release. Once in the cytoplasm, they are capable of activating the executioner caspases 3, 6 and or 7, converging on the intrinsic pathway (Ghobrial *et al*, 2005).

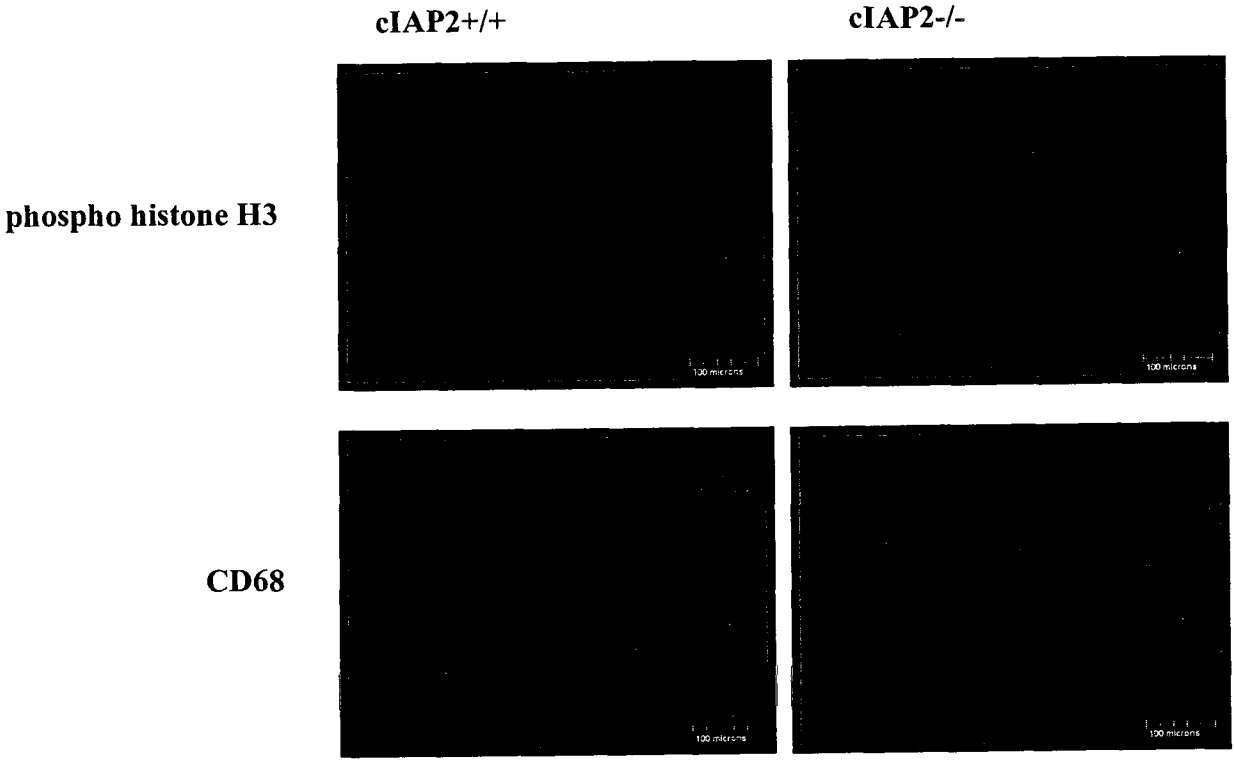
cIAP2+/+
cIAP2-/-
phospho histone H3
CD68
100 microns
100 microns
100 microns
100 microns

A.4.

Data collected by Min Ying Niu, a previous Pratt Lab technician (Niu, 2007; unpublished data).

Figure A.4 ErbB2 induced tumours in mice lacking cIAP2 expression do not show an increase in cell growth or levels of TAMs. Immunohistochemical analysis of representative 8μm frozen tumour sections from ErbB2 mice with and without cIAP2 expression to determine cellular mitototic index using an anti-phospho histone H3 antibody, and macrophage infiltration using an anti-CD68 antibody. Staining was visualized with a CY3 secondary antibody. Scale bar is 50 microns.

A

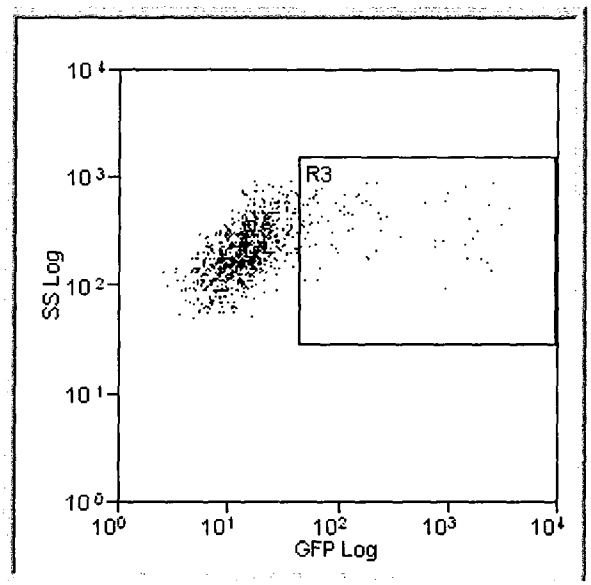
R3
SS Log
GFP Log
10^0
10^1
10^2
10^3
10^4

B

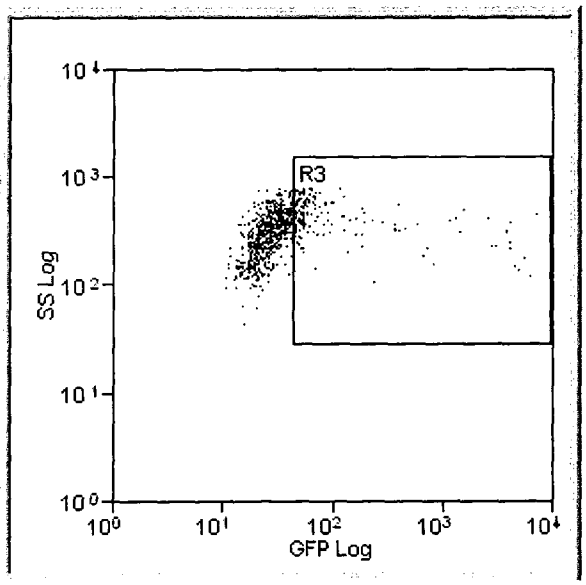
R3
SS Log
GFP Log
10^0
10^1
10^2
10^3
10^4

A.5

Negative flow cytometry data showing little to no EGFP expression. Flow cytometric analysis was completed as described in the text (Materials and Methods, and Results sections).

Figure A.5. NF-κB analysis of EGFP positive Ma-CFCs and MRUs. FACS analysis of mammary stem cell populations from *cis*-NF-κB reporter mice labeled with CD24PE and CD49F AlexaFluor antibodies. **A**, Analysis of EGFP expression in the MRU fraction (CD24med, CD49fhigh) of the mouse mammary stem cell population. **B**, EGFP fluorescence in the Ma-CFC fraction (CD24high, CD49flow) of the mouse mammary stem cell population. In both cases, less than 1% of cells had GFP fluorescence.

A.6

Interaction of PARP-1 with the cellular NHEJ machinery in V(D)J recombination and double stranded DNA break repair (Haché Lab (Sept. 2008 – May 2009))

LIST OF ABBREVIATIONS (used in Appendix A.6)

Abbreviation	Full Name
4-ANI	4-Amino-1,8-naphthalimide
ADP	Adenosine diphosphate
CAT	Chloramphenicol acetyl transferase
DNA-PKcs	DNA-dependent protein kinase catalytic subunit
DSBs	Double-stranded DNA breaks
EMSA	Electrophoretic mobility shift assay
GST	Glutathione-S-transferase
HEK	Human embryonic kidney
His-MBP	Histidine-maltose binding protein
HR	Homologous recombination
IPTG	Isopropyl-beta-D-thiogalactopyranoside
kDa	kiloDalton
NAD+	Nicotinamide adenine dinucleotide
NHEJ	Non-homologous end joining
PARP-1	Poly-ADP-ribose polymerase 1
RAG	Recombination activating gene
RSS	Recombination signal sequence
V(D)J	Variable diversity joining

A.6.1 Double stranded DNA break repair

Maintenance of genomic integrity and stability is an essential cellular function. Both metabolic processes and environmental factors can lead to DNA damage, and the ability of the cell to efficiently detect and repair the damage caused is fundamental to its survival (Lodish *et al.*, 2003). When a cell loses its ability to effectively repair DNA damage, it can enter a permanent state of dormancy or senescence, it can undergo programmed cell death via apoptosis or it can undergo an upregulation of cellular growth leading to transformation and a cancerous state (Weinberg, 2007). Double stranded DNA breaks (DSBs), which occur when both strands of the DNA double helix are damaged, can lead to genomic rearrangements. The cell has two mechanisms to repair DSBs, homologous recombination (HR) and non-homologous end joining (NHEJ) (Rothkamm *et al.*, 2003), which is the predominant pathway in higher eukaryotes, whereas HR requires the presence of identical or almost identical sequences between the broken DNA ends, or a template to complete the repair process (Sancar *et al.*, 2004).

A.6.2 The Ku heterodimer

NHEJ is an evolutionarily conserved process that uses short DNA sequence homologies called microhomologies typically present on the overhangs of the broken DNA ends to guide the repair process. A number of cellular proteins are required to initiate NHEJ, which begins with Ku binding to the broken DNA ends (Downs and Jackson, 2004). The Ku nuclear protein exists as a heterodimer of a 70 kiloDalton (kDa) subunit (Ku70) and an 80 kDa subunit (Ku80) with approximately $4X10^5$ copies per cell (Yoo, Kimzey, and Dynan, 1999). Although the primary role of Ku in a normal cell is to

mediate DSB repair, its high affinity for DNA ends and its abundance in the cell has implicated it in other processes, including the recombination of the variable (V), diversity (D) and joining (J) segments (V(D)J recombination) during lymphocyte development, telomere maintenance, anti-apoptosis, genomic stability, tumour suppression, and regulation of gene transcription (Bredemeyer *et al.*, 2008; Gao *et al.*, 2000; Gullo *et al.*, 2006; Mahaney, Meek, and Lees-Miller, 2009; Wang, Ghosh, and Hendrickson, 2009; Yu, Kim, and Kim, 2007).

The structure of the Ku heterodimer has been partially elucidated by X-ray crystallography; both Ku subunits exhibit common domain topology, and consist of an N-terminal α/β domain, a central β-barrel domain and a helical C-terminal arm which form a pseudo-symmetrical structure with a preformed ring extending from a broad base (Rivera-Calzada *et al.*, 2007; Walker, Corpina, and Goldberg, 2001). The Ku70 C-terminal arm contains a 5kDa SAP domain (Zhang *et al.*, 2001). The Ku70 SAP domain is thought to mediate DNA binding during the NHEJ process as SAP domains have been previously identified as DNA bindings regions (Aravind and Koonin, 2000).

A.6.3 The non-homologous end joining process

The NHEJ process involves a number of proteins that assemble at the site of the DNA break in a carefully controlled order. NHEJ is initiated when the Ku heterodimer binds at the site of the DSB, recruits DNA-dependent protein kinase catalytic sub-unit (DNA-PKcs), and slides inward on the DNA end (Lieber, 1999). The association of DNA-PKcs with Ku activates the serine/threonine kinase activity of DNA-PKcs, which leads to DNA-PKcs autophosphorylation and the phosphorylation of other NHEJ factors,

which are recruited to the site of the break, including Artermis, DNA ligase IV and XRCC4. Non-compatible DNA ends are processed by the endonuclease activity of phospho-Artemis, and the NHEJ process concludes with DNA end ligation by DNA ligase IV/XRCC4 (van Gent and van der Burg, 2007; Weterings and Chen, 2008).

The presence of Ku is an integral part of the NHEJ process. Until recently, the mechanism of Ku removal from the DNA was unknown; NHEJ results in a closed DNA conformation with no exposed ends for Ku to slide off of. However, our lab has recently proposed a model of Ku removal from ligated DNA ends via interaction with poly-adenosine diphosphate (ADP) ribose polymerase-1 (PARP-1).

A.6.4 Poly-ADP ribose polymerase-1

PARP-1 is a member of the DNA damage-dependent PARP family and is a molecular sensor of DNA damage in the cell (de Murcia *et al.*, 1997). When a DNA break occurs, PARP-1 uses nicotinamide adenine dinucleotide (NAD+) as a substrate to catalyze the attachment of ADP-ribosyl groups to aspartate and glutamate residues of acceptor proteins that are associated with DNA processes, or to itself. Due to its function as a DNA break sensor, it has been suggested that PARP-1 and Ku may compete for binding to DNA ends. Our lab has suggested that PARP-1 could regulate the association of Ku with DNA (Haché lab, unpublished data). It was shown that ADP-ribosylation of Ku by PARP-1 was efficient to cause the release of Ku from both linear and circular DNA ends under ADP-ribosylation permissive conditions. PARP-1 was also capable of ADP-ribosylating Ku, which likely leads to its removal from DNA ends. PARP-1 was shown to target three glutamate residues in the C-terminal SAP domain of Ku70, and

deletion of the SAP domain, or mutation of the glutamate residues targeted for ribosylation by PARP-1, prevented the release of Ku from the DNA. These mutants also showed increased sensitivity to DNA damage when expressed *in vivo*, suggesting that Ku ribosylation is necessary for an appropriate DNA damage response, and inhibition or prevention of Ku ribosylation causes an increased sensitivity to DNA damage (Haché lab, unpublished data).

A.6.5 The Ku heterodimer and V(D)J recombination

As well as having a role in NHEJ, the Ku heterodimer also has a role in V(D)J recombination, an essential step in the generation of B cell and T cell receptors in the vertebrate immune system. V(D)J recombination is a tightly controlled double-strand break and rejoining pathway needed to generate the region that codes for the variable domain of immunoglobulin and T-cell receptors (Gellert, 2002; Lieber *et al.*, 2004).

V(D)J recombination occurs at recombination signal sequences (RSSs) that lie adjacent to each V, D and J segment. The RSS is made up of well-conserved heptamer and nonamer sequences that are separated by non-conserved sequences of either 12 or 23 spacer DNA base pairs. Recombination only occurs between RSSs with 12 and 23 base pair sequences, known as the 12/23 rule (Tonegawa, 1983).

V(D)J recombination is initiated upon binding of two recombination activating genes (RAG) proteins, RAG1 and RAG2, at the RSS generating a nick in the DNA. Cleavage by RAG1/2 occurs in two steps. In the first step, a nick is made at the 5' end of the heptamer, resulting in a 5'-phosphoryl group on the RSS and a 3'-hydroxyl group on the coding end. The 3'-hydroxyl group initiates a nucleophilic attack on the phopshoryl

group on the opposite strand, resulting in a DNA hairpin at the coding end and a blunt signal end containing the RSS. The NHEJ components then repair the broken DNA strands, resulting in a circular signal joint and a coding joint containing the gene segment (Downs and Jackson, 2004; Gellert, 2002).

Previously, our lab looked at the role of Ku in the V(D)J recombination reaction. To determine if Ku was necessary for V(D)J, wild type and Ku knockout cells were used in an *in vivo* recombination reaction. It was found that recombination was unable to occur in the absence of Ku. It was suggested also that the cleavage step of Ku may be Ku-dependent: using an isolated RSS and extracts from Ku wild type or knockout cells, RSS cleavage did not occur in the absence of Ku. Since it appears that Ku is required for cleavage at the RSS, it is possible that Ku is interacting with one of the RAG proteins. Our lab was able to show that there may be an interaction between the Ku70 SAP domain and RAG1 using glutathione-S-transferase (GST) pulldowns and a number of Ku deletion mutants.

Using the Ku 70 C-terminal SAP domain mutants used in the PARP-1/Ku interaction studies, our lab looked at the functionality of these mutants in NHEJ using the *in vivo* recombination vector mentioned already. There was a severe impairment in V(D)J recombination when a Ku70 SAP deletion mutant (ΔSAP mutant) and another mutant with mutation of the three glutamate target residues of PARP-1 (3E mutant) were used in the recombination assay. There was a decrease in the recombination efficiency as well as an increase in the number of errors in the recombination products from the Ku70 SAP mutant or deletion cells compared to those from wild-type Ku70 cells. Since these

same Ku70 SAP mutants are rendered insensitive to ADP ribosylation by PARP-1, this suggests a potential role of PARP-1 in V(D)J recombination.

A.6.6 Hypothesis

I hypothesize that PARP-1 inhibition will significantly affect V(D)J recombination by reducing recombination efficiency, and potentially increasing the number of errors in both the signal and coding joints following V(D)J recombination.

A.6.7 Objectives

1. Determine the effects of PARP-1 inhibition on V(D)J recombination
2. Confirm that the interaction between Ku70 and RAG1 occurs via the Ku70 SAP domain

A.6.8 Results to date

A.6.8.1 The role of PARP-1 in V(D)J recombination

Given that PARP-1 modifies the Ku70 SAP domain, and that 1- the aforementioned mutants are rendered insensitive to ADP-ribosylation (PARylation) by PARP-1, and 2- the cells expressing the Ku70 ΔSAP and 3E constructs are V(D)J deficient, PARP-1 may also be playing a role in V(D)J recombination that is currently unknown. To determine the role of PARP-1 in V(D)J recombination, an *in vivo* V(D)J recombination system and the PARP inhibitor, 4-Amino-1,8-naphthalimide (4-ANI) was used.

The *in vivo* V(D)J recombination assay is a vector base system: a vector containing two RSSs is co-transfected into cells along with RAG1 and RAG2 vectors. Following RAG1 and RAG2 expression (48-72 hours after transfection) the recombination vector is purified from the cells using the Qiagen Miniprep small-scale alkaline lysis system. Signal and coding joint formation is assessed using two separate recombination vectors, pJH200 and pJH290, which are signal joint and coding joint vectors respectively. Using primers spanning the recombination site, recombination is assessed by PCR. If recombination is successfully completed in the pJH200 vector, a recombination product of 256bp is amplified. A 460bp fragment will be amplified if recombination has not occurred. With the pJH290 vector, recombined product will be amplified at 550bp whereas unrecombined product will yield an 800bp fragment.

The efficiency of V(D)J recombination can be assessed by transformation of the purified vector into *E. coli* and grown on LB plates with ampicillin or chloramphenicol and ampicillin. The recombination vectors have ampicillin resistance markers, and successful recombination removes a transcriptional terminator on a chloramphenicol acetyltransferase (CAT) gene that conveys chloramphenicol resistance. The recombination efficiency can be calculated by counting the number of recombined colonies (the number on the chloramphenicol + ampicillin plates) divided by the number of colonies on the ampicillin-only plates.

Human embryonic kidney (HEK) 293T cells were transfected with the signal or coding joint vector plus RAG1/2. The recombination success was assessed by PCR and the efficiency by transformation into *E. coli* as previously mentioned. V(D)J recombination was seen in cells transfected with the signal joint vector (pJH 200), but not

the coding joint vector (pJH290) (Figures A.1A and A.1B, respectively). The recombination efficiency of signal joint formation in HEK 293T cells was found to be 0.575, whereas coding joint recombination was much less efficient at 0.117 (Figure A1C). In a separate experiment, HEK 293T cells were transfected with the signal or coding joint vector plus RAG1/2 and were treated with the PARP inhibitor, 4-ANI. Cells were transfected with two concentrations of RAG1 and 2 to determine if this had an effect on recombination; recombination efficiency was determined by transforming *E. coli* as mentioned above. In all cases, treatment with 4-ANI decreased the efficiency of recombination, suggesting that PARP-1 may play a role in V(D)J recombination.

A.6.8.2 The Ku70 C-terminal SAP domain mediates the interaction between Ku and RAG1

It has been previously shown in our lab that there is an interaction between RAG1 and Ku that may occur via the Ku70 SAP domain using a series of Ku70 deletion mutants (Figure A.2-D) . These results have shown that the Ku-RAG1 interaction requires the SAP domain, but it is not known if the SAP domain is sufficient for the interaction alone. To determine this, a pulldown using the Ku70 SAP domain was completed.

Using primers flanking the Ku70 SAP domain, the SAP domain was cloned into a GST-tagged expression vector, pGEX. A Ku70 SAP domain-GST fusion protein was generated which will be used in the pulldown assay. Expression of the RAG1 protein was using the pET protein expression system. A pET-Histidine-maltose binding protein (His-MBP)-RAG1 construct will be transformed into BL21(DE3) *E. coli*, and protein

A

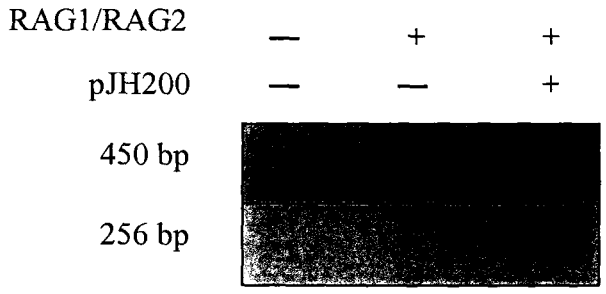

B

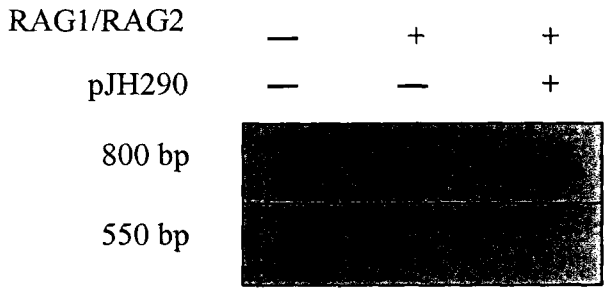

C

	Recombination Efficiency	
Cell Type	Signal Joint	Coding Joint
HEK293T	0.575	0.117

D

	Recombination Efficiency			
PARP-1 Status	Signal Joint		Coding Joint	
	Actual	Corrected	Actual	Corrected
Active	0.482	1.00	1.056	1.00
Inhibited	0.245	0.51	0.105	0.10
Active*	0.284	1.00	0.616	1.00
Inhibited	0	0	0.085	0.14

Figure A.6.1. ***In vivo*** **V(D)J recombination assay in HEK 293T cells.** 293T cells were transfected with RAG1 and RAG2 plasmids along with recombination substrates, were incubated for 48 hours and plasmid DNA was isolated from the cells using a Mini prep protocol. **A**, PCR analysis of signal joint (pJH200) recombination product. Recombination was determined using recombination specific primers, yielding a 450bp product if the signal joint substrate was unrecombined, and a 256bp product if recombined. **B**, PCR analysis of coding joint (pJH290) recombination product using recombination specific primers. Recombination yields a 550bp product, while unrecombined product yields an 800bp product. **C**, Recombination efficiency of HEK 293T cells transfected with RAG1 and 2 and either pJH200 or 290. Recombination efficiency was assessed by transforming DH5α E. coli with the recombination product from 293T cells, and plating the bacteria on ampicillin or chloramphenicol + ampicillin plates, and counting colonies. The recombination substrates contain ampicillin resistance, and when recombined, acquire chloramphenicol resistance. Actual recombination efficiency was calculated as: (number of colonies on (chloramphenicol + ampicillin) plates)/(number of colonies on ampicillin plates). **D**, Recombination efficiency of HEK 293T cells transfected with RAG1 and 2 with either pJH200 or 290 treated with and without the PARP inhibitor, 4-ANI. Cells were transfected with differing amounts of RAG1/2, 1.0ug or 0.8ug (*).

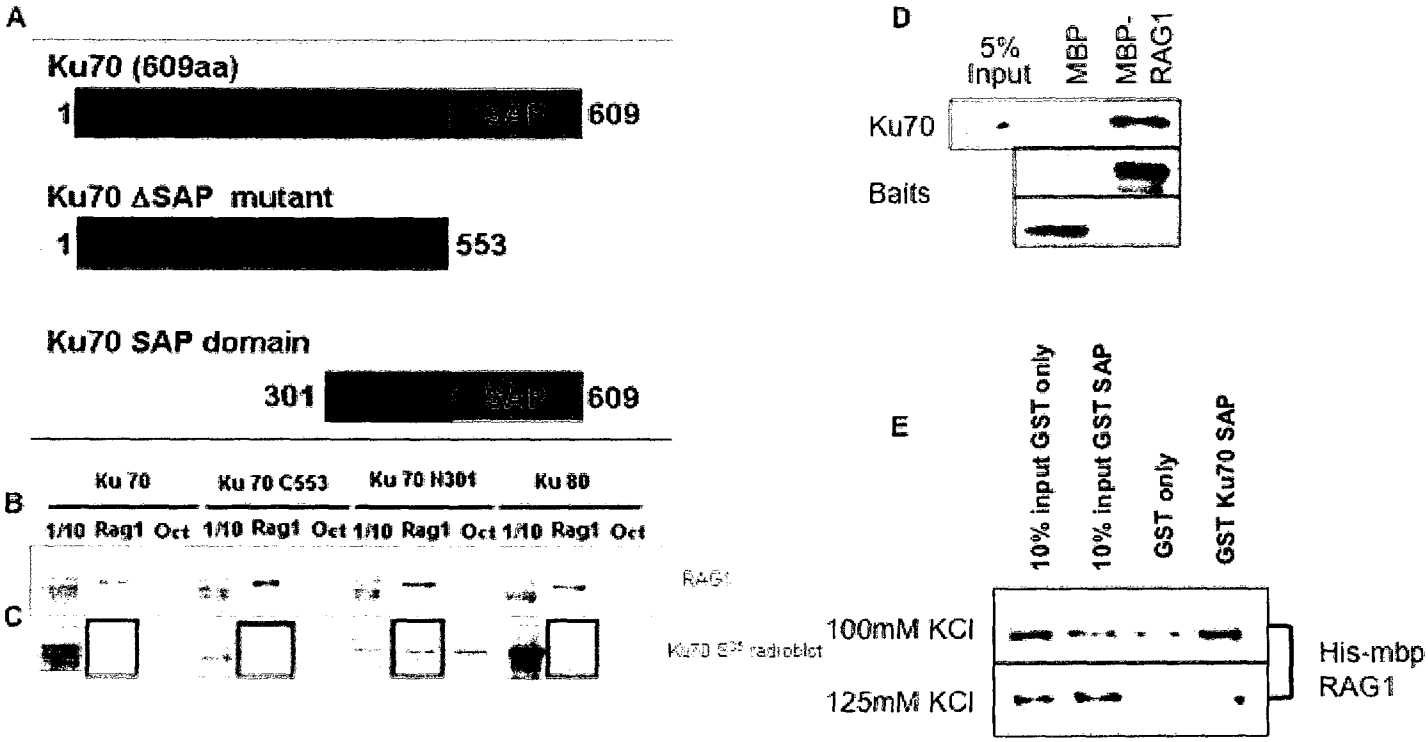
A
Ku70 (609aa)
1
609
Ku70 ΔSAP mutant
1
553
Ku70 SAP domain
301
609
B
Ku 70
Ku 70 C553
Ku 70 N301
Ku 80
1/10 Rag1 Oct 1/10 Rag1 Oct 1/10 Rag1 Oct 1/10 Rag1 Oct
C
RAG1
Ku70 SAP radioblot
D
5% Input
MBP
MBP-RAG1
Ku70
Baits
E
10% input GST only
10% input GST SAP
GST only
GST Ku70 SAP
100mM KCl
125mM KCl
His-mbp RAG1

Figure A.6.2. The C-terminal SAP domain of Ku70 mediates the interaction with RAG1. A, Deletion mutations of the Ku sub-unit and *in vitro* translated and radio-labeled with 35S. **B**, GST tagged RAG1 was isolated on GST-beads, and extraction was separated on 10% SDS polyacrylamide gel, followed by Coomasie staining and **C**, radioblotting. Wells labeled 1/10 contain crude extract used to test the interaction. **D**, His-tagged MBP fusion core RAG1 was tested for binding with purified Baculo Ku70/Ku80 (lane 3). The presence of Ku70/Ku80 was detected with an anti-Ku70 antibody (lanes 1 to 3). His-tagged MBP was employed as a negative control (lane 2). Ethidium bromide (200 mg/ml) was included in the reactions in lanes 2 and 3. Binding of core RAG1 to Ku70/Ku80 was compared with 5% of Baculo Ku input (lane 1). Input of his-tagged MBP fusion core RAG1 and his-tagged MBP were detected with an anti-MBP antibody. **E**, The C-terminal SAP domain of Ku70 mediates the interaction of Ku with RAG1. The Ku70 SAP domain on its own was expressed as a GST fusion protein and was incubated with bacterial His-mBP-RAG1 on GST beads in the presence of Ethidium bromide. After incubation, the resin was washed with wash buffer with 100mM or 125mM KCl. Increased salt in the wash buffer decreased non-specific binding to GST protein on its own. The resin was then loaded on a 10% SDS polyacrylamide gel, and binding was assessed using an anti-His antibody. Houssein Salem of the Haché lab completed figures A.2 A, B and C. Figure A.2. D was done by Kyna Mensch in the Haché lab.

expression was induced with isopropyl-β-D-thiogalactopyranoside (IPTG) following colony growth in LB with kanamycin. The pET-MBP-RAG1 protein was purified via its C-terminal histidine tag and TALON resin. TALON resin is a form of immobilized metal affinity chromatography using a cobalt resin that binds His-tagged proteins with an enhanced selectivity over nickel-based resins (Chaga *et al.*, 1999). A pulldown assay was done using the Ku70 SAP-GST fusion protein, and GST alone with His-MBP-RAG1 (previously generated) to determine if the Ku-RAG1 reaction is mediated via the Ku70 SAP domain. Full length Ku70 was unable to be expressed successfully. It was found, when the pull-down was performed in a buffer with 125mM KCl, 50mM $NaPO_4$ (pH 7.0), and ethidium bromide that RAG1 was capable of binding the Ku70 SAP-GST protein in a DNA independent manner, but not GST alone (Figure A.2E). Along with the other results from our lab, this suggests that the Ku70 C-terminal SAP domain is not only required, but is sufficient for the interaction between Ku and RAG1.

A.6.9 Discussion

A.6.9.1 The role of PARP-1 in V(D)J-recombination

It is difficult to come to any significant conclusions with regards to my work completed in the Haché lab presented herein. The role of PARP-1 in V(D)J recombination was unable to be sufficiently assessed due to a large number of issues that occurred during the experimental process. The experiments outlined in Figure A.1 were unfortunately unable to be replicated. The initial RAG1 and RAG2 plasmids that our lab had in possession were very difficult to express. The plasmid DNA was highly nicked and degraded, and even after cesium chloride prep, it was difficult to obtain any

indication that they were expressed in the cells that they were transfected into. The role of PARP-1 in V(D)J could have been further elucidated using the SAP domain mutants mentioned in the introduction. However, after it was difficult to repeat the results seen by a previous student, it was discovered that large errors in plasmid identification occurred, and re-cloning of these mutants was difficult. When the verified mutants were used in the V(D)J experiment, V(D)J recombination did not work. However, there does appear to be an involvement of PARP-1 in V(D)J recombination.

Previously, the role of PARP-1 in V(D)J has been difficult to assess, and there has been a number of contradictory studies suggesting that PARP-1 may aid in the resolution of coding joint formation during the NHEJ process of V(D)J, or that PARP-1 may actually antagonize V(D)J recombination altogether (Brown, Claudio, and Siebenlist, 2008; Dominguez-Bendala, Masutani, and McWhir, 2006). Our lab's proposed role for PARP1 in NHEJ repair is to aid in the movement of Ku from the DNA end by ribosylating the DNA bound SAP domain, and to regulate the association of Ku with RAG-induced DNA breaks.

A.6.9.2 The interaction between RAG1 and Ku

The process of V(D)J recombination has been well defined, with independent roles for Ku70 and RAG1; RAG1 initiates V(D)J recombination by introducing a DNA break at the RSS. It has long been assumed that Ku's involvement in V(D)J occurs following RAG1 cleavage. Ku senses the DNA break and recruits the NHEJ proteins to finish the process of V(D)J recombination. The direct interaction between RAG1 and Ku70 that our lab has shown suggests an earlier role for the Ku protein in V(D)J

recombination. Recently, another research group has found evidence for an interaction between Ku70 and RAG1 (Raval *et al.*, 2008). Using full length RAG1/core RAG2 and Ku70/Ku80, this group provided evidence that Ku70/Ku80 is capable of interacting in a DNA independent manner by electrophoretic mobility shift assay (EMSA). Ku70/Ku80 formed a RAG-RSS-Ku70/Ku80 complex that was capable of being supershifted with anti-Ku antibodies. In this study they were unable to show an interaction using full length RAG1 and Ku70/Ku80. These results contradict those from our lab as we have been able to show a direct interaction between RAG1 and Ku70/Ku80 that does not rely on the presence of DNA. In the literature, there is a significant amount of evidence that supports at least an indirect interaction between RAG1 and NHEJ components. RAG1 has been shown to mediate V(D)J recombination *in vitro*, better enforcing the 12/23 rule when Ku and other NHEJ components are included in the reaction (Sawchuk *et al.*, 2004). It has also been proposed that RAG proteins may aide in positioning Ku at the RSS prior to cleavage to guarantee that the nicked DNA is properly repaired during the V(D)J reaction (Raval *et al.*, 2008).

In summary, it appears that PARP-1 plays a role in V(D)J recombination that is currently unclear as inhibition of PARP-1 using the PARP inhibitor 4-ANI results in a decrease in V(D)J recombination efficiency. Based on these results, and previous results from our lab, we suggest that PARP-1 may be capable of facilitating the movement of Ku on the DNA via ribosylation of the Ku70 SAP domain to help regulate the association of Ku with the RAG-mediated DNA break. RAG1 is capable of interacting in a DNA-independent manner to the Ku70 SAP domain; the interaction requires the Ku70 SAP domain, which is sufficient to allow for this interaction to occur on its own.

A.7

Licences obtained for use of copyrighted material presented in introduction.

Figure 1.

License Number	2284881111969
License date	Oct 09, 2009
Licensed content publisher	Nature Publishing Group
Licensed content publication	Nature
Licensed content title	Purification and unique properties of mammary epithelial stem cells
Licensed content author	John Stingl, Peter Eirew, Ian Ricketson, Mark Shackleton, Francois Vaillant et al.
Volume number	439
Issue number	7079
Pages	pp993-997
Year of publication	2006
Portion used	Figures / tables
Requestor type	Student
Type of Use	Thesis / Dissertation
Billing Type	Invoice
Company	Kathleen M Hurst
Billing Address	1212-150 MacLaren Street Ottawa, ON K2P 0L2 Canada
Customer reference info	
Total	0.00 USD

Figure 2.B.

License Number	2284911341687
License date	Oct 09, 2009
Licensed content publisher	Nature Publishing Group
Licensed content publication	Nature Reviews Cancer
Licensed content title	The origin of the cancer stem cell: current controversies and new insights
Licensed content author	Rolf Bjerkvig, Berit B. Tysnes, Karen S. Aboody, Joseph Najbauer and A. J. A. Terzis
Volume number	5
Issue number	11
Pages	pp899-904
Year of publication	2005
Portion used	Figures / tables
Requestor type	Student
Type of Use	Thesis / Dissertation
Billing Type	Invoice
Company	Kathleen M Hurst
Billing Address	1212-150 MacLaren Street Ottawa, ON K2P 0L2 Canada
Customer reference info	
Total	0.00 USD